SCREENING AND CHARACTERIZATION OF CATALYTIC COMPOSITE
MEMBRANES FOR ETHYLLACTATE PRODUCTION

A THESIS SUBMITTED TO
THE GRADUATE SCHOOL OF NATURAL AND APPLIED SCIENCES
OF
MIDDLE EAST TECHNICAL UNIVERSITY

BY

ÖZGE OĞUZER

IN PARTIAL FULFILLMENT OF THE REQUIREMENTS
FOR
THE DEGREE OF MASTER OF SCIENCE
IN
CHEMICAL ENGINEERING

SEPTEMBER 2004

Approval of the Graduate School of Natural and Applied Sciences

_____

Prof. Dr. Canan Özgen
Director

I certify that this thesis satisfies all the requirements as a thesis for the degree of Master of Science.

_____

Prof. Dr. Timur Doğu
Head of the Department

This is to certify that we have read this thesis and that in our opinion it is fully adequate, in scope and quality, as a thesis for the degree of Master of Science.

_____   _____

Prof. Dr. Levent Yılmaz   Assoc. Prof. Dr. Gürkan Karakaş
Co-supervisor   Supervisor

Examining Committee Members

Prof.Dr. Haluk Hamamcı (METU, FE)   _____

Assoc.Prof.Dr. Gürkan Karakaş (METU, CHE)   _____

Prof.Dr. Levent Yılmaz (METU, CHE)   _____

Assoc.Prof.Dr. Pınar Çalık (METU, CHE)   _____

Assist.Prof.Dr. Halil Kalıpçılar (METU, CHE) _____

I hereby declare that all information in this document has been obtained and presented in accordance with academic rules and ethical conduct. I also declare that, as required by these rules and conduct, I have fully cited and referenced all material and results that are not original to this work.

Özge Oğuzer

ABSTRACT

SCREENING AND CHARACTERIZATION OF CATALYTIC COMPOSITE MEMBRANES FOR ETHYLLACTATE PRODUCTION

OĞUZER, Özge

M.Sc. Department of Chemical Engineering

Supervisor: Assoc.Prof.Dr. Gürkan Karakaş

Co-supervisor: Prof.Dr. Levent Yılmaz

September 2004, 138 pages

In this research, molybdophosphoric acid (PMo) was blended with polysulfone polymer (PSF) and form a film catalyst by using a common solvent dimethylformamide (DMF). Kinetic and mass transfer parameters were evaluated for catalytic films in ethanol lactic acid esterification reaction as film surface area, film thickness and catalyst loading were varied at 50°C, 1 atm and 1:1 ethyl alcohol to lactic acid mole ratio conditions. Also prepared films were characterized by DSC, TGA, FTIR, X-ray and SEM analysis.

It was observed that the catalytic films showed higher activities with respect to the unloaded form of PSF and activities were increased with the increasing loading levels. The stabilities of the loaded catalysts were tested by means of deactivation experiments. A decrease was observed after 5th trial for 10wt% PMo loaded PSF film and at 4th trial for 15wt% PMo loaded PSF film. However, activities of the loaded films gave still higher conversion results than the unloaded PSF film. Also it was proved

that with increasing film thickness conversion was decreased and increasing surface area conversion was increased. It was observed from the characterization studies that PMo catalysts have no chemical interaction with the PSF polymer and there was trace amount of DMF solvent was observed in the PMo-PSF catalytic film. Particulate structure of the PMo catalyst was observed and there is no catalyst agglomeration in the membrane network. However, along the thickness, catalyst particles were not homogeneously but finely dispersed in amorphous film structure.

ÖZ

KATALİTİK KOMPOZİT MEMBRANLARIN ETİLLAKTAT ÜRETİMİ İÇİN KARAKTERİZASYONU VE İNCELENMESİ

OĞUZER, Özge

Y. Lisans Kimya Mühendisliği Bölümü

Tez Yöneticisi: Doç.Dr. Gürkan Karakaş

Ortak Tez Yöneticisi: Prof. Dr. Levent Yılmaz

Eylül 2004, 138 sayfa

Bu çalışmada, Molibdofosforik Asit (PMo), Polisülfon (PSF) polİmeriyle birlikte ortak bir çözücüde (dimetilformamid, DMF) karıştırıldı ve bir film hazırlama yöntemiyle PMo-PSF katalitik film benzeri filmler elde edildi. Filmler etillaktat esterifikasyon reaksiyonunda, 50°C, 1 atm ve 1:1 etanol:laktik asit mol oranında, film yüzey alanları, film kalınlıkları ve katalist yükleri için TGA, DSC, X-ray ve SEM cihazlarıyla test edildi.

Yapılan analizler doğrultusunda, katalitik filmlerin, katalist yüklenmemiş PSF filmlerinden fazla aktivite gösterdikleri sonucu elde edildi. Ayrıca yükselen katalist yükleme miktarlarıyla katalitik aktivitenin arttığı da gözlendi. Katalizörlerin polimer matriks içindeki sabitliğini test etmek için deaktivasyon testleri yapıldı. %10 PMo yüklü PSF filmlerin aktivitesinde art arda yapılan 5. denemeden sonra düşüş gözlendi. %15 PMo yüklü PSF filmin aktivitesinde ise 4. denemeden sonra düşüş gözlendi. Her ne kadar 5. ve 4. denemelerdeki aktivitelerde düşme olsa da, aktiviteleri hala yüklenmemiş PSF filmininkinden yüksekti. Bunun

yanı sıra, artan film kalınlığıyla birlikte verimin azaldiği ve artan yüzey alanıyla birlikte verimin arttığı da yapılan analizlerle ispatlandı. Yapılan film karakterizasyon analizleri sonucunca PMo katalistinin polimerle kiyasal bir etkileşiminin olmadığı görüldü. Hazırlanan filmlerde az bir miktar DMF çözücüsü tespit edildi. PMo katalizörleri tanecik yapıda gözlendi ve filmin matriks yapısı içerisinde katalizör kümelenmesine rastlanmadı. Bununla beraber, dikey kesitte katalist tanecikleri homojen olarak dağılmadı ancak katalizör taneciklerinin amorf film yapısına ince dağıldığı ispatlandı.

Anahtar kelimeler: Esterifikasyon, Karakterizasyon, Heteropoli Asit, Polisulfon Membran

ACKNOWLEDGEMENTS

Dedicated to M.Kemal Atatürk..

TABLE of CONTENTS

LIST OF TABLES

LIST OF FIGURES

CHAPTER I

INTRODUCTION

Ethyllactate is an easily biodegradable product of esterification reaction of ethyl alcohol with lactic acid and has been approved by the U.S. Food and Drug Administration. It can replace most halogenated solvents (including ozone-depleting CFCs, carcinogenic methylene chloride, toxic ethylene glycol ethers, perchloroethylene, and chloroform) on a 1:1 basis.

One of the major defects of the current ethyllactate production processes is low purity and conversion. One of the reasons is that the reaction is equilibrium limited. In order to overcome this limitation, one of the esterification products should be removed from the reaction medium to shift the equilibrium to the product side. This means that suitable separation method should be applied. Distillation can be problematic since water (one of the ethyllactate esterification products) and alcohol (one of the reactants) forms an azeotropic mixture in the reaction medium. Therefore the production of high purity of ethyllactate is difficult. Namely, efficient separation processes are needed.

In the past few years, interest in the application of hybrid systems as membrane separation reactors to many chemical processes has substantially increased. When distillation process is difficult to apply, such as, close-boiling components, isomeric mixtures, fractionation of azeotropic mixtures, isomeric mixtures or alcohol-water mixtures, pervaporation is useful. In this respect, to increase the conversion by shifting the equilibrium to the right, using a membrane reactor for separation of a product seems to be an attractive method.

Pervaporation separation processes also considerably reduce the reaction time and save reactants. Therefore, pervaporation aided esterification hybrid processes may lead to the development of ecologically sound technologies for lactate esters [18]. In order to increase the esterification reaction rate and save more time, using a suitable type of catalyst seems also attractive. To benefit from both pervaporation process and catalyst properties, design of a new catalytic membrane for esterification reaction is necessary.

Direct esterification is traditionally catalyzed by strong mineral acids such as, sulfuric, hydrochloric, sulfonic and p-toluenesulfonic acids. The homogeneous catalysts had been used because of its low cost and high reaction rate. However, alkyl chlorides may form and dehydration, isomerization or polymerization side reactions may occur. In addition, removal from the reaction medium and their environmentally corrosive nature are the main disadvantages encountered with the use of these homogeneous catalysts.

Besides the disadvantages of using homogeneous catalysts, the use of strongly acidic heterogeneous catalysts for affecting esterification offers distinct advantages, such as eliminated side reactions, ease of removal and recycle, higher reaction rates and the environmentally safe operability and makes them attractive catalysts for this type of liquid-phase reactions.

In this research, applicability of heteropoly acid (HPA) loaded polymer membrane was investigated in ethanol-lactic acid esterification reaction. Polysulfone (PSF) hydrophilic polymer was chosen as the suitable polymer support and molybdophosphoric acid (PMo) type of heteropoly acid (HPA) was used as the active solid acid catalyst. PMo was blended with PSF polymer and membrane-like catalytic film was obtained by a membrane preparation method. Film was cut into 4mm^2 pieces and used in the batch type reactor. The effects of catalyst loading, film thickness, film surface area were investigated. The stabilities of the loaded catalysts were tested by means of deactivation

2

experiments. Lactic acid conversion changes and rate trends were examined. Also membranes were analysed with DSC, TGA, X-ray, SEM and FTIR in order to characterize the membrane, and to achieve optimum design parameters for a prepared membrane.

CHAPTER II

ESTERIFICATION REACTIONS

When a carboxylic acid and an alcohol are heated in the presence of an acid catalyst, equilibrium is established with the ester and water. Direct esterification of the carboxyl group with an alcohol is one of the best examples of the application of mass-action law by producing the ester as the desired end product [69].

R - CO**OH**   +   **H**O -R′   ⇔   R - COO - R′   +   **HOH**

   Acid   alcohol   ester   water
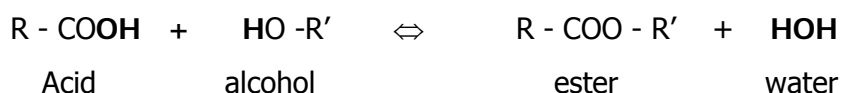
FigureII.1. General esterification reaction

Esterification proceeds by the attack of an alcohol molecule on the slightly positive carbonyl carbon of the acid. The larger the positive charge, the more rapid the reaction will be. Therefore, catalysts are used to increase the positive charge so that a given acid will esterify more rapidly [71].

Although the reaction is equilibrium, it can be used to make esters in high yield by shifting the equilibrium to the right. This can be accomplished in several ways. If either alcohol or the acid is inexpensive, a large excess can be used. Alternatively, the ester and/or water may be removed as formed (by distillation, pervaporation etc.), thus driving the reaction forward [69].

II.1. ETHYL LACTATE

Ethyllactate is product of esterification reaction of ethyl alcohol with lactic acid, has a good temperature performance range (boiling point:

154°C, melting point: 40°C), is compatible with both aqueous and organic systems, is easily biodegradable, and has been approved by the U.S. Food and Drug Administration for food. It can replace most halogenated solvents (including ozone-depleting CFCs, carcinogenic methylene chloride, toxic ethylene glycol ethers, perchloroethylene, and chloroform) on a 1:1 basis.

II.1.1. PROPERTIES of ETHYLLACTATE

Ethyllactate is a hydroxy ester, i.e.; one of its R groups is –OH. Therefore ethyllactate is a polar substance which is soluble in water.

Some physical and chemical properties of ethyllactate are given in TableII.1 below:

TableII.1. Ethyllactate properties

$C_5H_{10}O_3 = 118.13$

Color: Uncolored or yellowish transparent liquid.

Smell: Soft fruit odor

Specific Density (25/25 C):	1.029-1.032
Flash point c/c (°C)	47.2
Boiling point (°C)	154
Vapor density (air=1)	4.07
Vapor pressure (mmHg)	5 (at 30°C)
Evaporation rate (n-Buthyl Acetate=1)	0.21
Refraction Index (20 C):	1.410-1.420
Acid Value (mg * KOH/g) <-:	1.0
Ester Content % >-:	98.0
(As) Content % <-:	0.0002
Heavy Metal (Pb) % <-:	0.001

II.1.2. ETHYLLACTATE PRODUCTION

Lactic acid and ethylalcohol are heated in the presence of an acid catalyst and equilibrium is established with the ethyllactate and water as shown in figureII.2 and figureII.3.

$$\text{HOCHCH}_3 - \text{CO}\textbf{OH} \ + \ \text{C}_2\text{H}_5\textbf{OH} \quad \Leftrightarrow \quad \text{HOCHCH}_3 - \text{COO} - \text{CH}_2\text{CH}_3 \ + \ \textbf{H}_2\textbf{O}$$

Lactic acid   Ethanol   Ethyllactate   Water
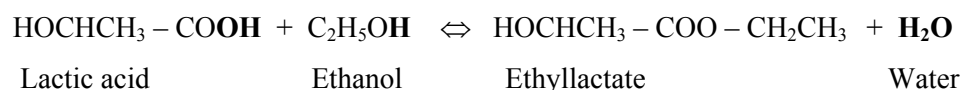
FigureII.2 : Thermodynamically limited reversible ethyllactate esterification reaction.

The carbonyl group of the acid is reversibly protonated by the acid catalyst. Increasing the positive charge on the carbonyl carbon, protonation enhances its reactivity toward nucleophiles. Ethyl alcohol, as a nucleophile, attacks the carbonyl carbon of the protonated lactic acid and new C-O bond is formed. The –OH group is protonated by oxygens. Protonation improves its leaving-group capacity. Finally deprotonation gives the ethyllactate (ester) and regenerates the acid catalyst [69].

Lactic acid being both an acid and an alcohol, is able to form an ester between two molecules, are acting one as acid and the other one as alcohol. Lactoyllactic acid, which is polyester of lactic acid, is formed. This is the reversible, slow, rate limiting ethyllactate side reaction.

$$\text{HOCHCH}_3\text{–CO}\textbf{OH} \ + \ \text{HOCHCH}_3\text{–CO}\textbf{OH} \quad \Leftrightarrow \quad \text{HOCHCH}_3 - \text{COO -CHCH}_3\text{COOH}$$

 lactic acid   lactic acid   lactoyllactic acid

$$+ \ \textbf{H}_2\textbf{O}$$

water
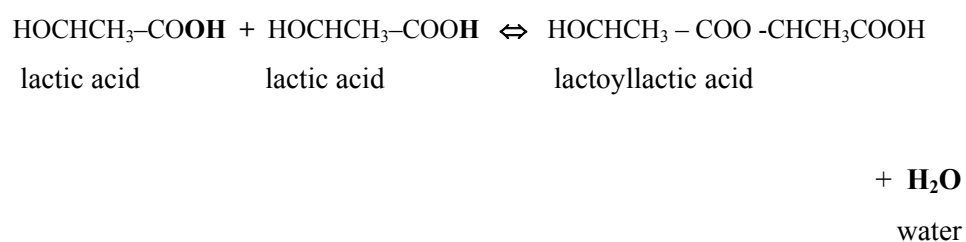
FigureII.3 Reversible lactic acid hydrolysis reaction

Direct esterification is traditionally catalyzed by strong mineral acids such as, sulfuric, hydrochloric, sulfonic and p-toluenesulfonic acids. However, formation of alkyl chlorides, dehydration, isomerization or polymerization side reactions may occur. In addition, removal from the reaction medium and their environmentally corrosive nature are the main disadvantages encountered with the use of these homogeneous catalysts [76,77,78,79].

The use of strongly acidic heterogeneous catalysts for affecting esterification offers distinct advantages over conventional methods, such as eliminated side reactions, ease of removal and recycle, higher reaction rates and the environmentally safe operability and makes them attractive catalysts for this type of liquid-phase reactions [2,3,5].

In this study, the super acidic heteropoly acids are doped in polymeric polysulfone membrane as the catalyst. Their importance, physical, chemical and catalytic properties will be discussed in detail in the next section.

CHAPTER III

HETEROPOLY ACID CATALYSTS

Catalysis by heteropoly acids (HPAs) and related compounds is a field of growing importance, attracting increasing attention worldwide, in which many new and exciting developments are taking place in both research and technology [6]. Heteropoly acids are polyoxometalates incorporating anions (heteropoly anions) having metal-oxygen octahedra as the basic structural units.

Heteropoly anions are polymeric oxoanions which are formed by the condensation of more than two different oxoanions [3]. Acidic elements such as Mo, W, V, Nb and Ta are present as oxoanions in aqueous solutions and polymerize to form polyanions at low pH. Free acids (or acid forms) of these species are called heteropoly and isopoly acids, respectively. Here, the term "heteropoly compounds" is used for heteropoly acids and their salts.

Although practical applications of heteropoly acid catalysts have been attempted for a long time, it was only recently that the relationships between the structure, chemical properties, and catalytic functions of these compounds were investigated in a systematic way [3]. Heteropoly compounds are suitable materials for both the catalyst design of practical processes and for fundamental studies regarding heterogeneous catalysis for their

- Strong Brϕnsted acidity approaching to the superacid region
- High solubility in water and in oxygenated solvents
- Ability to catalyze reversible redox reactions under mild conditions
- Fairly high stability in solid state

- High proton mobility
- Significantly higher catalytic activity compared to conventional acid catalysts
- Lack of side reactions (sulfonation, chlorination, nitration, etc.)
- No corrosion problem
- Easy operation in terms of catalyst re-use and recycle
- Pseudo-liquid phase

Catalytic tests reported to date indicate that heteropoly compounds are efficient for reactions of oxygen-containing molecules (water, ether and alcohol) such as dehydration, etheration, esterification, and related reactions at relatively low tempreratures [9,10,11,12]. A superior performance of heteropoly compounds is often observed under conditions that favor the pseudo-liquid phase (bulk-type reactions) or are likely to occur. They are also active for alkylation and transalkylation, but deactivation during reaction is significant, probably because of too strong acidity [3]. However, HPAs high solubility in water and other polar liquids prevents their usage in homogeneous phase esterification reactions. After HPAs dissolved in the reaction liquid, it is difficult to separate them from the reaction medium. In order to avoid this problem, HPAs may be loaded in polymeric or inorganic insoluble type supports when they are used as esterification reaction catalyst.

III.1. STRUCTURAL CHARACTERISTICS

III.1.1. MOLECULAR STRUCTURE

It is very important for understanding the heterogeneous catalysis of HPAs to distinguish between the two classes of structures which we call the primary and the secondary structures. HPAs in the solid state are ionic crystals (sometimes amorphous) consisting of large polyanions (primary structure), cations, water of crystallization, and other molecules. This three-dimensional arrangement is the "secondary structure" [4].
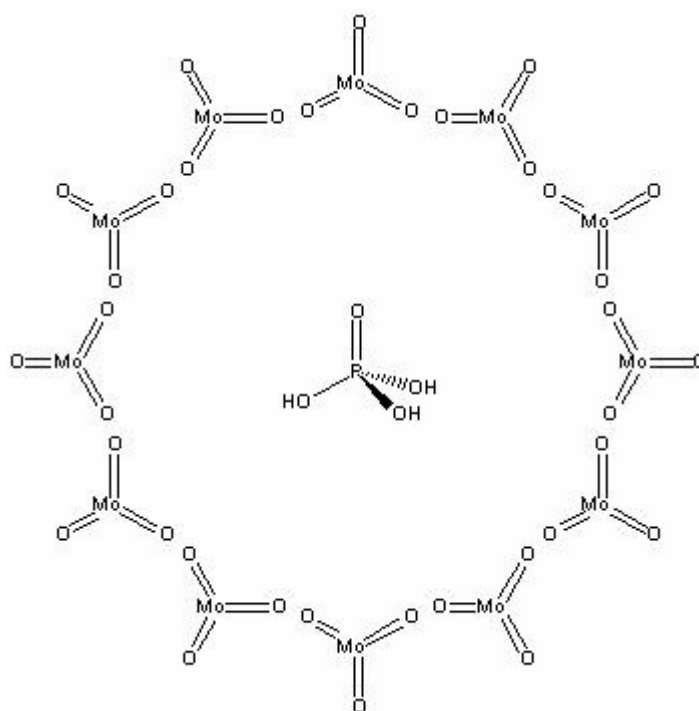
FigureIII.1 Molybdophosphoric acid structure

The primary structure having the Keggin structure, $XM_{12}O_{40}{}^{n-8}$ (X is the central atom (Si^{4+},P, etc.), n is the oxidation state, and M is the central metal ion (Mo^{6+},W^{6+},V^{5+}, etc.)) is shown in FigureIII.1. There are four different kinds of oxygen atoms: 4 O_i (internal oxygen connecting P and Mo), 12 O_e (edge sharing oxygen connecting Mo's), 12 O_c (corner-sharing oxygen connecting Mo_3O_{13} units), and 12 O_t (terminal oxygen bonding to 1 Mo atom). Mo atoms are displaced outward (0.3-0.4 A°) from the center of the O_6 octahedron, giving the Mo-O_t bond a double-bond character. O_i is located inside the anion and the Mo- O_iP bond is long and weak. In the free Keggin anion, edge-bridging oxygens (edge sharing and corner sharing) are assumed to be the most significant protonation sites. On the other hand, in solid HPAs, the protons take part in the formation of the heteropoly acid crystal structure, linking the neighboring heteropoly anions, which enables the more accessible terminal oxygens to be protonated. The structure is

essentially the same for $PMo_{12}O_{40}^{3-}$, although in some cases the positions of Mo are further distorted [3].

Figure III.2 Primary Keggin Structure

In secondary structure case, polyanions constitute two sets of three-dimensional networks in which polyanions are connected by $H^+(H_2O)_2$ bridges. Quasi-planar $H^+(H_2O)_2$ ions hydrogen-bonded to the therminal oxygens of four polyanions. The protons in the hexahydrate rapidly exchange with water. In more hydrated heteropoly anions, $H^+(H_2O)_2$ connects the four Keggin anions [1]. On dehydration, a proton occupies the same position as the $H^+(H_2O)_2$ ion and interacts with the four terminal oxygens.
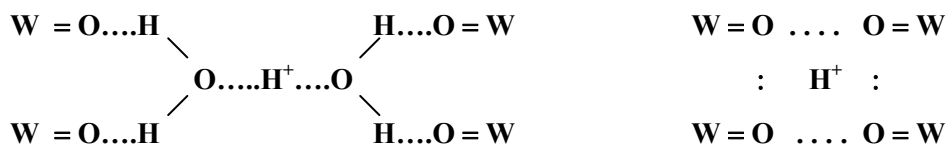
Figure III.3.a Solid HPW hexahydrate   **III.3.b.** Solid dehydrated HPW

III.1.2. THERMAL STABILITY AND WATER CONTENT

Thermal stability in solution changes very much depending on the kind of HPAs. The thermal stability of hydrogen forms of HPAs changes with heteroatom, polyatom, and polyanion structure as follows [4]:

$$H_3PW_{12}O_{40} > H_3SiW_{12}O_{40} > H_3PMo_{12}O_{40} > H_3SiMo_{12}O_{40}$$
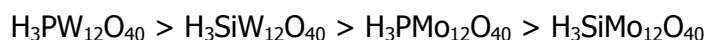
Decomposition, which takes place at 350-600 °C, is believed to be, for example [3]:

$$H_3PMo_{12}O_{40} \rightarrow 1/2\ P_2O_5 + 12\ MoO_3 + 3/2\ H_2O$$
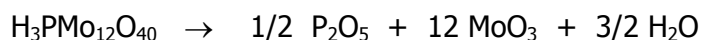
However, thermally decomposed molybdenum HPAs can be reconstructed under exposure to water vapors and enhances stability at higher temperatures.

The thermal behavior of metal salts are discussed in somewhere else [3,4,6,65].

III.2. ACIDIC PROPERTIES

The catalytic function of solid acids is closely related to the acidic properties (amount, strength, and type of acid sites) of the catalyst surface. In the case of heteropoly compounds, "bulk acidity" as well as "surface acidity" must be taken into account, since reactions sometimes proceed in the catalyst bulk [3])

Acidic properties (and redox properties) can be controlled by varying the constituent elements of polyanions and the counter cations [2]. Acidity may be generated by protons which act as counter ions in heteropoly acids (i.e., in $H_3PW_{12}O_{40}$), and in mixed acidic salts, or by protons, which developed by other mechanisms such as; dissociation of water coordinating to metal cations and formation of protons by the reduction of metal in the structure. All heteropoly acids are strong acids, which are much stronger than mineral acids as H_2SO_4, HCl, p-toluene sulfonic acid etc. The strong acidity is caused by dispersion of the negative charge over many atoms of the polyanion and the polarization of the outer M=O bond [2].

The acid strength can be expressed by the Hammett acidity function H_0;

$$H_0 = pK_{BH+} - \log([BH^+] / [B])$$

$$BH^+ \rightarrow B + H^+$$
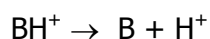
Where [B] is the concentration of the indicator B, [BH$^+$] is the concentration of the conjugated acid, and K_{BH+} is the equilibrium constant for the above reaction. The H_0 value of 100% H_2SO_4 (-11.94) is taken as a reference number, and acids with values lower than -12 are classified as superacids. Superacids with H_0 values of -20, that is 10^8 times stronger than 100% H_2SO_4. The values of the Hammett function for the a number of solid acids, including $H_3PW_{12}O_{40}$ are as follows [65]:

TableIII.1 Hammett function values of solid acids

Solid Acid	-H_0	Solid Acid	-H_0
H_2SO_4	11.94	SbF_5/SiO_2-Al_2O_3	13.7
Nafion	12	SO_4^{2-}/ TiO_2	14.5
$H_3PW_{12}O_{40}$	13.2	SO_4^{2-}/ ZrO_2	16.1
$AlCl_3$-$CuCl_2$	13.7	-	-

III.2.1. **HETEROPOLY ACIDS IN SOLUTION**

In solutions, the acid properties of heteropoly acids are quite well documented in terms of dissociation constants and Hammett acidity function. Heteropoly acids have very high solubilities in polar solvents such as water, lower alcohols, ketones, ethers, esters, etc. on the contrary, they are insoluble in nonpolar solvents like hydrocarbons [65].

A great deal of works is dedicated to the study of HPA acidity in solutions. However, data for the dissociation constants of HPAs are quite limited. In aqueous solution HPAs are completely dissociated at the first three steps, the consecutive dissociation usually being unnoticeable because of leveling effect of the solvent [5].

Using a potentiometric method the dissociation constants of some heteropoly acids in various solvents at 25°C are obtained [5]. Note that the value of dissociation constants of HPAs does not vary considerably, while the distinctions between value of dissociation constants of inorganic acids are more considerable. This may be explained by taking into account a large size and low surface density of the polyanion charge as well as by the peculiarity of the HPAs proton structure. Nonaqoeous and mixed solvents exhibit differentiating effect on the acid dissociation constants of HPAs. Moreover, HPAs are considerably more stable in organic solutions. In the table below, the dissociation constants in ethanol are given in the form of $pK_i = - \log K_i$, where K_i is the acid dissociation constant. For comparison, the dissociation constants of some inorganic acids are presented.

TableIII.2 Dissociation constants of HPAs in ethanol at 25°C

	PK_1	pK_2	pK_3
$H_3PMo_{12}O_{40}$	1.8	3.4	5.3
$H_3PW_{12}O_{40}$	1.6	3.0	4.1
HNO_3	3.6	-	-

It is seen that HPAs are stronger than the usual inorganic acids. This is of fundamental importance for the HPAs application in acid catalysis. Also it is realised that acidic properties of HPAs in ethanol do not vary significantly depending on the HPAs composition and structure [5].

Keggin anions can be characterised as having a very weak basicity and great softness. The softness of the heteropoly anions is assumed to play an important role in stabilizing organic intermediates. The order of

softness of heteropoly anions in aqueous solution was estimated as follows:

$$SiW_{12}O_{40}^{4-} > GeW_{12}O_{40}^{4-} > PW_{12}O_{40}^{3-} > PMo_{12}O_{40}^{3-} > SiMo_{12}O_{40}^{3-} > NO_3^{4-} > TsO^- > SO_4^{2-}$$
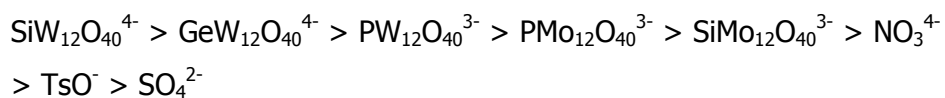
III.2.2. SOLID HETEROPOLY ACIDS

Solid heteropoly acids posses purely Bronsted acidity and are stronger than conventional solid acids as $SiO_2 - Al_2O_3$, H_3PO_4 / SiO_2 , and HX and HY zeolites [6]. The acid strength of the crystalline heteropoly acids decreases in series:

$$H_3PW_{12}O_{40} > H_4SiW_{12}O_{40} \approx H_3PMo_{12}O_{40} > H_5PMo_{10}V_2O_{40} > H_4SiMo_{12}O_{40}$$
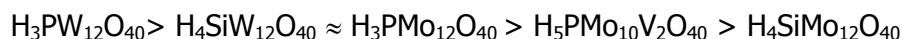
Like other strong acids, HPAs are capable of generating carbocations from adsorbed olefins and arenes.

III.2.3. PSEUDO-LIQUID PHASE

Owing to the flexible nature of the secondary structure of the acid forms and group A salts, polar molecules such as alcohols and amines are readily absorbed into the solid bulk, by substituting water molecules and / or by expanding the interdistance between polyanions [2]. Thus, this is not a diffusion process in micropores. Upon absorption the volumes of heteropoly compounds increase and sometimes deliquescence is observed.

Heteropoly acids which have absorbed a significant amount of polar molecules resemble in a sense a concentrated solution and are in a state between a solid and a solution. Therefore, this state is called "pseudo-liquid phase".

The tendency to form a pseudo-liquid phase depends on the kind of heteropoly compound, the molecules to be absorbed and on the

reaction conditions. The acid-forms extensively absorb polar molecules into the solid bulk, but non-polar molecules are adsorbed only on the surface.

The rate of absorption varies depending on the basicity of the molecule and on the molecular size. The rate of absorption depends also on the water content of heteropoly compounds, and there is sometimes a critical pressure at which the rate changes abruptly [2].

III.3. REDOX PROPERTIES

III.3.1. MECHANISM of REDUCTION and OXIDATION

The two-step mechanisms shown in figureIII.4 for the reduction by H_2 of 12-molybdophosphoric acid and its alkali salts is proposed. The first step is $H_2 \rightarrow 2H^+ + 2e$. Electrons are trapped by Mo atoms ($Mo^{6+} + e \rightarrow Mo^{5+}$; the number of electrons per anion is not certain) but are mobile in a polyanion, and protons are weakly associated with the water of crystallization or the outer surfaces of the anions. In the second step, protons react with the oxygen of the polyanion to form water. Corresponding to the two-step reduction, there are two redox cycles (I $\Leftrightarrow$ II and II $\Leftrightarrow$ 1). Upon reoxidation, water is evolved in II $\Leftrightarrow$ 1 but not III $\Leftrightarrow$ I. Both redox cycles naturally satisfy the overall stoichiometry of $H_2 + \frac{1}{2} O_2 \rightarrow H_2O$. The second redox cycle (I $\Leftrightarrow$ III) tends to dominate at high temperatures and for an extensive reduction [3].

$$\begin{array}{ccc}
\overset{O}{\underset{6+}{\|}} \quad \overset{O}{\underset{6+}{\|}} & \overset{O}{\underset{5+}{\|}} \quad \overset{O}{\underset{5+}{\|}} & \overset{O}{\underset{5+}{\|}} \quad \overset{O}{\underset{5+}{\|}} \\
-Mo-O-Mo \; + \; H_2 \; \rightarrow & -Mo-O-Mo- \; + \; 2H^+ \; \rightarrow & -Mo \qquad -Mo \; + \; H_2O \\
I & II & or
\end{array}$$

$$\begin{array}{c}
\overset{O}{\|} \qquad {}_{4+} \\
-Mo-O-Mo- \\
III
\end{array}$$

$$II + \tfrac{1}{2}\,O_2 \rightarrow I + H_2O$$

$$III + \tfrac{1}{2}\,O_2 \rightarrow I$$
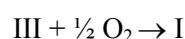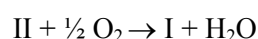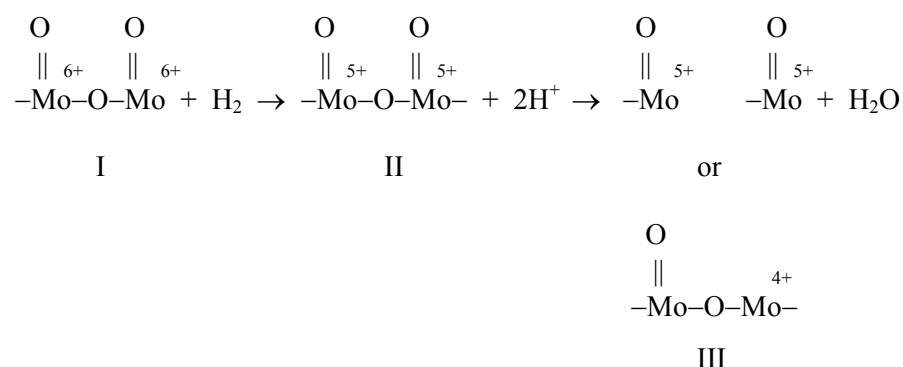
FigureIII.4 Two step redox cycle of molybdophosphoric acid

The rate and reversibility of the redox cycles shown in figureIII.4 are as follows:

I.   The first redox cycle is the most rapid and reversible

II.   The second redox cycle is rapid and reversible near the surface at a low extent of reduction

III. An excess reduction at high temperatures makes the cycle irreversible.

III.3.2. **REDOX PROPERTIES AND CONSTITUENT ELEMENTS**

Redox properties of 12-heteropoly compounds depend on both the constituent elements of polyanions and countercations. The oxidizing ability (or the reducability) has been estimated from the reduction of heteropoly compounds by H_2, CO, and organic compounds. Although the orders of oxidizing ability observed differ a little for the various methods adopted and the investigators, the following trends have been noted [3].

I. When the activation of a reducing agent proceeds easily, the reduction rate of polyanions approximately parallels the oxidation potential in solution. For example, in the case of heteropoly acids

mixed with Pd/carbon powders, the order for the reduction by H_2 was $PMo_{10}V_2$ > PMo_{12} > PMo_6W_6 > PW_{12} . This order is often reflected in oxidation catalysis.

II. For a given polyanion, the effects of metal counterions are divided into two groups:

metal ions which can be reduced (Pd, Ag, Cu) and metals which can be reduced respectively [3].

III.4. HETEROPOLY ACID CATALYSIS IN HOMOGENEOUS PHASE

Catalysis by heteropoly compounds, reactions of esters and esterification catalyzed by heteropoly acids in a homogeneous liquid phase, effects of the central atom of heteropoly anions having tungsten as the addenda atom was studied in 1993 [10]. Decomposition of isobuthyl propionate (IBP) (rxn1), ester exchange of IBP with acetic acid (rxn2), ester exchange of IBP with n-propyl alcohol (rxn3), and esterification of propionic acid with isobuthyl alcohol (rxn4) have been studied in a homogeneous liquid phase using heteropoly acids $H_mXW_{12}O_{40}$ (X = P, Si, Ge, B, and Co) having the Keggin structure and $H_6P_2W_{18}O_{62}$. It was concluded that the catalytic behavior of the heteropoly acids remarkably depended on the kind of reaction system, namely, the basicity of the reactants.

Synthesis of esters under microwave irradiation using heteropoly acids as catalysts was studied in 2003 [13]. The esters were prepared by the reaction of alcohols (butanol, heptanol, octanol and benzyl alcohol) with acetic acid and benzoic acid, using heteropoly acids (both homogeneous HPAs and their Cs salts) and sulfuric acid as catalysts under microwave irradiation and conventional heating in the absence of solvent. It was concluded that the combination of heteropoly acid and microwave energy for the synthesis of ester shortened the reaction time from hours to minutes as environmentally benign.

III.5. SUPPORTED HETEROPOLY COMPOUNDS

Dispersing HPAs on solid supports with high surface areas is important for catalytic applications. Because the surface area of unsupported HPAs are usually low ($1-5 m^2/g$) [6]. In general, HPAs strongly interact with supports at low loading levels, while the bulk properties of HPAs prevail at high loading levels.

Acidic or neutral substances such as SiO_2, active carbon, acidic ion exchange resin are suitable supports. Solids having basicity such as Al_2O_3 and MgO tend to decompose HPAs [4].

Esterification of phthalic anhydride with 2-ethylhexanol by solid superacidic catalysts was studied in 1992 [12]. Efficacy of several solid superacidic catalysts was delineated in the preparation of the industrially important plsticizer, dioctyl phthalate (DOP), from 2-ethylhexanol and phthalic anhydride. The HPAs used in this study were phosphotungstic acid and dodecatungstophosphoric acid. HPAs on various supports (SiO_2, r-Al_2O_3, TiO_2, ZrO_2) were prepared by the incipient wetness method. A complete kinetic study with sulphated zirconia was also examined in this study. In case of supported heteropoly acids the support was found to play an important role in defining the final activity of the catalyst.

The preparation of encaged heteropoly acid catalyst by synthesizing 12-molybdophosphoric (12-PMo) acid in the supercages of Y-type zeolite was studied in 1997 [57]. 12-molybdophosphoric acid encaged in the supercages of Y-type zeolite was synthesized from molybdenum oxide and phosphoric acid, in a slurry mixture of Y-type zeolite crystals and deionized water. After thorough washing in hot water, the 12-PMo was found to remain in the Y-type zeolite. Catalysts thus obtained were found to show activity for the esterification of acetic acid with ethanol, indicating that this catalyst could be used as a solid acid catalyst in various liquid phase reactions that involve water.

The stability of MCM-41-supported heteropoly acids under liquid- and gas-phase esterification conditions was studied in 1999 [58]. MCM-41-supported HPAs ($H_3PW_{12}O_{40}$ (PW_{12}) and $H_4SiW_{12}O_{40}$ (SiW_{12})) are used as catalysts in the liquid-phase esterification of 1-propanol and hexanoic acid, and in the gas-phase esterification of acetic acid and 1-butanol. For both reactions MCM-41 supported HPAs proved to be active catalysts. However, X-ray diffraction (XRD) and transmission electron microscopy (TEM) studies show that the initially high dispersion of HPA units is lost during reaction. Large clusters (~10nm) of HPA are formed on the outer surface of the MCM-41 support. Since this clustering also occurred when less polar substrates were applied, not the polarity of the substrates is responsible for the cluster formation only. HPA tendency to form clusters has been observed both in liquid phase reactions and, to a lesser extent, in vapour phase reactions.

Esterification of maleic acid with ethanol over cation-exchange resin catalysts was studied in 2002 [31]. In this study, the efficacy of several heterogeneous catalysts, such as Indion-170, Amberlyst-36, Amberlyst-15, Amberlite IRA 120, 20% DTP/K-10 (dodecatungstophosphoric acid supported on K-10 clay) were delineated in the esterification of maleic acid with ethanol at reflux. Amongst these Indion-170, Amberlyst-36, Amberlyst-15 were observed to be the most effective. It was also observed that the catalyst chosen has excellent reusability and was not deactivated. The effects of various parameters on the rate of reaction demonstrated that the reaction was intrinsically kinetically controlled and there were no intraparticle and interparticle mass transfer limitations. A pseudo-homogeneous kinetic model was developed from the experimental data and activation energy was found. The result also suggested that this reaction was intrinsically kinetically controlled.

Although application of polymer materials to chemical reactions at high temperatures has been restricted due to their thermal and mechanical instability, much attention has been paid to the polymer materials because of their flexible applicability. There are two promising

approaches to the modification of novel catalysis of HPAs. In the first approach, polymer materials have been utilized as supporting materials. Taking advantage of of the overall negative charge of heteropolyanion, e.g., HPAs have been combined with polymer materials such as ion-exchange resin [65] or conjugating conducting polymer [80]. Other approach is the HPA-polymer composite film catalysts [48-55]. HPAs have been successfully blended with polymer materials using a common or a mixed solvent to prepare the membrane-like HPA-polymer composite film catalysts. They have potential applications as catalytic membranes to be used in membrane separation units.

CHAPTER IV

PERVAPORATION

Membrane technologies have recently emerged as an additional alternative to the well-established separation processes [18]. Membrane separation technologies offer advantages over existing methodologies. Such as

- High selectivity
- Low energy consumption
- Moderate cost to performance ratio
- Compact and modular design

Pervaporation membrane reactors (PVMR) are recently attracting attention as one of the most promising membrane technology [21]. Pervaporation itself is becoming, in recent years, a promising technology, potentially usefull in applications such as the dehydration and removal/recovery of organic compounds from aqueous solutions, as well as the separation of organic mixtures. Pervaporation is a membrane separation process where the upstream side of the membrane is in contact with feed liquid while vacuum is applied on the downstream side of the membrane, and permeate is obtained as vapor. PV is often applied in combination with other technology as a hybrid process; among these, PV-distillation systems and PVMR are already finding industrial applications [18]. In PVMR the membrane either removes the desired product or the byproduct (e.g., water for esterification reactions).

Though attracting current attention, PVMR are not a recent discovery. Their use was proposed in the early patent literature (Jennings & Binning, 1960). Pearse (1987) describes a PVMR for the esterification study. As with the more conventional membrane reactors (MR), PVMR systems are designed as two configurations; reactor and membrane are housed in separate units, or membrane and reactor are incorporated into one unit. Esterifications are the main class of reactions that have been studied in PVMR.

The major pervaporation applications include

- the removal of small amounts of water from organic solutions (e.g., ethanol-water azeotropes to produce a relatively pure organic chemical)
- the drying of organic liquids by removing small volumes (few percent) of water from nearly pure organics
- removal of small amounts of organics from water (e.g., wastewater clean up)

The performance and the efficiency of a pervaporation membrane are determined by two parameters: flux and selectivity. Flux is defined as the amount of material flowing through the membrane per unit area per unit time. The selectivity of a membrane towards a mixture is expressed by a dimensionless parameter called separation factor (α). Separation factor $\alpha_{A/B}$, which express the selectivity of A to B is defined as follows:

$$\alpha_{A/B} = (y_A / y_B) / (x_A / x_B)$$

Where, y_I denotes the concentration of species i in the permeate, and x_i denotes the concentration of species i in the feed. When the separation factor is unity, no separation occurs. When it approaches to infinity, the membrane becomes perfectly semipermeable. The membrane is evaluated according to its closeness to the perfectly semipermeable side. However the performance of a membrane is

23

determined not only by its structure but also some other operating parameters.

The main factors affecting the selectivity and flux in pervaporation are concentration of feed solution, temperature and downstream pressure in the system, the chemical nature of the permeating species and interactions between them and between the membrane [68].

IV.1. MEMBRANE MATERIALS AND PROPERTIES

Synthetic membranes are thin, solid-phase barriers that allow preferential passage of certain substances under the influence of driving force [17]. In pervaporation, nonporous membranes, which are generally either composite, or asymmetric, or composite and asymmetric, are used. For such membranes, the performance is determined by the properties of the membrane material, the choice of which is done according to the type of application. In pervaporation, the driving force for mass transfer is the chemical potential gradient across the membrane. Mass transfer in pervaporation is described by the solution-diffusion model [68].

IV.1.1. SOLUTION-DIFFUSION MODEL

According to the solution-diffusion model, as a first step permeants dissolve in the membrane material and then, as a second step, diffuse through the membrane down a concentration gradient. Separation of the different permeants is achieved because of the differences in the solubilities in the membrane and the rate at which they diffuse through the membrane. It is assumed that the pressure within a membrane is uniform and that the chemical potential gradient across the membrane is expressed only as a concentration gradient [81].

IV.1.2. POLYMERIC MEMBRANES

Polymers provide a range of properties important for separations, and modifying them can improve membrane selectivity. A material with a high glass-transition temperature (T_g), high melting point, and high crystallinity is preferred. Glassy polymers (i.e., polymers below their T_g) have stiffer polymer backbones and therefore let smaller molecules such as hydrogen and helium pass more quickly; larger molecules such as hydrocarbons permeate the membrane more slowly. Rubbery polymers (i.e., polymers above their T_g), in contrast, allow the hydrocarbons to permeate more readily than the smaller gas molecules.

Membranes can be classified into two main groups according to their behavior towards water: hydrophilic and hydrophobic membranes. Although hydrophilic membranes, which are composed of polymers like polyvinylalcohol (PVA), polyacrylonitrile (PAN), are selective to water and they are used to separate water from aqueous mixtures; hydrophobic membranes (generally composed of silicon containing polymers) are more selective to the organics than water [68].

Esterification of oleic acid with ethanol accompanied by membrane separation was studied [35] in order to shift the equilibrium and increase the conversion of the esterification by removal of water vapor from the gaseous mixture consisting of alcohol and water. A porous ceramic tubing was used as the substrate to support a membrane and it was dipped in the solution of perfluorinated ionexchange resin (Nafion 117), chitosan (FLONAC #250), or polyimide (Ultem). The perfect conversion due to equilibrium shift was obtained by using a polyimide membrane for removal of water vapor generated by the esterification.

Separation of ethanol-water mixtures by pervaporation-membrane separation process was studied in 1987 [27]. The separation of ethanol-water mixtures by pervaporation are presented and evaluated

with the purification of alcohol dilute aqueous solution from fermentation and the separation of an ethanol-water azeotropic mixture with ethanol permeable and water permeable polymeric membranes, including cellulose acetate (CA-Me84), cellulose triacetate (DT05, DT06) , polydimethylsiloxane (PDMS) , polyvinylidene fluoride (PVF) and polysulfone (Psf) membranes. the results demonstrated that in polysulfone membrane, the diffusivity coefficient in the membrane is the dominant factor in the separation process. Plots of the separation factor versus feed concentration and the molar fraction of the product versus feed sample show that PDMS and PDMS/PVF) are preferentially ethanol permeable. Besides that DT05, Psf are preferentially water-permeable, especially for azeotropic mixtures and in the high ethanol concentration range. The changes in the permeation flux and permeability over the whole range of concentrations of the mixture clearly illustrate the mechanism of separation for ethanol-water systems. It was indicated that for PDMS membrane, solubility of alcohol is dominant, whereas water just slightly dissolves and is adsorbed on the membrane. However, DT05 and PSF were found to be permeable both for pure ethanol and pure water. In general, it was concluded that the use of pervaporation membrane process to separate the azeotrope of ethanol-water is feasible and can greatly reduce the energy consumption; unfortunately, the separation factor and permeation flux are not very high.

Esterification of carboxylic acid with ethanol accompanied by pervaporation was studied in 1988 [30]. The mixture of oleic acid and acetic acid and ethanol with a catalytic amount of p-toluenesulfonic acid was used. The membrane materials are polyetherimide (PEI), asymmetric PEI, Chitosan (39) and perfluorinated ion-exchange membrane (175). The perfect conversion due to the equilibrium shift was obtained by using an asymmetric polyetherimide membrane for removal of water generated by the esterification.

The influence of composite membrane structure on pervaporation was studied in 1991 [19]. Different composite membranes consisting of

polyethersulfone phase-inversion membranes as sublayer and polydimethylsiloxane coatings as toplayer have been prepared and characterized by water-ethanol pervaporation and oxygen/nitrogen gas separation experiments. Two general statements can be made comparing the sublayers with the respective composite membranes; the flux decrease after coating, the selectivities shift towards the water-selective side.

Pervaporation-aided esterification of oleic acid with ethanol in the presence of p-toluenesulfonic acid was studied in 1993 [29]. The esterification, aided with pervaporation through asymmetric polyimide membranes, was carried out at 348K and 371K under atmospheric and elevated pressures respectively. Only water and ethanol permeated through the membranes. The pervaporation system may perform more effectively at higher temperatures, at least above 360K. Also optimum alcohol/acid mole ratio and other operating parameters were determined.

Esterification of tartaric acid with ethanol (kinetics and shifting the equilibrium by means of pervaporation) was studied in 1994 [34]. The reaction is catalyzed by methanesulfonic acid and used membrane is polyvinyl alcohol-based composite membrane. Kinetic parameters have been determined for the esterification of tartaric acid with ethanol. When pervaporation is used to remove the water produced in this reaction, the equilibrium composition can be shifted significantly towards the formation of the final product diethyltartrate. The membrane surface area to be installed has a clear optimum: when the A/V chosen is too low the water removal is too slow and when the A/V chosen is too high, too much of the ethanol is removed also.

Continuous pervaporation membrane reactor was used for the study of esterification reactions using a composite polymeric/ceramic membrane in 1996 [33]. The membranes used in the experiments were prepared by the dip-coating method. (A polyetherimide (PEI) coated on the ceramic support). For a range of experimental conditions reactor

conversions were observed which are higher than the corresponding calculated equilibrium values due to the ability of the membrane to remove water, a product of the reaction. The membranes also show reasonable fluxes and separation efficiencies towards water. A theoretical model has been developed which gives a reasonable fit of the experimental results.

Application of zeolite-filled pervaporation membrane for separation of alcohol-water mixtures was studied in 1996 [62]. Composite hydrophilic membranes, consisting of KA, NaA, CaA and NaX zeolites and polyvinylalcohol (PVA) polymer were prepared. The pervaporation and separation characteristics of different alcohol-water systems (such as methanol, ethanol, isopropyl alcohol and tert-butanol) through these membranes were investigated at temperatures ranging from 293-323 K. Pervaporation-aided catalytic esterification of acetic acid with ethanol and salicylic acid with methanol hve been carried out in a membrane reactor, leading to a considerable increase in conversion and a reduction in reaction time as a result of continuous removal of water through the membrane. Acetone-water separation by pervaporation on KA- and CaA- filled PVA membrane has been studied as well, which gives even better separation results than that of the ethanol-water system. Application of the zeolite-filled pervaporation membrane to the methanol-acetone condensation reaction also promotes the reaction.

The coupling of esterification with pervaporation was studied in 2001 [28]. The crosslinked PVA membranes were prepared and its separation characteristics were studied by the pervaporation separation of the liquid mixtures of both water/acetic acid and water/acetic acid/n-butanol/butyl acetate. The permeation fluxes of water and acetic acid as a function of compositions were presented. The esterification of acetic acid with n-butanol catalysed by $Zr(SO_4).4H_2O$ was carried out at a temperature range of 60-90 °C. A kinetic model equation was developed for the esterification; then, it was taken as a model reaction to study the coupling of pervaporation with esterification. Experiments

were conducted to investigate the effects of several operating parameters, such as reaction temperature, initial molar ratio of acetic acid to n-butanol, ratio of the membrane area to the reacting mixture volume (S/V) and catalyst concentration, on the coupling process. It was found that water content in the mixture increased earlier during the reaction and then decreased when it reached to the maximum amplitude. Before water content passed through the maximum amplitude, it increased and the ratio of the rate of water removal to water production (coupling factor,F) was less than 1, and after water content reached to the maximum amplitude, it decreased and F was larger than 1. S/V had a different effect on F from the other cases in that F increased earlier and then decreased with the increase of S/V. The increase of temperature or catalyst content resulted in water content increase earlier and then decrease later. Analysis show that the concentration has a sharper decrease at a higher temperature or at a higher catalyst concentration.

Pervaporation separation water/ethanol mixture through lithiated polysulfone membrane was studied in 2001 [37]. For dehydrating water/ethanol mixture by pervaporation, a lithiated polysulfone (Psf) membrane was prepared. The separation performance of water and ethanol strongly depend on the degree of lithiation of Psf membrane. The water permeation rate decreased and separation factor increased with increasing the degree of lithiation of Psf membrane up to 0.75. Beyond the degree of substitution 0.75, the permeation rate increased and separation factor decreased with increasing the substitution. Also it was found that the diffusion selectivity was the dominant contribution to overall permselectivity. The diffusivity differences between permeates through lithiated membrane was the dominant factor for separating water/ethanol mixture. It was also indicated that the separation performance of lithiated membrane was strongly affected by ethanol concentration, and that diffusion selectivity decreased and sorption selectivity increased with increasing ethanol composition in feed. The permeation flux is strongly dependent on the operating

temperature and, the separation factor decreased with increasing the operating temperature.

Zeolite membranes were applied to esterification reactors in 2001 [60}. Pervaporation-aided esterification of acetic acid with ethanol was investigated at 343 K using zeolite T membranes. Almost complete conversion was reached within 8 h when initial molar ratios of alcohol to acetic acid were 1.5 and 2. The reaction time courses were well described by a simple model based on the assumptions that the reaction obeyed second-order kinetics and the permeation flux of each component was proportional to its concentration. The influence of operating parameters on variation in conversion with reaction time was investigated by means of the simulation using the model. The conversion for every PV-aided reaction exceeded the thermodynamic equilibrium. Almost complete conversion of 100% was reached for the reactions of mole ratio 1.5 and 2 within 8 h. It ıs evident that the selective removal of water by PV separation shifted the equilibrium in favor of ester formation.

Performance of hydrophilic pervaporation membranes for ethyl lactate-water-ethanol mixtures was evaluated in 2001 [68]. Four possible hybrid systems of esterification and pervaporation are developed for ethyl lactate production. To investigate feasibility of these proposed systems,performances of commercial hydrophilic pervaporation membranes, namely PERVAP 2201 and PERVAP 2205 from Sulzer, are screened for this chemical system. PERVAP 2201 membrane is used for the removal of water from binary ethanol-water, ethyl lactate-water and ethyl lactate-water-ethanol systems, whereas PERVAP 2205 is used only for the ethanol-water system. It was found that, PERVAP 2201 membrane is very selective to water for ethanol-water and it has higher selectivities and lower flux than PERVAP 2205. Moreover,it is seen that successful separation of ethyl lactate-water mixtures is possible with PERVAP 2201 membrane. However, the ternary system results in lower selectivities and higher fluxes with respect to both of the binary systems, meaning that there is a coupling effect. It is finally

concluded that PERVAP 2201 is a suitable hydrophilic membrane that can be used in hybrid esterification-pervaporation systems for the production of ethyl lactate.

Zeolite-T membrane was applied to vapor-permeation-aided esterification of lactic acid with ethanol in 2002 [59]. The hybric process provided almost complete comversion within a short reaction time by removing water from the reaction mixture. Zeolite T membrane worked steadily for a long time. The reaction time-courses were described by a model based on the assumptions that the esterification obeyed second order kinetics and the permeation flux of each component was proportional to its concentration in the reaction mixture. The final reaction liquid mixtures consisted mostly of ethyllactate and ethanol with little ester of polylactic acids, although concentrated lactic acid solution was used as a source.

IV.2. CATALYTIC MEMBRANES

Membrane separation technology in chemical reaction processes has received increasing attention during recent two decades [20]. Since membranes permit selective permeation of a component from a mixture, the conversion of a thermodynamically limited reaction can be enhanced through controlled removal of one or more product species from the reacting mixture. For example, in the coupling of pervaporation with esterification, the conversion of esterification can be increased greatly through dehydration with pervaporation. The membrane itself can be catalytically active or catalyst blended polymer membranes can be prepared by a membrane preparation method. With composite catalytic membranes, catalyst removal (from the reaction medium) problem has been solved. These membranes have both catalytic and separative properties together. As catalytic materials, composite catalytic membranes have the following advantages [52]:

- preparation procedure is quite simple

- highly dispersed catalysts (e.g., HPAs) in/on polymer supports can be obtained and catalyst dispersion can be easily controlled
- acid and redox properties of catalysts can be modified by selecting suitable solvents polymeric materials.
- pore characteristics of the polymer matrix can be modulated by a membrane preparation technique

Pervaporation membranes endowed with catalytic properties, based on polymer blends was used in 1992 [22]. Membranes endowed with both catalytic and separative properties were designed by using the polymer blend concept. Two polymer blend systems were studied: polyacrylonitrile (PAN)-polystyrene sulfonic acid (PSSA) and polyvinylalcohol (PVA)-PSSA blend for esterification of 1-propanol by propionic acid. Sodium polystyrene sulfonate in its acidic form, mainly used in ion-exchange resins due to its strong acidic character, appears to be a suitable catalyst. However, it exhibits low selectivity towards water in alcohol or acidic media and its highly soluble in water and polar solvents. Its blending with insoluble and highly hydrophilic polymers such as PVA or PAN increases the selectivity and resistance to solvent and solvent mixtures. Based on miscibility and extraction studies, it appeared that PAN-PSSA could not be employed due to polymer segregation and extraction of PSSA to the liquid mixture. In the case of PVA-PSSA, miscibility was observed at high PVA content but, whatever relative polymer concentration in the blend, PSSA extraction occurred. To circumvent this extraction problem, PVA crosslinking was carried out by heat treatment. Good catalytic and separative properties were observed during the esterification reaction tests.

Catalytically active pervaporation membranes were used in esterification reactions to simultaneously increase product yield, membrane permselectivity and flux [36]. Nafion tubes that function both as catalyst and a pervarporation membrane have been used to increase the yield in the esterification of acetic acid with methanol and n-butanol by selectively removing products, mainly water, from the

reaction mixture. The effect of the membrane's catalytic activity on its permselectivity was investigated. The catalytically active membranes showed significantly higher permselectivities for water at the same or higher flux, compared to when no reaction was taking place within the membrane phase.

Pervaporation separation and pervaporation-esterification coupling using crosslinked PVA composite catalytic membranes on porous ceramic plate was studied in 1998 [32]. A composite catalytic membrane with crosslinked PVA dense active layer coated on a porous ceramic plate support was prepared using a novel method and evaluated with a pervaporation setup for the separation of several organic aqueous mixtures. $Zr(SO_4)_2.4H_2O$, an inorganic solid acid was immobilized on the dense active layer. N-buthyl alcohol- acetic acid esterification was used as a model system for investigating into the coupling of reaction with pervaporation in a batch reactor. Almost complete conversion was achieved when crosslinked PVA pervaporation catalytic membrane was used. The order of the permeation flux are: water> acid> alcohol > acetate.

Esterification reaction yield was enhanced using zeolite A vapour permeation membrane in 2002 [61]. A tubular zeolite NaA membrane, prepared on a carbon/zirconia support, was tested for the removal of water from water/isopropanol and water/ethanol mixtures, in both pervaporation and vapour permeation modes, and shown to give high selectivity. A series of 12 experiments were undertaken with no loss of membrane performance. The esterification of lactic acid with ethanol to give ethyllactate was studied in a batch reactor, without catalyst and with p-toluenesulfonic acid as catalyst. The use of a zeolite A vapour permeation membrane to remove water generated by the reaction gave substantially enhanced yields of product, compared to control experiments carried out without the membrane and with the membrane but without vacuum being applied.

Coupling of reaction and separation at the microscopic level: esterification processes in a H-ZSM-5 membrane reactor was studied in 2002 [56]. A catalytically active zeolite membrane has been used to displace equilibrium by selective water permeation during ethanol-acetic acid esterification. The H-ZSM-5 catalytic membrane used in this work had sufficient catalytic activity to carry out the esterification reaction and at the same time was selective to water permeation. As a consequence, the reaction and separation functions could be coupled very efficiently, and the conversion obtained at the same feed rate and catalyst loading was greater than in conventional fixed bed reactors.

IV.2.1. HETEROPOLY ACID DOPED POLYMER MEMBRANES

A heteropoly acid compound is highly soluble in some organic solvents. Taking advantage of this property, heteropoly acid can be blended with a polymer to form a film by using a common solvent which dissolves both the heteropoly compound and the polymer.

$H_3PMo_{12}O_{40}$-doped polyacetylene as a catalyst for ethyl alcohol conversion was studied in 1991 [80]. 12-Molybdophosphoric acid, 20.8 wt%, was introduced into the polymer. A uniform distribution of HPA over the cross section of the polymer film was found. However, the concentration of HPA seemed to be higher at the surface of the polymer fibers than in their bulk. The conversion of ethyl alcohol was used as a catalyst test reaction. The catalyst exhibited both acid-base activity (formation of ethylene and diethyl ether) as well as redox activity (formation of acetaldehyde). The acid-base activity was 10 times higher than that of unsupported PMo., and the redox activity was about 40 times higher.

Esterification of acetic acid with n-butanol reaction with catalytic membrane of $H_3PW_{12}O_{40}$ (HPW) entrapped in polyvinylalcohol (PVA) was studied in 1999 [20]. In this work, HPW/PVA catalytic membranes on ceramic plates were prepared. SEM (scanning electron microscopy) and XPS (X-ray photoelectron spectrometry) were used to characterize

the membrane nature. The separative and catalytic properties of the membrane were tested by the esterification of acetic acid with n-butanol. It was found that the different ways of crosslinking (with glutaraldehyde [GA]) played an obvious role in the membranes' performance. The membrane possess both good separative characteristics and good catalytic activity. Also it was indicated that the membrane before and after 120 h reaction had a similar surface morphology and nearly the same absorption intensities.

IV.3. POLYSULFONE BASED MEMBRANES

Polymeric materials are widely used in advanced separation technology and biomedical fields. However, the only polymers that are used at present are conventional materials, such as cellulose acetate (CA), polymethylmethacrylate (PMMA), polyethylene (PE), polypropylene (PP), polyacrylonitrile (PAN), ethylene vinyl alcohol copolymer (EVAL), polyvinyl alcohol (PVA), polysulfone (PSF) and polyethersulfone (PES). Among the materials, polysulfone is one of the most important polymeric materials, and the PSF and PSF-based membranes show outstanding oxidative, thermal and hydrolytic stability as well as good mechanical and film-forming properties [39].

Polysulfone is a high performance polymer used for numerous applications across the wide spectrum of membrane separation processes. Polysulfone films have the inherent advantage that they are applicable to a wide range of pH and temperature (378K).

In addition to being commonly used for ultrafiltration membranes, this material serves as the selective layer in membrane gas separations, as a support layer for thin film composite membranes and as a substrate for enzyme attachment.

VI.3.1. MOLECULAR STRUCTURE OF POLYSULFONE

Poylsulfone repeat unit is given in figureVI.1. A single polysulfone chain has an apparent diameter of 9-12 A in the transmission electron microscope.
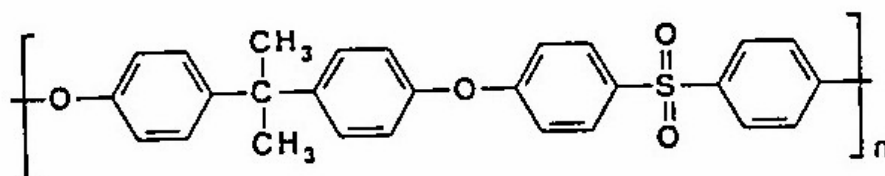
FigureVI.1 Polysulfone molecular structure

IV.3.2. PHYSICAL AND CHEMICAL PROPERTIES

Polysulfone (PSU) is an amber semi-transparent, heat-resistant, high performance engineering thermoplastic. It offers excellent mechanical, electrical and improved chemical resistance properties relative to polycarbonate.

Polysulfone is hydrolysis resistant for continuous use in hot water and steam at temperatures up to 300°F.

Polysulfone offers high chemical resistance to acidic and salt solutions, and good resistance to detergents, hot water and steam. In addition, polysulfone has excellent radiation stability, and offers low ionic impurity levels. Polysulfone often replaces polycarbonate when higher temperatures, improved chemical resistance or autoclavability is required.

Some physical and chemical properties of polysulfone is given as:

nominal average molecular weight: 10,000 Daltons
flash ignition temperature: 550°C / 1022 F

odor: essentially odorless

glass transition temperature: 190°C / 374 F

solubility in water: negligible, below 0.1% (strongly hydrophobic)

volatile content: <1%

spesific gravity: 1.24

stability at room temperature: stable

IV.3.3. MODIFICATION OF POLYSULFONE MEMBRANES

The addition of functional groups to the polymer can enhance some properties of the material in certain ways. For example, the addition of carboxyl groups increases hydrophilicity and alters the solubility characteristics, allowing greater water permeability and better separation. In addition, functional groups are an intrinsic requirement for affinity, ion exchange and other specialty membranes [45]. Polysulfone membranes with functional groups may be prepared by casting functionalized polymer or by chemical modification of a preformed membrane. In the former case, the membrane material is distinct and may have solubility characteristics unlike the parent polymer, resulting in a functionalized membrane that has a quite different microstructure and pore size. In the latter case, functional groups can be added to an existing polysulfone membrane, without altering the defined microstructure and pore size.

Homogeneous modification of polysulfones has been achieved by a number of methods. Sulfonation techniques have resulted in hydrophilic and negatively charged membranes. Polysulfones have been halomethylated to provide useful intermediates that have been subsequently derivatized or quaternized to cationic membranes. Several types of functional group polymers have been derived from lithiated and brominated polysulfones. Other functionalization techniques have led to nitro, amino, and aminomethyl derivatives [45].

IV.4. HETEROPOLY ACID DOPED POLYSULFONE MEMBRANES AND THEIR CHARACTERIZATION

$H_3PMo_{12}O_{40}$ (PMo) −blended polysulfone (PSF) film was prepared and its catalytic activity for the ethanol conversion reaction was investigated in 1993 [53]. The small pieces (2mm×2mm) of the PMo-PSF film were used as catalyst in a fixed-bed reactor. Products were analysed with an online GC using a column packed with Porapak-Q. Thermal analysis showed that the glass transition (T_g) temperature of PSF was 176°C and the thermal decomposition temperature of PMo was 430 °C. The prepared PMo-PSF film was annealed at 150 °C, before the reaction was carried out at 170°C. From the IR spectra of PMo, PSF and PMo-PSF film, the primary structure (Keggin structure) of PMo can be identified by the four characteristic bands ranging from 700 to 1200 cm^{-1}. This fact suggests that the PMo in the PMo-PSF film keeps the primary structure of PMo. In order to investigate any interaction between PMo and PSF, the oxidation state of molybdenum in PMo and PMo-PSF film was measured by XPS. It was confirmed that there is only one type of molybdenum (IV) in both PMo and PMo-PSF film. A TPD experiment of dimethylformamide (DMF) adsorbed on the PMo catalyst (powder) revealed that DMF desorption was initiated at 150 °C and reached maximum points at 270 and 337 °C. this fact suggests that the chemically adsorbed MDF (organic base) on the Bronsted acid site of PMo in the PMo-PSF film can remain at a reaction temperature of 170 °C. SEM micrographs of PSF film and PMo-PSF film show that there is no distinctive difference between the two. No visible evidence representing PMo was found in the PMo-PSF film. This may indicate that PMo was not recrystallized into large particles but was finely distributed as fine particles invisible in the SEM in the PMo-PSF film. The PMo-PSF film showed higher activity for the oxidation reaction and a lower activity for the acid-catalyzed reaction than did PMo. The decrease of an acidic activity of the film is mainly due to DMF adsorbed on its acid sites. Also a slight decrease of the catalytic activity over the film at higher temperatures than 170 °C may have resulted from the thermal deformation of the PSF above the T_g of 176 °C.

Modification of 12-molybdophosphoric acid catalyst by blending with polysulfone was studied and its catalytic activity for 2-propanol conversion reaction was evaluated in 1996 [51]. $H_3PMo_{12}O_{40}$ (PMo) embedded in a polysulfone film was prepared by blending PMo with PSF using DMF as a common solvent and its catalytic acitivity for 2-propanol conversion reaction was examined in different reactor systems. Systems are conventional fixed bed reactor packed with unsupported PMo , fixed bed reactor packed with 2mm$\times$2mm pieces of PMo-PSF film (PMo-PSF-F), a pseudo membrane reactor using PMo-PSF film as a catalytic membrane (PMo-PSF-M). the prepared film catalyst showed a higher yield for acetone but lower yield for propylene than PMo itself. The decrease of an acidic activity of the film is mainly due to DMF adsorbed on its acid sites. When the film catalyst was used as a membrane, it showed higher ratio of acetone to propylene than PMo itself. This is mainly due to higher permeability of acetone through PSF film than propylene.

Selective oxidation catalysis over heteropoly acid supported on polymer ws studied in 1997 [49]. Membrane-like heteropoly acid (PMo)-blended polymer (polysulfone (PSF), polyphenylene oxide (PPO)) film catalysts were prepared using a common solvent (dimethylformamide (DMF)) or mixed solvents (chloroform (C) – methanol (M)) ad they were tested as fixed-bed catalysts for the ethanol conversion reaction in a continuous flow reactor. The film catalysts were characterized by IR, TPD, SEM, EDX, DSC. It was found that heteropoly acid catalyst was finely and uniformly distributed through the polymer matrix. All the film catalysts showed the higher selectivity to acetaldeyde than the bulk solid catalysts. It was revealed that PMo –imbedded PPO film showed much higher oxidation catalytic activity than the corresponding bulk heteropoly acids. This may be due to the interaction (or bonding) of proton of HPA with PPO; judging from the fact that glass transition temperature of PPO was increased after blending with HPA. Conversion and selectivity over the film catalyst were also affected by the nature of solvent and polymer.It was concluded that the film catalyst could be

applied to the low temperature oxidation reactions to obtain high yield and selectivity for oxidation product by enhancing catalyst dispersion and by suppressing the acid-catalyzed reaction.

Modification of pore characteristics and catalytic activities of HPA-polymer composite catalysis by membrane technology was studied in 1998 [50]. $H_3PMo_{12}O_{40}$ (PMo) embedded in a polysulfone film was prepared by blending PMo with PSF using DMF as a common solvent or mixed solvents (chloroform (C) – methanol (M)) and its catalytic acitivity for the vapor-phase ethanol conversion in a continuous flow reactor. The composite catalysts showed the modified catalysis compared to the bulk acid. The effects of solvent on the pore characteristics and catalytic activities of these composite film catalysts were investigated. It is concluded that the pore characteristics of HPA-PSF composite film catalysts could be controlled by the phase inversion method.

Heterogeneous liquid-phase hydration of isobutene by heteropoly acid-polymer composite film catalyst was studied in 1999 [54]. PMo-polymer composite film catalysts were prepared by blending these two materials using a methanol-chloroform mixture by a membrane preparation technique. Polysulfone (PSF), polyphenylene oxide (PPO), polyethersulfone (PES) were used as blending polymers. A PMo-PPO composite catalyst coated on Al_2O_3 was also prepared. These catalysts were used as hetergeneous catalysts for the liquid-phase tert-butanol (TBA) synthesis from isobutene and water. ıt was found that all the composite film catalysts showed higher catalytic activities than homogeneous PMo in the TBA synthesis. Among the composite film catalysts, PMo-PPO showed the best catalytic performance. Not only high absorption capability of PMo-PPO for isobutene but also stability of it in the reaction medium was presponsible for such a catalytic performance. The PMo-PPO/ Al_2O_3 also showed a higher activity than a homogeneous solution of PMo.

Heteropoly acid-polymer composite films wew used as catalytic materials for heterogeneous reactions in 2002 [52]. In this work, PMo-polymer composite film catalysts were prepared by blending these two materials using a methanol (M) –chloroform (C) mixture or ethanol (E) –chloroform (C) by a membrane preparation technique. Polysulfone (PSF) and polyphenylene oxide (PPO) were used as blending polymers because of their excellent thermal and mechanical stability. The composite film catalysts were cut into small pieces and applied as heterogeneous catalysts to the liquid-phase TBA synthesis and to the vapor-phase ETBE (ethyl tert-butyl ether) synthesis. It was observed that PMo was finely dispersed throughout the polymer supports, and the blending patterns of the composite film catalysts were different depending on the identity of polymer material used. In the liquid-phase TBA synthesis, catalytic activities were in the following order; PMo-PPO-MC > PMo-PSF-MC > homogeneous PMo. Not only high absorption capability of PMo-PPO-MC for isobutene but also high stability of it during he reaction was responsible for its enhanced catalytic performance. In the vapor-phase ETBE synthesis, catalytic activities were in the following order; PMo-PPO-EC > PMo-PSF-EC > homogeneous PMo. It was revealed that the residual ethanol in the composite film catalysts played an important role to improve and maintain the catalytic activities of the composite film catalysts.

Heteropoly acid- polymer composite films were used as heterogeneous catalysts and its catalytic properties were evaluated in 2003 [55]. Preparation, characterization and performance of catalytic membranes were reported in this work. PMo-polymer composite film catalysts were prepared by blending these two materials using a methanol (M) – chloroform (C) mixture by a membrane preparation technique. The composite film catalysts were cut into small pieces and applied as heterogeneous catalysts to the liquid-phase TBA synthesis, to the vapor-phase ETBE (ethyl tert-butyl ether) synthesis and to the vapor-phase ethanol conversion. It was observed that PMo was finely dispersed throughout the polymer supports, and the blending patterns of the composite film catalysts were different depending on the identity

of the solvent and polymer material used. The HPA-polymer composite films showed enhanced catalytic activities in these reactions compared to the mother HPAs. Pore characteristics of the composite film catalysts could be controlled by a conventional membrane preparation technique, and they were related to the catalytic performance of the film catalysts. Shell and tube type membrane reactors comprising inert polymer membranes and HPAs were designed and applied to the vapor-phase methyl tert-butyl ether (MTBE) decomposition. Simulation and experimental results revealed that PPO-based membrane reactor showed the best performance, among some polymer membranes examined. Selective removal of methanol through the polymer membrane inhibited the unfavorable reverse reaction (MTBE synthesis), and at the sam time accelerated the MTBE decomposition. Shell and tube-type catalytic membrane reactors (CMRs) utilizing HPA-polymer composite catalytic membranes not only showed catalytic reactivity for the reaction, but also were permselective for methanol with respect to isobutene and MTBE. It has been demonstrated that HPA-polymer composite catalytic membranes have potential application in a membrane reactor for the MTBE decomposition.

Pervaporation separation processes results in a considerable reduction in the reaction time and saving of reactants by enabling the *in-situ* separation of reaction products and shifting the conversion. Therefore, pervaporation aided esterification hybrid processes may lead to the development of ecologically sound technologies for lactate esters. To achieve these goals, design of a new catalytic membrane for esterification reaction is necessary.

CHAPTER V

EXPERIMENTAL

In order to examine the catalytic activity of the molybdophosphoric acid, by taking advantage of heteropoly acids high solubility in organic solvents, series of catalytic films were prepared. Molybdophosphoric acid ($H_3PMo_{12}O_{40}.27H_2O$) was blended with polysulfone (PSF) by using dimethylformamide (DMF) as the solvent for the catalytic film preparation. Prepared catalytic films were characterized by various characterization methods (X-Ray, SEM, DSC, TGA, FTIR) and tested in the typical ethyllactate esterification reaction conditions (50°C & 1 atm, 1:1 etOH:LA mole ratio) .

V.1. FILM PREPARATION

V.1.1 PARAMETERS IN FILM PREPARATION

While preparing the films, effect of catalyst loading (as weight percent), catalytic film thickness and films external surface area were investigated as the parameters.

Polysulfone (PSF) were chosen among those conventional polymers used in separation technology (cellulose acetate (CA), polymethylmethacrylate (PMMA), polyethersulfone (PES), polyacrylonitrile (PAN), etc.). PSF films have the inherent advantage that they are applicable to a wide range of pH and temperature (378K).

Among the heteropoly acid catalysts, molybdophosphoric acid (PMo) was chosen as the solid acid catalyst because of its high acidity and

proven activity on the Lactic acid esterification reactions [65] and DMF is the common suitable polar solvent for both PSF and PMo.

Before preparing the films, drying and annealing conditions were set as 80°C & 0.2 bar N_2 atm and 100°C & 0.9 bar respectively.

The following sets of catalytic film samples were prepared and tested in order to characterize the mass transfer and kinetic effects.

i.   films which have constant thicknes, but four different catalyst loading (0,5,10 and 15 wt% in polymer)

ii.   films which have constant catalyst loading (chosen as 10wt% in polymer), but four different thickness (47,78,150 and 300 μm)

V.1.2 MATERIALS

The following materials were used to prepare the catalytic films.

$H_3PMo_{12}O_{40}.27H_2O$ [phosphomolybdic acid]: Marketed by Acros Organics, New Jersey-USA, under CAS number 51429-74-4 was used as solid catalyst

PSF [polysulfone]: Marketed by Aldrich Chemical Company, Inc., Milwaukee, USA, under CAS number 25154-01-2 was used as polymer matrix

DMF [dimethylformamide]: Marketed by Lab-Scan Ltd., Dublin, Ireland, under CAS number 68-12-2 was used as solvent for PSF

V.1.3 EQUIPMENT

To prepare PMo-PSF catalytic film, Carbolite MTF model tube furnace operating at 300 °C was used for the calcination of the heteropoly acid catalysts by using air as the calcination medium, and after calcination, they were mixed properly in DMF solvent put in a beaker by using

magnetic hot plate stirrer with 0-250 °C heating and 0-1400 rev./min. stirring ranges. This solvent poured in a glass petri-dish (called drop casting) then kept in vacuum oven with heating range between 0-200 °C and vacuum range between 0-1000 mbar for film preparation using nitrogen as the ambient gas.

V.1.4 METHOD

Before dissolving in dimethylformamide (DMF), PMo is calcinated at 300 °C for 1 hr. and polysulfone (PSF) is dried at 110 °C for 12 hr. PMo and PSF are dissolved in DMF for 3 hr. The solution is casted on a petri-dish and dried at 80 °C & 0.2 bar in N_2 atm, in vacuum oven for 12 hr followed with annealing at 100 °C & 0.9 bar for 24 hr.

V.2. PREPARED FILMS

V.2.1 FILMS USED TO ANALYSE THE EFFECT OF CATALYST LOADING

To examine the effect of catalyst loading in lactic acid esterification, 0wt%, 5wt%, 10wt% and 15wt% PMo loaded PSF films were prepared. In order to reduce the mass transfer effects, the thickness and external surface area of the film samples for the reaction experiments were kept constant. These four films prepared in the same conditions and films were prepared in the same drying and annealing conditions to eliminate their effects.

TableV.1 Prepared films used in reaction

	0wt%	5wt%	10wt%	15wt%
Used area (cm^2)	18	18	18	18
Thickness (μm)	78	75	78	78
used polymer + cat.weight in rxn (g)	0.051	0.052	0.053	0.056
cat. charge in used film (g.cat/lt liq.rxn)	-	0.11	0.23	0.34

Prepared films were cut into 4mm^2 pieces to mix the catalytic film particles with the liquid reaction medium properly.

V.2.2. FILMS USED TO ANALYSE THE EFFECT OF SURFACE AREA

In this set of experiments it is aimed that the catalyst loading and film thickness in the film samples were kept constant but the external film surface area was changed in order to test the importance of external mass transfer effects.

i.   **effect of surface area on the reaction rate keeping amount of catalyst constant**

In this set of experiments, aim was to obtain three films having three different external surface area, keeping film thickness and amount of catalyst charge in liquid reaction volume constant. In order to achieve this, 5,10 and 15wt% PMo loaded 78μm-thick PSF films were prepared and proper amount of films were used in reaction experiments. By this way, three films having three different surface area and constant catalyst amount and thickness were obtained. The samples used for this set of experiments are summarised in Table V.2

TableV.2 Prepared films

	12cm^2	18cm^2	36cm^2
Thickness (μm)	78	78	78
Catalyst wt%	15	10	5
used polymer + cat.weight in rxn (g)	0.032	0.053	0.10
cat.charge.in used film (g cat./lt liq.rxn)	0.27	0.24	0.22

ii.   **effect of surface area on the reaction rate keeping weight percent of catalyst constant**

In this experimental set, 10wt% PMo loaded 78 μm PSF film was prepared, then 12,18, 36 and 72 cm^2 pieces were cut to be tested in ethyllactate reaction. Assuming that the solid heteropoly acid is

homogeneously distributed through the film area, for each area series, catalyst charge (in gram catalyst/ lt reaction mixture) included in reaction were changed with changing film area but the ratio of the catalyst in used films (in reaction medium) per polymer amount included in reaction was kept constant i.e., for each film included in reaction medium, weight percent of catalyst loaded in polymer network was kept constant.

Table V.3 Prepared films

	12cm^2	18cm^2	36cm^2	72cm^2
Thickness (μm)	78	78	78	78
Catalyst wt%	10	10	10	10
used polymer + cat. weight in rxn (g)	0.035	0.053	0.11	0.21
cat.charge in used film (g.cat / lt. Liq.rxn)	0.16	0.23	0.47	0.94

Aim was to see whether reaction rate increased with increasing film area or not, and to examine polymer-catalyst interaction keeping catalyst/polymer weight ratio constant.

V.2.3 EFFECT OF FILM THICKNESS

In order to understand the effect of mass transfer resistance, films were prepared with different thicknesses,but with the same amount of catalyst and film area.

Four different films having four different thickness and same loading (10wt%), same area (18cm^2) were prepared and tested in esterification reaction medium. These films are summarised in Table V.4.

TableV.4 Prepared films

	45μm	78μm	150μm	300μm
Area (cm^2)	18	18	18	18
Cat. wt%	10	10	10	10
Used polymer + cat weight in rxn (g)	0.028	0.053	0.10	0.19
Cat.charge in used film (g.cat / lt liq.rxn)	0.21	0.23	0.21	0.21

V.3. ETHYLLACTATE ESTERIFICATION EXPERIMENTS

Experiments were carried out in a batch reactor with constant temperature and pressure (323K & 1atm) and mole ratio of lactic acid to ethanol was kept constant (1:1) for all experiments in order to see the effect of catalyst. A weighted amount of liquid sample was withdrawn at 2 hours time intervals for analysis. Titration and gas chromatography were carried out simultaneously during the experimental runs.

V.3.1 MATERIALS

$C_3H_6O_3$ [Lactic Acid, 92wt% Total Acidity]: Marketed by Merck, Darmstadt-Germany, under CAS number 79-33-4 was used as an esterification reactant

C_2H_5OH [Ethyl Alcohol, 99.5%]: Marketed by Grup Deltalar, Ankara-Turkiye, under CAS number 64-17-5 was used as an esterification reactant

$C_5H_{10}O_3$ [(-)- Ethyl L-Lactate, 99%]: Marketed by Fluka Chemie, Steinheim-Switzerland, under CAS number 97-64-3 was used for GC calibration

KOH [Potassium Hydroxide Pellets, 85%]: Marketed by Merck, Darmstadt-Germany, under CAS number 1310-58-3 was used for titration analysis

HCL [Hydrochloric Acid, 37wt%]: Marketed by Merck, Darmstadt-Germany, under CAS number 7647-01-0 was used for titration analysis

$C_{20}H_{14}O_4$ [Phenolphthalein]: Marketed by Merck, Darmstadt-Germany, under CAS number 77-09-8 was used as indicator solution for titration analysis

$C_{15}H_{15}N_3O_2$ [Methyl Red]: Marketed by Across Organics, New Jersey-USA, under CAS number 493-52-7 was used as indicator solution for titration analysis

V.3.2 EQUIPMENT

Prepared catalytic films, which were cut into $4mm^2$ small pieces to mix catalyst with the reactants homogeneously, put into a 25 ml glass bottle with the reactants (ethanol and lactic acid in 1:1 mole ratio). The reaction solution was mixed by a Clifton model constant temperature water bath, with an inside shaker trolley operating between 0-400 strokes/min and with a PID temperature controller within control capability of $\pm$ 0.1 °C water temperature range within 0-100 °C range was used.

At two-hour reaction intervals, samples were taken from the reactor (small bottle) and liquid product compositions were analysed by titration and GC analysis. For titration analysis, CAT M6 / 1 magnetic hot plate stirrer with 0-250 °C heating and 0-1400 rev./min. stirring ranges and standard laboratory glassware set up were used, and for GC analysis Hewlett-Packard 5890A Gas Chromatograph equipped with a TCD Detector and a 10% packed FFAP / Chromosorb (60/80) Column operating at 120 °C oven temperature, 170 °C injection temperature, 180 °C detector temperature and at 150 kPa head pressure using Helium as a carrier gas for reactant weight percent determination was used. Also a 1 μL Hamilton micro-liter syringe was used for sample injection. GC calibration method was given in appendix-A (p.108).

V.3.3 REACTION EXPERIMENTS

Lactic acid and film catalysts (prepared film cut into $4mm^2$ pieces) were mixed properly (alcohols can be dehydrated by heating them with a strong acid), after reaching steady temperature value, ethylalcohol was added.

Samples were taken at specific time intervals and titrated then were analyzed in GC (to measure the ethyllactate, water and ethyl alcohol amount). GC data and titration data gave the product distribution while reaction proceed. However, since lactic acid has a tendency to form polymeric lactic esters by self-polymerization, the analysis requires hydrolysis step to determine the total acid content. Therefore, examination of the unconverted lactic acid and the amount of lactoyllactic acid present in the product sample are done by means of two sequential acid-base titrations. These titration procedures and all experimental calculations are put in appendix-A.
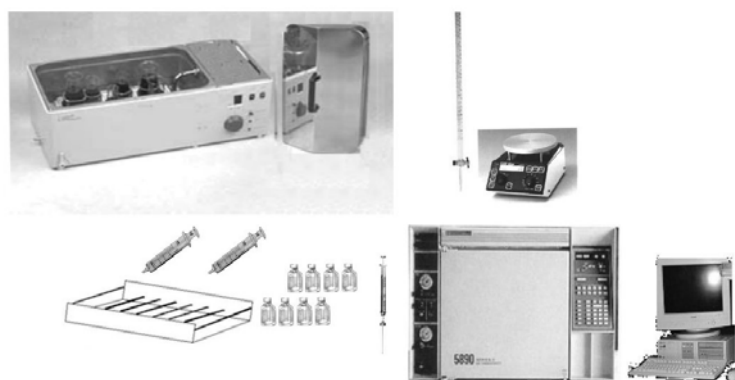
FigureV.1 Experimental set up

V.4. FILM CHARACTERIZATION

Film samples were characterised by using Scanning Electron Microscope (SEM), X-Ray diffractometer, Differential Scaning Calorimetry (DSC), Thermo Gravimetric Analysis (TGA), Fourier Transform Infrared (FTIR) Spectroscopy.

V.4.1 EQUIPMENT

Hitachi 270-30 I.R. Spectrophotometer, Philips PW 1840 X-Ray Diffractometer using nickel filtered CuK_α radiation, SEM (JSM.6400), DSC

(General V4.1C DuPont 2000) were used for the catalytic film characterization studies.

V.4.2 FILM CHARACTERIZATION METHODS

V.4.2.1 <u>Infrared Spectroscopy</u>

In this study, FTIR was applied to pure PSF film and also PMo loaded PSF films between 400-4000 cm^{-1} wavelength and percent transmittence was examined. Their comparison was made to see the PMo crystalline absorption bands in the PMo-PSF films.

V.4.2.2 <u>X-RAY Diffraction Analysis</u>

X-ray diffraction was applied to pure PSF and PMo loaded PSF films in order to see the PSF polymer blendıng effect on the PMo crystal. Film samples were scanned between 5 and 60 2θ (degree) with 5 deg/ min scan speed. The pure PSF and PMo loaded PSF films intensities were compared.

V.4.2.3 <u>Scanning Electron Microscopy</u>

SEM analysis were applied to films having different thickness and loading in order to see the PMo distribution thoughout the film (in the bulk and surface of them), to analyse effect of thickness in catalytic films, or effect of catalyst loading whether make any difference in image and morphologies of the films or not. In the preparation stage, films were broken with liquid nitrogen and adhered on the disks, which are the SEM apparatus. Final preparation step is the coating the film particles with gold. SEM results should support X-ray and FTIR results also i.e., if characteristic Keggin structure of PMo peaks are observed in X-ray and FTIR, there should be image of PMo Keggin crystals in SEM image.

V.4.2.4 <u>Differential Scanning Calorimetry</u>

DSC was applied to PSF and PMo loaded psf films. Samples were first heated from 25 to 230°C at a heating rate of 10°C/min and then cooled to 25°C by liquid nitrogen (75 cc/min). Most of the moisture (solvent) in the film was removed during the first scan, the glass transition temperature (T_g) was measured at the second scan. Their glass transition temperatures were compared to see whether loading effected the polymers physical or chemical properties or not.

V.4.2.5 <u>Thermogravimetric Analyis</u>

TGA analysis was applied to pellet PSF, pure PSF film and one of the prepared catalytic films in order to see the amount of residual solvent in the film. Film samples were heated from 25°C to 200°C at a 10°C/min heating rate and weight loss was followed.

V.5 DEACTIVATION TESTS

After used in esterification reaction, 10wt% pmo loaded and 15wt% pmo loaded psf catalytic film pieces were investigated under deactivation conditions (50°C & 1atm, 1:1 etOH:LA mole ratio). After each sequential run lasting 13.5 hours, catalytic film particles were washed with distilled water and dried at 80 °C & 0.8 bar vacuum conditions. In order to see the reusability of prepared catalytic films, dried film particles were used in ethyl lactate reactions several times.

CHAPTER VI

RESULTS AND DISCUSSIONS

In this study, application of PMo loaded PSF films to the ethyllactate esterification reaction as heterogeneous acid catalysts was investigated. Film characterization methods including DSC, TGA, X-ray diffraction, FTIR and SEM analysis were applied to the prepared catalytic films and possible characteristics were discussed.

Taking advantage of HPAs high solubility in organic solvents, both heteropoly acid (molybdophosphoric acid, PMo) and polymer (polysulfone, PSF) was dissolved in a common organic solvent (dimethylformamide, DMF). The solution was used to prepare a membrane-like catalytic films by a film preparation method described earlier (Chapter V, Section V.1.). Films were cut into $4mm^2$ pieces in order to achieve a better contact with liquid phase and obtain enhanced mixing conditions and used in the batch type reactor. The effects of catalyst loading, film thickness, film surface area were investigated. Prepared catalytic films were analysed by DSC, TGA, FTIR, X-ray and SEM in order to determine optimum design parameters for a prepared film. The film samples were tested in ethlyllactate conversion reaction. Reaction mixture was analysed by GC to determine the liquid product composition. The samples were succesively tested in ethyllactate esterification reaction for several times to see the reusability or the deactivation properties of the prepared catalytic films.

VI.1 CHARACTERIZATION STUDIES

In order to determine the kinetic and mass transfer effects of catalytic films in ethyllactate esterification reaction, a set of films was prepared as described in the experimental part. To analyse their physical properties, DSC (differential scanning calorimetry), TGA (thermogravimetric analyser), X-Ray Diffraction method, SEM (scanning electron microscopy) and IR-spectrophotometer characterization techniques were applied to prepared films. Amount of residual solvent was confirmed by thermal analysis. The primary structure of PMo in PMo-PSF film catalysts was also confirmed by observing four characteristic bands ranging from 700 to 1200 cm^{-1} [48]. SEM images of PMo-PSF film catalysts revealed the morphologies of them.

VI.1.1 RESULTS of DSC ANALYSIS

DSC measurements were carried out in order to measure the glass transition temperatures of the prepared composite film catalysts and to confirm the blending patterns of them. Table VI.1 shows the glass transition temperatures of the composite films and their corresponding PMo-free polymer film. After most of the moisture (solvent) in the film was removed during the first scan from room temperature to 300°C , the glass transition temperature (T_g) was measured at the second scan. Original DSC thermograms of each film are given in Appendix-D.

TableVI.1 T_g values of prepared membrane-like films

T_g (ºC) values of	1st RUN	2nd RUN
pellet PSF	-	192
only PSF (and literature value [52])	142	187 (185)
5wt% PMO loaded PSF	142	187
10wt% PMO loaded PSF	145	189
15wt% PMO loaded PSF	143	182

From DSC analysis it is evidenced that some part of the solvent, DMF, is absorbed in the bulk side of the prepared film.

There were no important difference between the T_g of pure PSF film and PMo loaded PSF films. This means that there is no significant chemical interaction between the PSF and the acid sides of the PMo catalyst, i.e., PMo only served as a filler for PSF in the PMo-PSF composite film catalysts.

VI.1.2 TGA RESULTS

TGA analysis were done in order to measure the amount of solvent trapped in the prepared PMo-PSF films. Results in TableVI.2 show that the pellet PSF has trace amount of volatile compound (moisture) inside of it (0.07wt%) as also observed from the DSC results. Pure PSF film and 5,10,15 wt% PMo loaded PSF films all have small amounts of volatile impurity. Catalyst loading affected the absorbed solvent amount in polymer matrix, but this is not the function of catalyst amount. Certain weight loss occuring around 150 °C, (boiling point of DMF is 153°C) was concluded to be the DMF loss. Around 2.375wt% of the sample film were vaporized as DMF. Original TGA thermograms of each film are given in appendix-D.

Table VI.2 TGA results of prepared films

weight loss at 150 C (wt%) for	
pellet psf	-
pure psf film	2.3
5wt% pmo loaded psf film	3.1
10wt% pmo loaded psf film	3.5
15wt% pmo loaded psf film	3.2

VI.1.3 XRD RESULTS

In order to indicate whether HPA loading results in structural changes in polymer, x-ray powder diffraction patterns for the prepared films and the powder PMo catalyst was scanned. In x-ray diffraction patterns of PMo, peaks belong to typical Keggin structures were apparent. On the

other hand, pure polysulfone polymer were also scanned between $2\theta =$ 5-60 angle and appearent amorphous phase of polymer was observed.

As it can be seen from the figures (figureVI.1 to figureVI.9), peaks belonging to powder PMo catalyst are not observed over the PMo-PSF film, indicating the finely dispersed amorphous film structure. However, above the 10wt% catalyst loading and below 50μm thickness, some peaks representing the original Keggin structure which indicates crystallites were observed. Above 78μm thickness at 10wt% loading levels, Keggin peaks were not observable because of bulk polymer. X-ray result of 300μm-thick prepared film and that of the pure PSF film were almost the same.
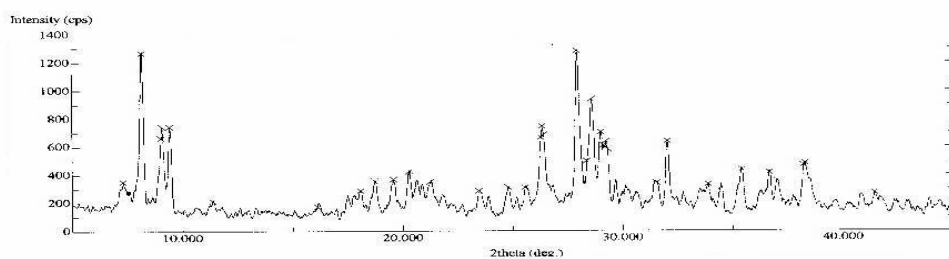
FigureVI.1 x-ray result for pure powder PMo
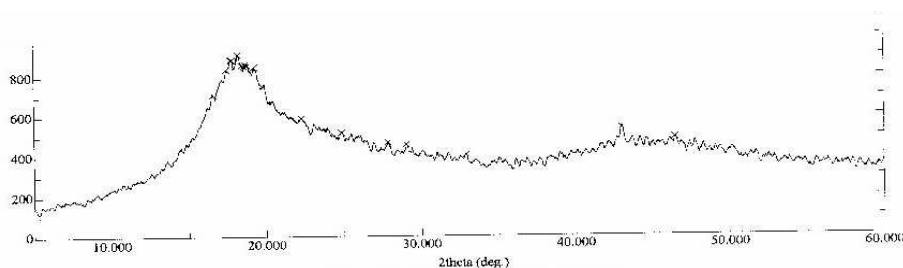
FigureVI.2 x-ray result for pure psf polymer

56
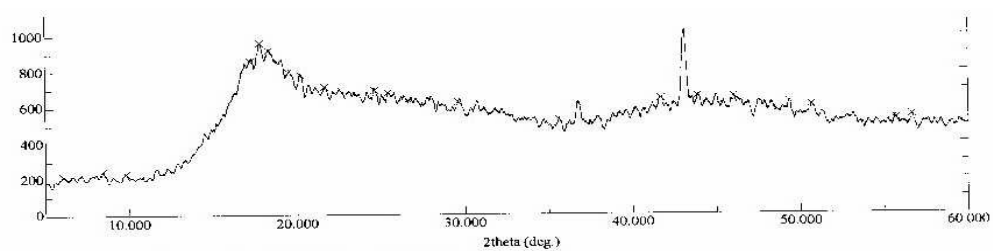
FigureVI.3 x-ray result for 5wt% pmo loaded 78μm-psf catalytic film
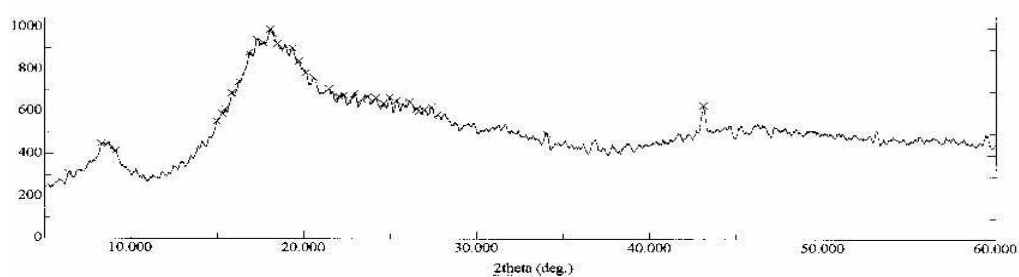
FigureVI.4 x-ray result for 10wt% pmo loaded 78μm- thick psf catalytic film
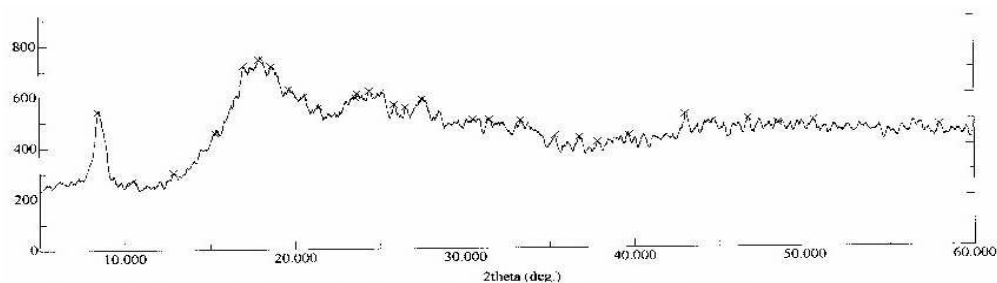
FigureVI.5 x-ray result for 15wt% pmo loaded 78 μm-psf catalytic film
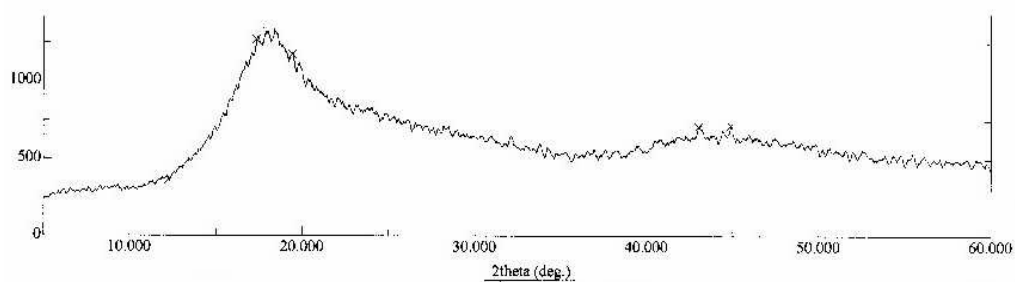
FigureVI.6 x-ray result for 10wt% pmo loaded 300μm-psf catalytic film
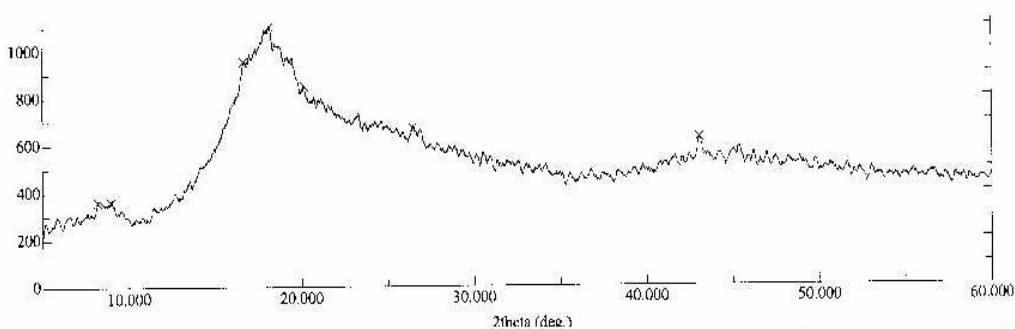
FigureVI.7 x-ray result for 10wt% pmo loaded 150μm-psf catalytic film
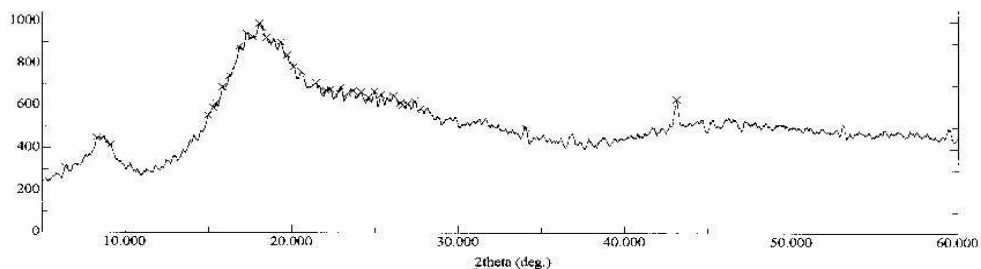
FigureVI.8 x-ray result for 10wt% pmo loaded 78μm- psf catalytic film
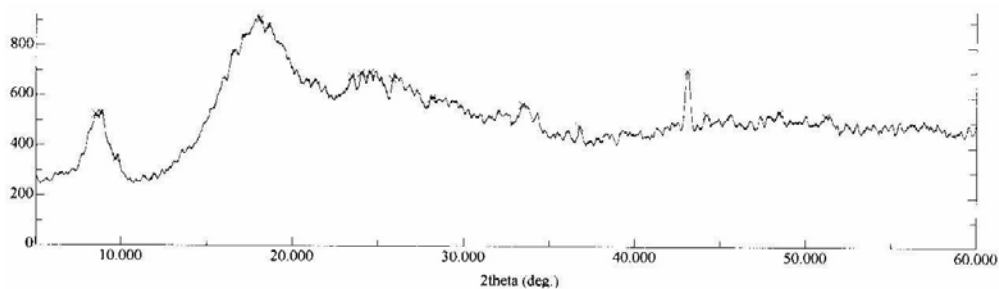
FigureVI.9 x-ray result for 10wt% pmo loaded 47μm-psf catalytic film

VI.1.4 SEM RESULTS

In order to see the catalyst distribution in the polymer network structure and effect of catalyst loading on the morphology of the films, SEM (scanning electron microscope) was used. From the SEM analysis particulate structure of the PMo catalyst was observed and there is no catalyst agglomeration in the polymer network. However, along the thickness, catalyst particles were not homogeneously dispersed.

It was observed that, in 47-μm thick-film (figVI.12 and fig.VI.13) , catalyst particles tears the surface of the film and the exposed catalyst particles can be seen over the surface by means of SEM. Also it can be seen from the figures that with decreasing film thickness micro-voids occurred. Figure VI.10 and Figure VI.12 reveals that with decreasing film thickness, catalyst's particle size increases. with decreasing film thickness, DMF vaporisation rate increase, as a result catalyst particles stick together.

It may also be referred from the SEM images that as the catalyst weight percent increased (Fig.VI.10 and Fig.VI.11), cleavages are increased in the polymer film. This is due to the fact that the stress points of the polymer network increased when catalyst particles are added. The remaining SEM images are given in Appendix-D.
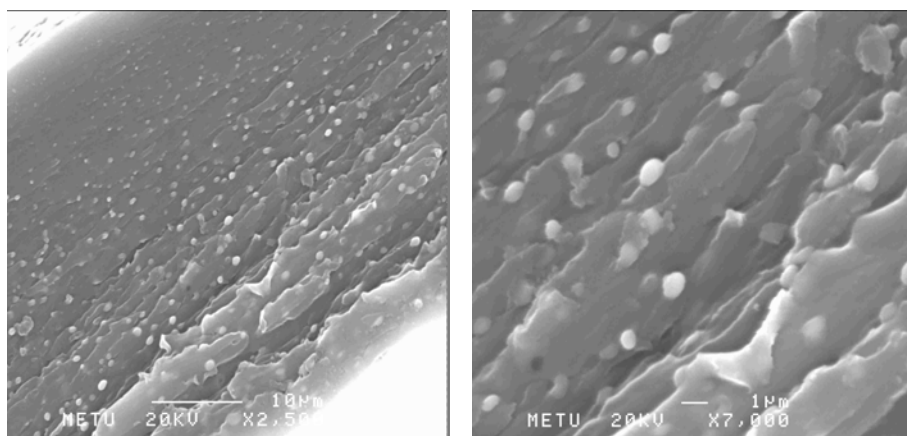
FigureVI.10 Cross-sectional view of 10wt% PMo loaded 78μm-PSF film
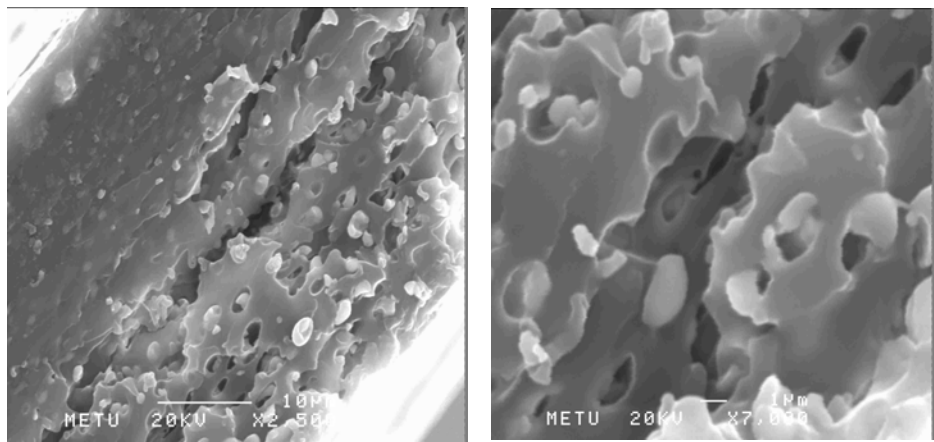
FigureVI.11 Cross-sectional view of 15wt% PMo loaded 78μm-PSF film
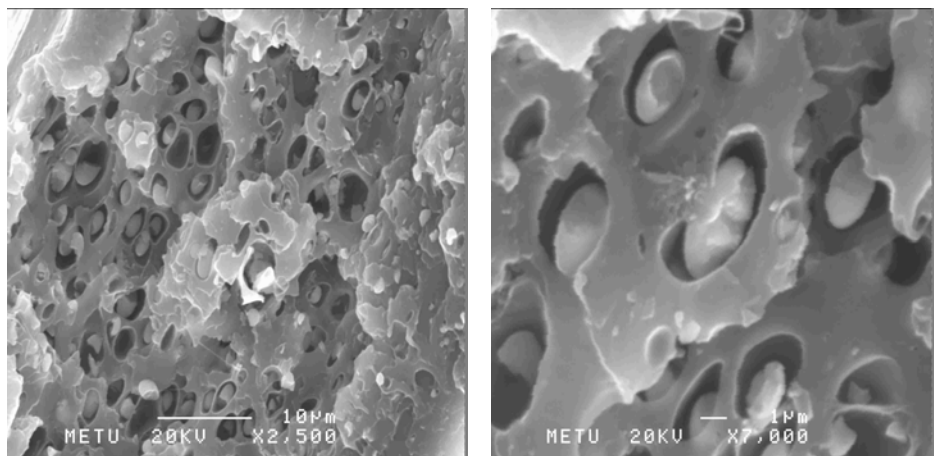
FigureVI.12 Cross-sectional view of 10wt% PMo loaded 47μm-PSF film
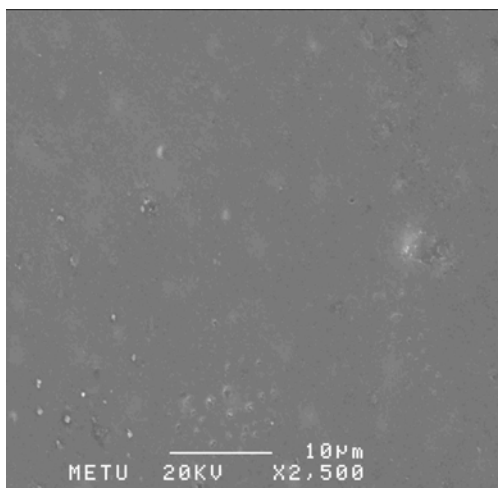
FigureVI.13 Top view of 10wt% PMo loaded 47μm-PSF film

VI.1.5 FTIR RESULTS

IR spectra of the 10wt% Pmo loaded 78μm-thick PSF film was studied. Figure.VI.14 and 15 show the IR spectra of PSF and PMo-PSF film respectively. The primary (Keggin) structure of PMo can be identified by the four characteristic bands ranging from 700-1200 cm^{-1}. Bands at 788 and 863 cm^{-1}, which represent Mo-O-Mo bonding. Bands at 965 and 1064 cm^{-1} signify Mo=O and P-O bonds, respectively [48]. As shown in Figure.15, the four characteristic bands of PMo are shown in PMo-PSF film. IR bonds other than those due to PMo in the PMo-PSF film are due to the PSF film. This fact indicates that the primary structure of the PMo is not altered by the PSF.
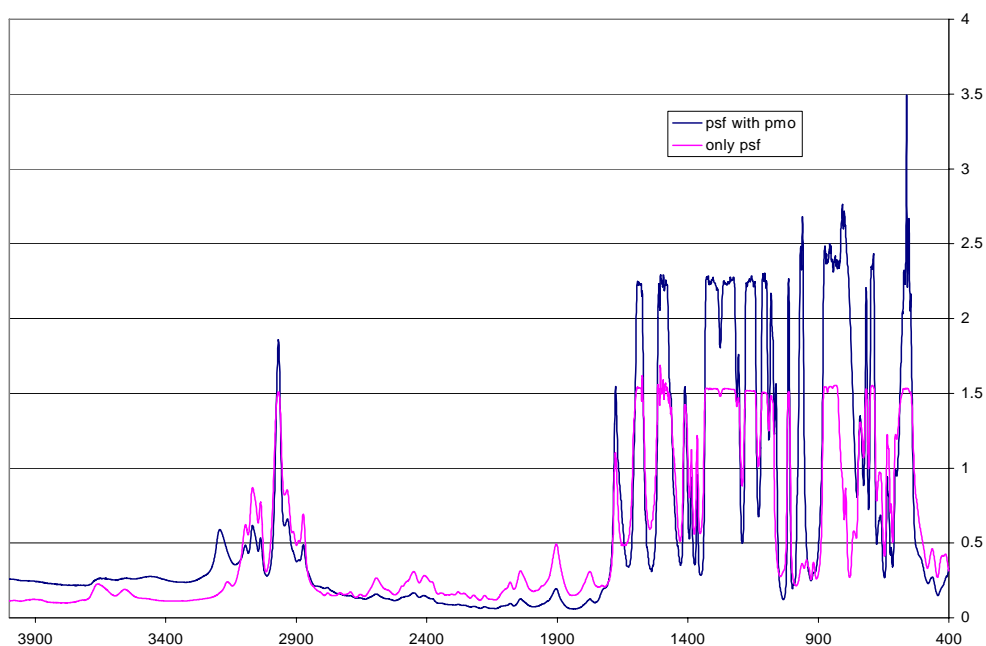
FigureVI.14 % transmittance vs cm^{-1} IR-spectra of pure psf film and 10WT5 pmo loaded 78μm-thick pmo-psf film
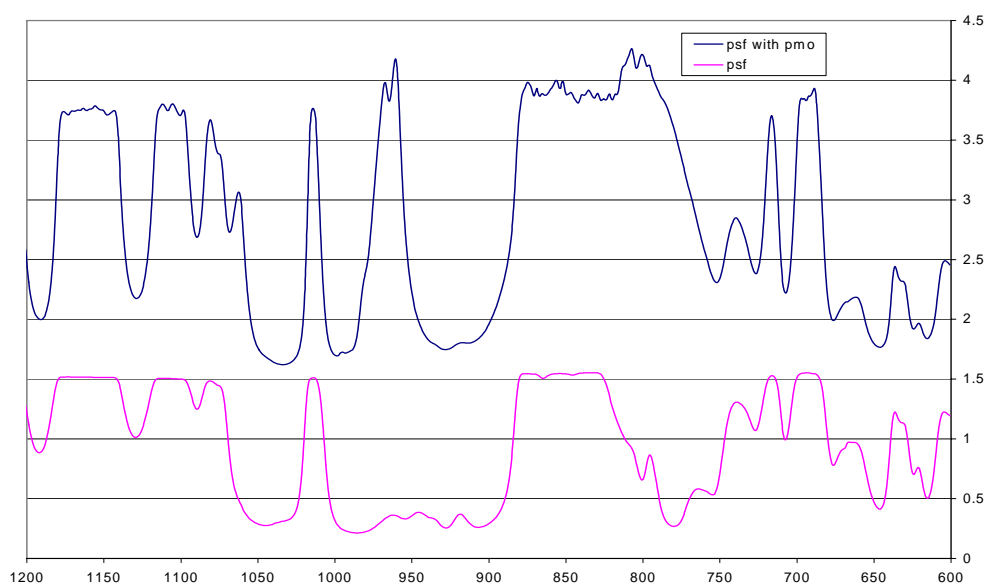
FigureVI.15 % transmittance vs cm^{-1} IR-spectra of pure psf film and 10wt% pmo loaded 78μm-psf film

VI.2. EXPERIMENTAL RESULTS

In experimental analysis, prepared catalytic membranes were tested in esterification reaction at 50°C and 1:1 etOH:LA mole ratio reaction medium, and liquid product compositions were determined by titration and gas chromatograph analysis.

VI.2.1 SYSTEMATIC APPROACH TO VARIABLE PARAMETERS

Kinetic and mass transfer parameters were tested for catalytic films in ethanol lactic acid esterification reaction as film surface area, film thickness and catalyst loading at 50°C, 1 atm and 1:1 ethyl alcohol to lactic acid mole ratio conditions. In this section, how can these parameters effect the rate of the esterification reaction is explained.

In order to show these kinetic and mass transfer parameters effect on ethyllactate reaction, rate equation based on weight of catalyst may be utilized;

Esterification reaction of lactic acid with ethyl alcohol was carried out in a batch reactor, then the general form of the mole balance is

$$dN_J / dt = \int_V r_J \, dV$$

With the perfect mixing assumption, the variations in the rate of reaction through out the reactor volume was neglected. Then, the balance equation becomes

$$dN_J / dt = rj.V$$

with the constant-volume reactor assumption, reactor mole balance is expressed as

$$(1 / V).(dN_J / dt) = [d(N_j / V) / dt] = dC_j / dt = r_j$$

So, for the proposed esterification reactions, which are both reversible, to see the catalytic activity on the reaction rate, simple procedure was followed (for detailed rate calculation, see Engin Aytürk Ms Thesis,2001 [65])

$$r_{LA} = - (dc_{LA} / dt).(\text{liquid volume/amount of catalyst})$$

$$r_{LA} = - (\Delta C_i / \Delta t_i). (\text{liquid volume/amount of catalyst})$$

$$r_{LA} = - [(C_2-C_1) / (t_2-t_1)] \mid$$
$$t_1+ (t_2-t_1)/2$$

For a reversible reaction
$$A + B \Leftrightarrow C + D$$
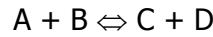
Rate equation for reactant A can be also written as

$$-r'_A= (k'_{hom}+ k'_{cat}.\beta). C_A. C_B - (k''_{hom}+ k''_{cat}.\beta). C_C. C_D$$

where

r'_A: reaction rate based on weight of catalyst (mol reacted/g cat.min)

k_{hom} : homogeneous liquid phase reaction rate constant (lt/mol.min)

k_{cat} : catalytic reaction rate constant (lt^2/g cat.mol.min)

β: catalyst concentration (gram catalyst / lt solution)

C_A: concentration of species A (moles/lt)

t: time (s)

In order to analyse the effect of change in catalyst loading in 78μm thick films, 0wt% (unloaded), 5, 10, 15 wt% PMo loaded PSF films were tested at 50°C & 1 atm reaction conditions and 1:1 etOH:LA mole ratio. Keeping their thickness (78μm) and used film area for the reaction (18cm^2) as constant (as mass transfer parameters) is essential to see the loading effect on the reaction rate, where mass transfer parameters

are kept constant. These four films prepared under the same conditions (same glass petri and oven were used and films were prepared in the same drying and annealing conditions) to eliminate their effects. Weighted amount of samples were withdrawn from the reaction medium at spesific time intervals. Product composition and reaction rate calculations are given in in appendix-A and B respectively.

To see the effect of catalytic film external surface area and film thickness on ethyllactate reaction, schematic representation in figureVI.16 can be examined.

As can be seen from the Figure VI.16, with increasing catalyst surface area, liquid reaction medium-film interfacial area/ volume of the reactor ratio increased. This results in more reactant to diffuse through the film and reach catalysts active sites, i.e., increase in the esterification reaction product.
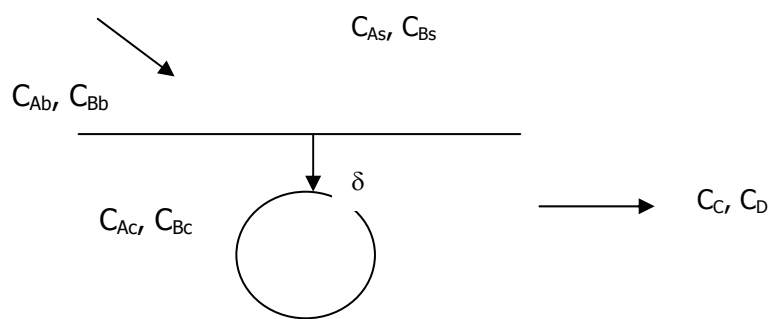
Figure VI.16 Schematic representation of catalytic film

δ represents the distance between external surface of the film and catalyst surface in the film. δ is important in diffusional point of view. As the δ increases, mass transfer resistance increases and the reactants are prevented to reach catalyst active site.

In order to analyse these parameters effect, three set of experiment were performed and evaluated. Calculation methods for conversion and rate are presented in appendix-A and B.

VI.2.2. EFFECT OF CATALYST LOADING

To compare different wt% PMo loaded PSF films effects on the reaction, lactic acid conversion with respect to time were analysed. When the liquid product compositions were calculated, it was seen that all the catalytic films result in higher reaction conversion profile than that of pure PSF polymer film. When figure VI.17 is examined, it is realised that with increasing catalyst loading ethyllactate conversion also increased. Up to 400th min, conversion trend was almost the same for all catalytic films in spite of increasing catalyst loading. Because of this trend, it can be concluded that up to the vicinity of 400th min, reaction is very fast because of the high concentration of the reactants (forward reaction is faster than the backward reaction) and it was infered that catalyst loading has no importance in this region. Kinetically or equilibrium controlled region were observed after the vicinity of 400th min, where the reaction was slow and catalyst loading was effective in this area. After 400th minute, in spite of the fact that the reactants concentration decreased in the reaction volume, lactic acid conversion continued to increase. This increase was due to the increase in catalyst concentration (β) value (in rate equation given in previous section). Esterification reactions suffer from low conversions because of their equilibrium-limited nature. To overcome this difficulty, the equilibrium is displaced by the removal of one of the reaction products by pervaporation or azeotropic distillation for example, to increase the product yield and conversion. In ethyllactate esterification reaction, water as one of the products, can be removed by the membrane separation method, and equilibrium limitation can be overcomed.

To compare the reaction rates, simply one LA conversion data is chosen, such as point 0.3 LA wt%. It is clearly seen that reaction with

catalytic film having highest catalyst loading (15wt%) is reached 0.3 conversion value first, and with decreasing catalyst loading level, time period to reach 0.3wt% LA conversion value for reaction increase. This conclusion can be seen clearly from table VI.3.

To reach 0.3 LA wt% conversion;

Table VI.3. Time versus catalyst loading comparison table to reach 0.3 LA conversion point

cat.load. Wt%	time(min)	Rate (-r_A)
0	800	0.004
5	570	0.012
10	400	0.010
15	330	0.090

Also it can be seen in the LA wt% conversion vs time graph, increase in the lactic acid conversion at any time after the 400th min is clear between the loading levels (i.e., with increasing loading, LA conversion increases linearly). This is resulted form the fact that ethyllactate reaction was kinetically controlled and mass transfer almost has no effect with respect to variable catalyst loading set.

Ethyllactate reaction was proceeded not only on the surface of the heteropoly acid catalysts but also on the bulk phase of them because of their pseudo-liquid behaviour. Owing to the flexible nature of the acid forms and group A salts, polar substances like alcohol and water, can be absorbed into the bulk phase of the heteropoly acids. And heteropoly acids which have absorbed a significant amount of polar molecules resemble in a sense and are in a state between solid and a liquid. Increasing catalyst loading in each experimental run, keeping the other parameters effecting the mass transfer constant, results in the more volume for the reaction to proceed because of the pseudo-liquid behaviour of the heteropoly acid catalyst.

Resulting high activities were also explained by remaining heteropoly acids molecular structure in the polymer network as the same as molecular structure in the solution. From characterization studies, it was prooved that the heteropoly acids kept their primary Keggin structure in the polymer network. Heteropoly acids have extremely high proton mobility and protonate lactic acids carbonyl group. Protonation of the carbonyl group of the lactic acid increase lactic acids reactivity toward ethylalcohol, as a nucleophile. Therefore, heteropoly acids high proton mobility results in increase in the esterification reaction rate.
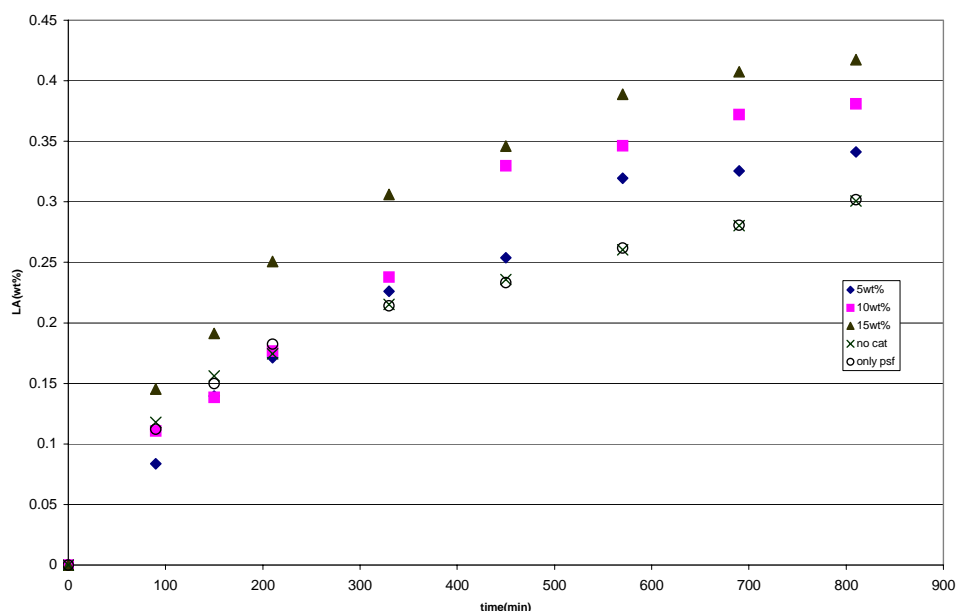
FigureVI.**17** LA conversion graph for esterification reaction at 50°C & 1:1 etOH:LA ratio for variable loading

VI.2.3 EFFECT OF EXTERNAL SURFACE AREA

In this analysis it is claimed that film surface area is directly related with the catalyst surface area, in other words, increasing film surface area (keeping film thickness constant), including the same amount of solid catalyst, result in increase in the esterification reaction rate. To check this is correct or not, two set of surface area experiments were done.

i. effect of surface area on the reaction rate keeping amount of catalyst constant

Three different films having 12,18,36 cm^2 areas were analysed in esterification reaction medium, and compared with pure PSF film results to check catalytic film performance. Catalyst amount was kept constant for all three piece of films having different areas but the catalyst/polymer weight percentage was not constant, i.e., with increasing catalytic film area, polymer amount increased.
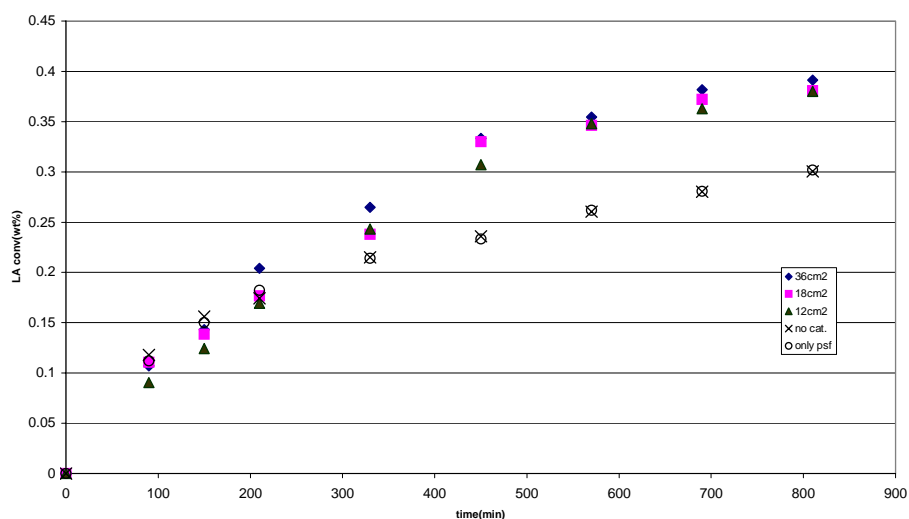
FigureVI.18 LA conversion graphs for esterification reaction at 50°C & 1:1 etOH:LA ratio with constant thickness (78 μm), constant loading (10wt%), variable area

LA conversion versus time graph were plotted (figureVI.18) and it is obvious that 12,18 and 36 cm^2 films resulted almost same conversion profile with each other. On the other hand, their catalytic effect were noticable from the graphs. Therefore, knowing that the catalyst amount in each film was the same, it can be concluded that external mass transfer rate is high enough (figureVI.19) and does not bring any limitation to the reaction rate for the experimental conditions

applied.(e.g. mixing rate) (reaction is much more slower than the liquid phase mass transfer)
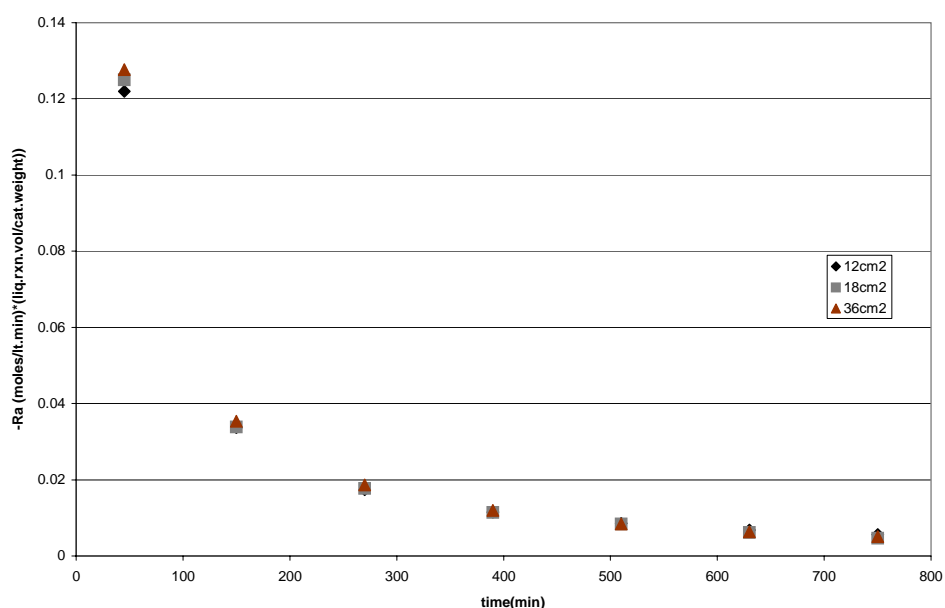
Figure VI.19 Rate of reaction comparison graphs for variable area set

ii.   effect of surface area on the reaction rate keeping weight percent of catalyst constant

In this experimental set, 10wt% PMo loaded 78 μm PSF film was prepared according to the preparation method described in experimental section, then 12,18, 36 and 72 cm^2 pieces were cut, tested in ethyllactate reaction at 50°C & 1 atm conditions and 1:1 etOH:LA mole ratio. Samples were taken from liquid reaction mixture at spesific time intervals and product distribution were analysed by titration and GC analysis methods.

Aim was to see whether reaction rate increased with increasing film area or not, and to examine polymer-catalyst interaction keeping catalyst/polymer weight ratio constant. For each area series, catalyst amount (in gram) per polymer amount (in gram) included in reaction were kept constant with different films but catalyst amount included liquid esterification reaction in each film was not constant.

İt was expected that with increasing area reaction rate also increase because catalyst amount included in reaction increase with increasing film area. However, polymer amount also increase in film having greater area. To check whether catalysts active sites were occupied by the polymer network or not and to see reactants can or can not reach heteropoly acids active sites, this series of experiments were done.

To compare films effect on reaction results, LA conversion versus time graph was plotted again (figureVI.20). And it was observed that with increasing film area LA conversion also increased at any time. This means that reaction is kinetically controlled and there is no external mass transfer limitation. Mass transfer rate is greater than the reaction rate, i.e., it does not matter whether polymer amount increased or decreased (for same thickness) in catalytic film. Because catalyst amount (in gr) in film was increased with increasing film area, LA conversion also increased. Reaction rate tendency was compared in another graph (figureVI.21) and it was proved that the reaction was kinetically controlled and mass transfer resistance has not importance. Difference in reaction rate values are much greater at the beginning of the reaction. While equilibrium is approached, reaction rate values become closer but still film having highest area results in the highest reaction rate.
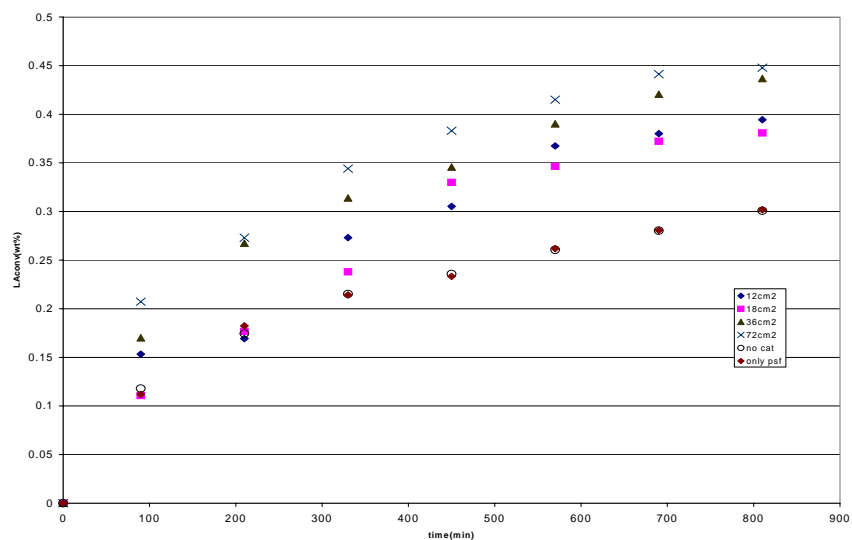
FigureVI.20 LA conversion graphs for esterification reaction at 50C & 1:1 etOH :LA mole ratio with different area series
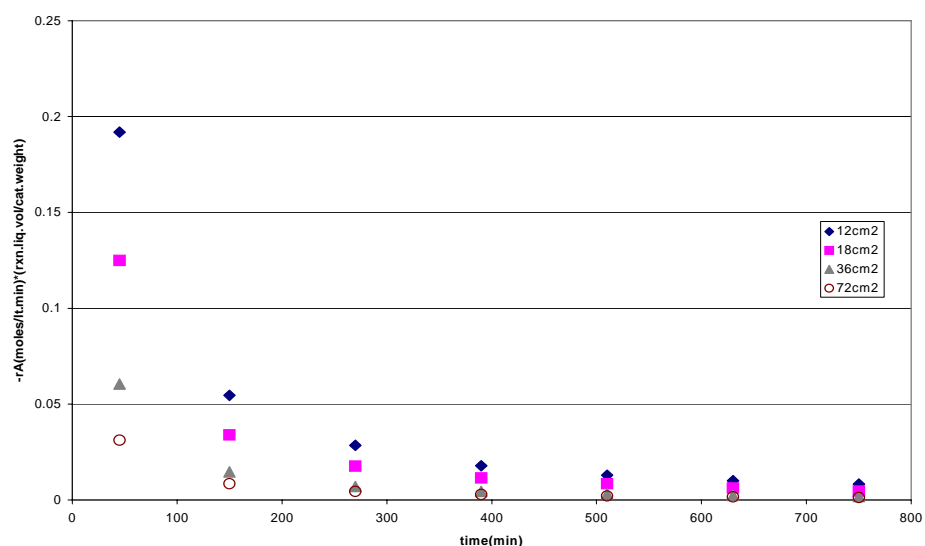
Figure VI.21 Rate of reaction comparison for esterification reaction at 50C & 1:1 etOH :LA mole ratio with different area series

VI.2.4. EFFECT OF FILM THICKNESS

Importance of the catalytic film thickness on the reaction rate was discussed at the begining of the chapter. In order to see whether reaction rate is increased with the decreasing film thickness or not, four

different films having four different thickness and same loading (10wt% in psf film), same area (18cm^2) were prepared and tested in esterification reaction medium and the liquid product concentrations were analysed using titration and gc analysis method.

LA conversion versus time graph was prepared to compare effect of films having different thickness on the liquid product compositions (figureVI.22). For 45 and 78 μm thickness series, internal mass transfer is faster than the reaction where slow reaction conditions exists (reaction is slow between 300th and 800th minutes), i.e., the reaction was controlled by equilibrium limitations. It was observed from the graph that increase in thickness resulted in the lower conversion in LA and this means that internal mass transfer resistance was gained importance as the film thickness increased. Following FigureVI.22, it was observed that between 45 and 150 μm thickness series, LA conversion decrease with increasing thickness almost linearly. After 150 μm, decreasing rate is definitely smaller than that of before 150 μm. and this means that there is a thickness interval in which the mass transfer limitation is important and out of this interval, mass transfer is not changed. In this analysis, the upper limit of this interval is assumed to be in between 150 and 300 μm. Above 300μm, catalyst particles can not be reached by the reactants and film have no longer catalytic effect on the reaction. I.e., the film having thickness greater than 300 μm has much larger mass transfer resistance than its reaction resistance.

Reaction rate tendencies of these catalytic films were also examined (figureVI.23), and it was clearly seen that with decreasing film thickness reaction rate increases. This result arises from the fact that with decreasing film thickness, catalyst availability increases. I.e., reactant can pass through the film more easily (mass transfer resistance decreases) and reach the catalysts active sites. As the reaction proceeds, the difference in reaction rates of films having different thicknesses decrease.
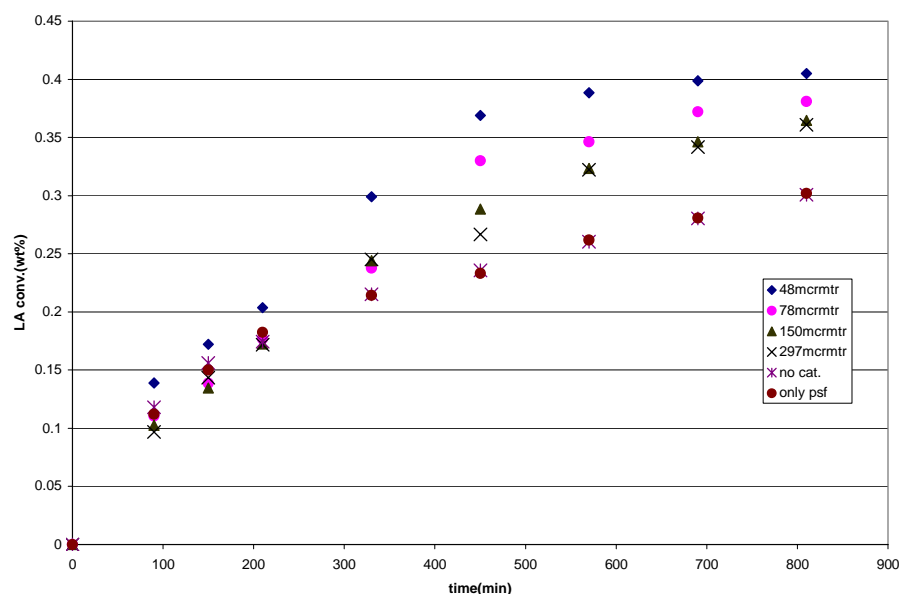
FigureVI.22 LA conversion graphs for esterification reaction at 50°C & 1:1 etOH:LA ratio with constant area (18cm^2), constant loading (10wt%),variable thickness
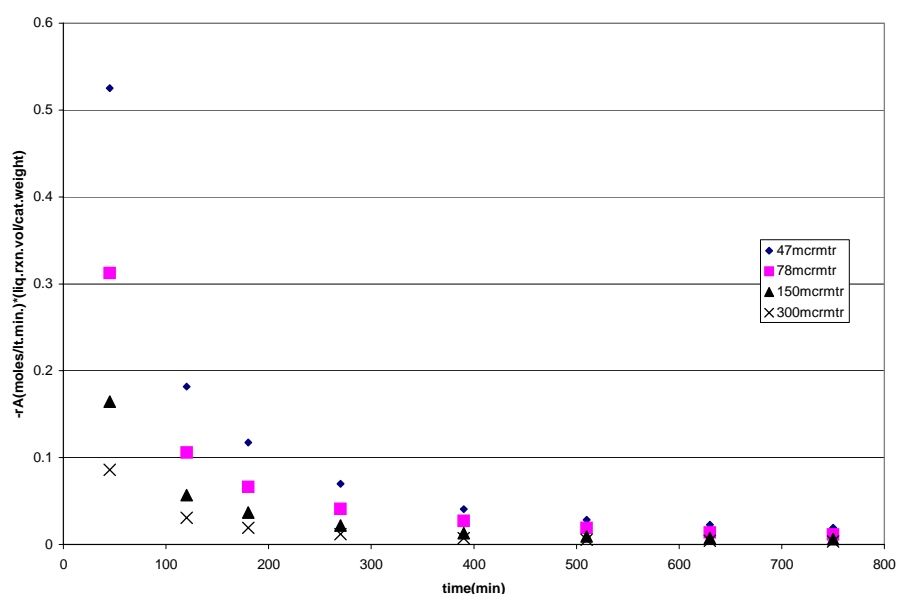
FigureVI.23 rate of reaction comparison graphs for variable thickness set

When "catalyst loading" (sec.VI.2.2) and "external surface area" (sec.VI.2.3.ii) effects were compared following figureVI.17 and figure VI.20, it was seen that LA conversion trends were almost the same. The main difference between the "catalyst loading" and "external surface area" analysis was their preparation method. When tableV.2

and tableV.3 are examined, it is seen that in both analysis, catalyst amount were increased, film thickness were kept constant. Surface area of the prepared films were increased with increasing polymer amount in "effect of external surface area" analysis, on the other hand, surface area of the prepared films were kept constant in "effect of catalyst loading" analysis. In both figureVI.17 and figureVI.20, it was seen that with increasing catalyst amount in films, LA conversion was increased.

When the thickness of the film was decreased up to 47μm, microvoids occurred. These voids are clearly seen in SEM images of the prepared films (appendix-D). Occurance of these voids also increases the internal mass transfer rate

In general, when these four set of analysis were compared, some general trends were obtained;

Up to 400th min, conversion trend was almost the same for all catalytic films. Up to the vicinity of 400th min, reaction is very fast because of the high concentration of the reactants and it was inferred that catalytic effect has no importance in this region. Kinetically or equilibrium controlled region were observed after the vicinity of 400th min, where the reaction was slow and catalytic effect can be followed in this area. Also mass transfer has no effect on these set of reaction experiments because the reactants were well-mixed.

VI.2.5. DEACTIVATION TESTS

In deactivation tests, 10 and 15wt% PMo loaded PSF films were inverstigated under deactivation conditions at 50°C & 1 atm and 1:1 etOH:LA mole ratio for 6 and 4 sequential run lasting 13.5 hours each respectively in order to understand the stability of the produced catalytic films. After each run, film particles were removed from the reaction medium, washed and dried. Observed activities for 6 run of the 10wt% loaded film catalysts were still higher than catalyic activity

of the unloaded film (figureVI.24). Until the 5th run there was no distinct decrease in conversion. In 6th run, conversion decreased but was still higher than the unloaded film. For 15wt% PMo loaded PSF film, distinct conversion decrease was seen in 4th run but conversion was still higher than that of unloaded PSF film (figureVI.25). This means that in 15wt% PMo loaded PSF film, catalysts in the surface of the film dissolved in reaction medium more easily than 10wt% PMo loaded PSF film.
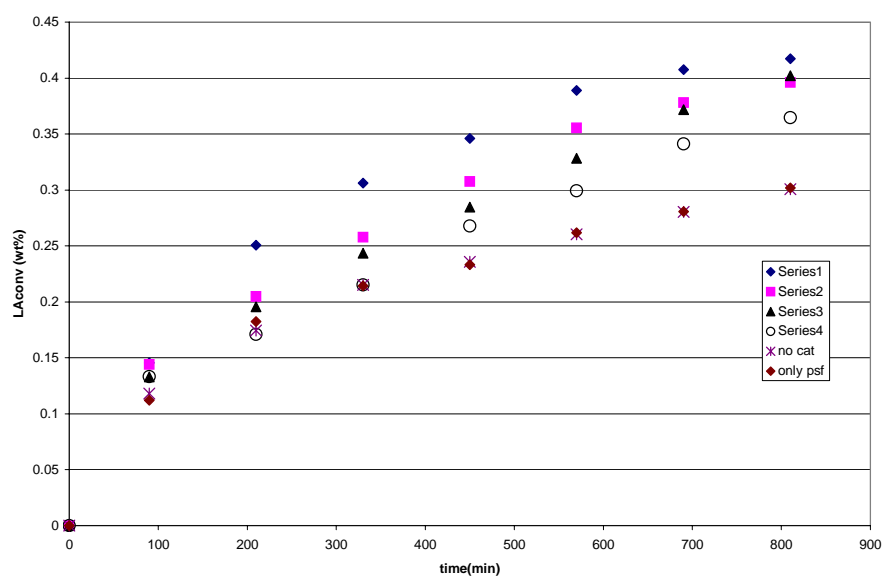
FigureVI.24 LA conversion graphs for deactivation series of esterification reaction at 50C & 1:1 etOH:LA mole ratio with 10wt% PMo loaded PSF film
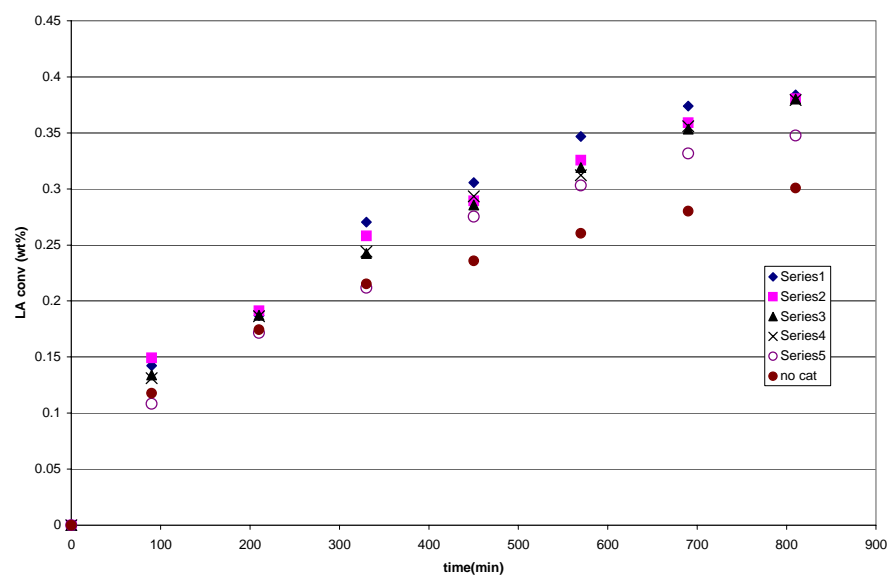
FigureVI.25 LA conversion graph for deactivation series for 15wt% PMo loaded PSF film

CHAPTER VII

CONCLUSIONS

In the present study, catalytic PMo loaded PSF films were prepared and film characterization methods were applied to them. The catalytic performance of the films was tested in ethyllacte esterification reaction at spesific reaction conditions. The following conclusions were withdrawn;

1. PMo loaded PSF film membranes exhibited catalytic activity while unloaded form of the PSF films does not alter the self catalysed homogeneous esterification rate. Rate of reaction was increased with higher loadings of PMo.

2. By DSC analysis T_g of pure PSF and PMo loaded PSF films were compared. T_g values were all within the range of 190°C, which is the glass transition temperature of the pure PSF. This result reveals that PMo loading does not alter the chemical structure of PSF films. Further characterization studies with TGA analysis showed that trace amount of solvent, DMF, was absorbed in the bulk of the PSF matrix.

3. The X-ray analysis results showed that the original crystalline structure of the PMo can not be retained after drop casting of PMo with DMF solvent which indicates finely dispersed amorphous structure. However, above the 10wt% catalyst loading and below 50μm thickness, the original Keggin structure in the form of small crystallites was observed.

4. FTIR analysis indicated that the primary structure of the PMo is not altered by the PSF film and DMF solvent.

5. From the SEM analysis it was observed that there is no catalyst agglomeration in the film network. However, the catalyst particles were not homogeneously dispersed along the thickness. This is due to the slow evaporation rate of the DMF solvent and sedimentation of the crystallites while casting the films.

6. As the catalyst weight percent increased, cleavages are increased in the polymer film as can be seen from the SEM images. This is due to the fact that the stress points of the polymer network increased when catalyst particles are added.

7. In variable area sets (i), it is obvious that 12,18 and 36 cm^2 films resulted almost the same conversion profile with each other. On the other hand, their catalytic effect were noticable from the graphs. Therefore, knowing that the catalyst amount in each activity test was the same, it can be concluded that external mass transfer rate is high enough (figureVI.19) and does not contribute any limitation to the reaction rate for the experimental conditions applied

8. In variable area series (ii), it was observed that with increasing film area LA conversion also increased at any time. This means that reaction is kinetically controlled and there is no external mass transfer limitation. Mass transfer rate is greater than the reaction rate, i.e., it does not matter whether polymer amount increased or decreased (for same thickness) in catalytic film.

9. In variable thickness series it was observed that increase in thickness resulted in the lower conversion in LA and internal mass transfer resistance has gain importance here. After 150 μm, decrease in rate is definitely smaller than that of before 150 μm. This means that there is an interval in which the mass transfer limitation is important.

10. As the thickness of the film decreases, the rate of evaporation of the DMF solvent increases. As a result, the catalyst particles were more homogeneously dispersed as the film thickness decreased. However, SEM results showed that, in 47 μm thick-film, catalyst particles tear the surface of the film and catalyst particles can be exposed over the film surface. This result is important for PMo wash-down in the reaction medium and the main cause of the catalyst deactivation for the subsequent activity tests.

11. In deactivation series it was observed that catalyst in the surface of 15wt% PMo loaded PSF film may be dissolved in the polar reaction medium more easily than the 10wt% loaded PSF film. However the PMo solubilization in reaction medium is very slow step and the higher catalytic activity can be well retained after 5 sequential run.

CHAPTER VIII

RECOMMENDATIONS

1. To prevent the polymeric film absorbing the solvent (DMF), evaporation time may be kept longer and evaporation temperature may be higher (but not higher than Tg value)

2. Ultrasonic bath may be used to prevent the nonhomogeneous catalyst dispersion

3. Film prepared for pervaporation should not be thinner than 50 μm, because catalyst particles tears the surface of the film and this is important in pervaporation point of wiev.

REFERENCES

1. Dias J.A. , Osegovic J.P. , and Drago R.S.,J. Catal. 183, 83-90 (1999)

    The Solid Acidity of 12-Tungstophosphoric Acid

2. Misono M., Materials Chemistry and Physics,17 (1987) 103-120

    Acidic and Catalytic Properties of Heteropoly Compounds

3. Misono M., Catal.Rev.- Sci.Eng., 29 (2&3), 269-321 (1987)

    Heterogeneous Catalysis by Heteropoly Compounds of Molybdenum and Tungsten

4. Mizuno N., Misono M., Chem.Rev., 1998, 98, 199-217

    Heterogeneous Catalysis

5. Timofeeva M.N., Appl. Cat. A: General 256 (2003) 19-35

    Acid Catalysis by Heteropoly Acids

6. Kozhevnikov I.V.,Catal.Rev.-Sci.Eng., 37(2), 311-352 (1995)

    Heteropoly Acids and Related Compounds as Catalysts for Fine Chemical Synthesis

7. Cavani F., Catalysis Today 41 (1998) 73-86

    Heteropolycompound-based catalysts: A blend of acid and oxidizing properties

8. Mizuno N.,Katamura K., Yoneda Y., Misono M., Journal of Catalysis 83, 384-392 (1983)

    Catalysis by Heteropoly Compounds V. The Reduction Mechanism of $H_3PMo_{12}O_{40}$

9. Okuhara T., Hashimoto T., Hibi T., Misono M., Journal of Catalysis 93, 224-230 (1985)

    Catalysis by Heteropoly Compounds IX. Role of Water in Catalytic Dehydration of 2-Propanol over Copper Salts of $H_3PMo_{12}O_{40}$

10. Hu C., Hashimoto M., Okuhara T., Misono M., Journal of Catalysis 143, 437-448 (1993)

Catalysis by Heteropoly Compounds XXII. Reactions of Esters and Esterification Catalyzed by Heteropolyacids in a Homogeneous Liquid Phase- Effects of the Central Atom of Heteropolyanions Having Tungsten as the Addenda Atom

11. Hayashi H., Moffat J.B., Journal of Catalysis 77, 473-484 (1982)
    The Properties of Heteropoly Acids and the Conversion of Methanol to Hydrocarbons

12. Throat T.S., Yadav V.M., Yadav G.D., Applied Catalysis A: General, 90 (1992) 73-96
    Esterification of phthalic anhydride with 2-ethylhexanol by solid superacidic catalysts

13. Öztürk G., Gümgüm B., Akba O., Catalysis Letters, vol 82, no 3-4, October 2002
    Synthesis of esters under microwave irradiation using heteropoly acids as catalysts

14. Liew M.K.H., Tanaka S., Morita M., Desalination 101 (1995) 269-277
    Separation and Purification of Lactic Acid: Fundamental Studies on the Reverse Osmosis Down-Stream Process

15. Sanz M.T., Murga R., Beltran S., Cabezas J.L., Coca J., Ind.Eng.Chem.Res. 2002, 41, 512-517
    Autocatalyzed and Ion-Exchange-Resin-Catayzed Esterification Kinetics of Lactic Acid with Methanol

16. Altıokka M.R., Çıtak A., Applied Catalysis A: General 6205 (2002) 1-8
    Kinetics study of esterification of acetic acid with isobutanol in the presence of amberlyte catalyst

17. Singh R., Chemtech, April 1998 33,
    Industrial membrane separation processes

18. Lipnizki F., Field R.W., Ten P-K., Journal of Membrane Science 153 (1999) 183-210
    Pervaporation-based hybrid process: a review of process design, applications and economics

19. Gudernatsch W., Menzel Th., Strathmann H., Journal of Membrane Science 61 (1991)19-30

Influence of composite membrane structure on pervaporation

20. Liu Q., Jia P., Chen H., Journal of Membrane Science 159 (1999) 233-241

Study on catalytic membranes of $H_3PW_{12}O_{40}$ entrapped in PVA

21. Lim S.Y., Park B., Hung F., Sahimi M., Tsotsis T.T, Chem.Eng.Sci. 57 (2002) 4933-4946

Design issues of pervaporation membrane reactors for esterification

22. David M.O., Nguyen Q.T., Neel J., Journal of Membrane Science, 73 (1992) 129-141

Pervaporation membranes endowed with catalytic properties, based on polymer blends

23. Martinez L., Florido-Diaz F.J., Hernandez A., Pradanoz P., J. Membr. Sci. 203 (2002) 15-27

Characterization of three hydrophobic porous membranes used in membrane distillation Modelling and evaluation of their water vapour permeabilities

24. Krupiczka R., Koszorz Z., Separation and Purification Technology 16 (1999) 55-59

Activity-based model of the hybrid process of an esterification reaction coupled with pervaporation

25. Feng. X., Huang R.Y.M., Chemical Engineering Science, vol51, no.20, pp.4673-4679, 1996

Studies of a Membrane Reactor: Esterification Facilitated by Pervaporation

26. Xuehui L., Lefu W., Journal of Membrane Science 186 (2001) 19-24

Kinetic model for an estefication process coupled by pervaporation

27. Changluo Z., Moe L., Wei X.., Desalinatination, 62 (1987) 299-313

Separation of Ethanol-Water Mixtures by Pervaporation-Membrane Separation Process

28. Liu Q., Zhang Z., Chen H., Journal of Membrane Science 182 (2001) 173-181

Study on the coupling of esterification with pervaporation

29. Okamoto K.,Yamamoto M., Otoshi Y., Semoto T., Yano M., Tanaka K., Kita H., Journal of Chemical Engineering of Japan, vol.26 no.5 1993

Pervaporation-aided Esterification of Oleic Acid

30. Kita H., Sasaki S., Tanaka K., Okamoto K.,Yamamoto M.,Chemistry Letters, pp.2025-2028, 1988

Esterification of Carboxylic Acid with Ethanol Accompanied by Pervaporation

31. Yadav G.D., Thathagar M.B., Reactive and Functional Polymers 52 (2002) 99-110

Esterification of maleic acid with ethanol over cation-exchange resin catalyst

32. Zhu.Y., Chen H.,Journal of Membrane Science 138 (1998) 123-134

Pervaportion separation and pervaporation-esterification coupling using crosslinked PVA composite catalytic membranes on porous ceramic plate

33. Zhu Y., Minet G., Tsotsis T.T., Chem.Eng.Sci., vol.51, no.17, pp. 4103-4113, 1996

A continious pervaporation membrane reactor for the study of esterification reactions using a composite polymeric/ ceramic membrane

34. Keurentjes J.T.F., Janssen G.H.R., Gorissen J.J., Chem.Eng.Sci., vol.49., no.24A, pp. 4681-4689, 1994

The esterification of tartaric acid with ethanol: kinetics and shifting the equilibrium by means of pervaporation

35. Kita H., Tanaka K., Okamoto K., Yamamoto M., Chem.Lett., pp. 2053-2056, 1987

The esterification of oleic acid with ethanol accompanied by membrane separation

36. Bagnell L., Cavell K., Hodges A.M., Mau A. W., Seen A.J., J. Membr. Sci., 85 (1993) 291-299

The use of catalytically active pervaporation membranes in esterification reactions to simultaneously increase product yield, membrane permselectivity and flux

37. Chen. S., Liou R., Hsu C., Chang D., Yu K.,Chang C., J Membr.Sci., 193 (2001) 59-67

Pervaporation separation water / ethanol mixture through lithiated polysulfone membrane

38. Nowak K.M., Desalination, 71 (1989) 83-95

Synthesis and Properties of Polysulfone Membranes

39. Zhao C., Liu X., Rikimaru S., Nomizu M., Nishi N., J. Membr. Sci. 214 (2003) 179-189

Surface characterization of polysulfone membranes modified by DNA immobilization

40. Tweddle T.A., Striez C., Tam C.M., Hazlett J.D., Desalination, 86 (1992) 27-41

Polysulfone Membranes I. Performance Comparison of Commertially Available Ultrafiltration Membranes

41. Tam C.M., Tweedle T.A., Kutowy O., Hazlett J.D., Desalination, 89 (1993) 275-287

Polysulfone Membranes II. Performance comparison of polysulfone-poly-(N-vinyl-pyrrolidone) membranes

42. Tam C.M., Mauro D., Guiver M.D., J Membr.Sci., 78 (1993) 123-134

Polysulfone Membranes IV. Performance evaluation of Radel A / PVP membranes

43. Radovanovic P., Thiel S.W., Hwang S., J Membr.Sci., 65 (1992) 213-229

Formation of asymmetric polysulfone membranes by immersion precipitation. Part I. Modelling mass transport during gelation

44. Gür M.T., J. Membr.Sci., 93 (1994) 283-289

Permselectivity of zeolite filled polysulfone gas separation membranes

45. Guiver M.D., Black P., Tam C.M., Deslandes Y., J. Appl. Pol.Sci., vol.48, 1597-1606 (1993)

Functionalized Polysulfone Membranes by Heterogeneous Lithiation

46. Kim J.Y., Lee H.K., Kim S.C., J Membr.Sci. 163 (1999) 159-166

Surface structure and phase separation mechanism of polysulfone membranes by atomic force microscopy

47. Tsai H.A., Lee K.R., Wang Y.C., Li C.L., Huang J., Lai J.Y., J Membr. Sci., 176 (2000) 97-103

Effect of surfactant addition on the morphology and pervaporation performance of asymmetric polysulfone membranes

48. Lee J.K., Song I.K., Lee W.Y., J Mol.Catal.A:Chemical 120 (1997) 207-216

Design of novel catalyst imbedding heteropoly acids in polymer films: Catalytic activity for ethanol conversion

49. Song I.K., Lee J.K., Park G.I., Lee W.Y., 3rd World Congress on Oxidation Catalysis, pp.1183-1193, 1997

Selective oxidation catalysis over heteropoly acid supported on polymer

50. Park G.I., Lim S.S., Choi J.S., Song I.K., Lee W.Y., J Catal. 178, 378-381 (1998)

Modification of pore characteristics and catalytic activities of heteropoly acid- polymer composite catalysis by membrane technology

51. Lee J.K., Song I.K., Lee W.Y., Kim J.J., J Mol.Catal. A: Chemical 104 (1996) 311-318

Modification of 12-molybdophosphoric acid catalyst by blencing with polysulfone and its catalytic activity for 2-propanol conversion reaction

52. Lim S.S., Park G.I., Song I.K., Lee W.Y., J Mol. Cat. A: Chemical 182-183 (2002) 175-183

Heteropolyacid (HPA)- polymer composite films as catalytic materials for heterogeneous reactions

53. Song I.K., Shin K.S., Lee W.Y., J Catal. 144, 348-351 (1993)

Catalytic activity of $H_3PW_{12}O_{40}$ – blended polysulfone film in the oxidation of ethanol to acetaldehyde

54. Lim S.S., Kim Y.H., Park G.I., Lee W.Y., Song I.K., Youn H.K., Catal.Lett. 60 (1999) 199-204

Heterogeneous liquid-phase hydration of isobutene by heteropoly acid-polymer composite film catalyst

55. Song I.K., Lee W.Y., Appl. Catal. A: General 256 (2003) 77-98

Heteropoly acid (HPA)- polymer composite films as heterogeneous catalysts and catalytic membranes

56. Bernal M.P.,Coronas J., Menendez M., Santamaria J., Chem.Eng.Sci., 57 (2002) 1557-1562

Coupling of reaction and separation at the microscopic level: esterification process in a H-ZSM-5 membrane reactor

57. Mukai S.R., Masuda T., Ogino I., Hashimoto K., Appl.Cat. A: General 165 (1997) 219-226

Preparation of encaged heteropoly acid catalyst by synthesizing 12-molybdophosphoric acid in the supercages of Y-type zeolite

58. Verhoef M.J., Kooyman P.J., Peters J.A., Bekkum H., Microporous and Mesoporous Materials 27 (1999) 365-371

A study on the stability of MCM-41-supported heteropoly acids under liquid- and gas-phase esterification conditions

59. Tanaka K., Yoshikawa R., Ying C., Kita H., Okamoto K., Chem.Eng.Sci. 57 (2002) 1577-1584

Application of zeolite T membrane to vapor-permeation-aided esterification of lactic acid with ethanol

60. Tanaka K.,Yoshikawa R., Ying C., Kita H., Okamoto K., Catalysis Today 67 (2001) 121-125

Application of zeolite membranes to esterification reactions

61. Jafar J.J., Budd P.M., Hughes R., J. Membr. Sci. 199 (2002) 117-123

Enhancement of esterification reaction yield using zeolite A vapour permeation membrane

62. Gao Z., Yue Y., Li W., Zeolites 16: 70-74, 1996

Application of zeolite- filled pervaporation membrane

63. Süer M.,Baç N., Yilmaz L., J. Membr.Sci., 91 (1994) 77-86

Gas permeation characteristics of polymer-zeolite mixed matrix membranes

64. From M., Adlercreutz P. Mattiasson B., Biotech.Lett., vol. 19, no.4, April 1997, pp. 315-317

Lipase catalyzed esterification of lactic acid

65. Aytürk M.E., Ms Thesis in Chemical Engineering, August 2001, METU

Liquid-phase synthesis of lactic acid esters catalyzed by heteropoly acid supported ion-exchange resins

66. Süer M.G., Ms Thesis in Chemical Engineering, April 1993, METU
Gas permeation studies with novel polymer-zeolite membranes

67. Battal T., Ms Thesis in Chemical Engineering, August 1994, METU
Separation of binary gas mixtures with zeolite-polymer mixed matrix membranes

68. Korkut S., Ms Thesis in Chemical Engineering, August 2001, METU
Evaluation of performance of hydrophilic pervaporation membranes for ethyllactate-water-ethanol mixtures

69. Solomons T.W.G., "Organic Chemistry", 5th edition, Wiley, 1992

70. Levenspiel O., "Chemical Reaction Engineering", 2nd edition, Wiley, 1992

71. Groggins P.H., "Unit Process in Organic Synthesis", 5th edition, McGraw-Hill, 1958

72. Wijmans J.G., Baker R.W., J. Membr. Sci., vol.107, p.1-21, 1995
The solution-diffusion model: a review

73. Okumus E., Ms Thesis in Chemical Engineering, 1998, METU
Development of PAN-based composite membranes for pervaporation

74. Gupta B.D., Mukherjer A.K., Marcel Dekker, 1990, p.299-329
Separation of liquid mixtures by pervaporation

75. Neel J., "Membrane Separations Technology, Principles and Applications", Elsevier Science B.V., p.143-171, 1995

76. Rönnback R., Salmi T., Vuori A., Haario H., Lehtonen J., Sundqvist A., Tirronen E., Chem. Eng. Sci., vol 52, pp. 3369-3381, 1997
Development of a kinetic model for the esterification of acetic acid with methanol in the presence of a homogeneous acid catalyst

77. Lehtonen J., Immonen K., Salmi T., Paatero E., Nyholm P., Chem. Eng. Sci., vol. 51, pp. 2799-2804, 1996
Kinetic analysis of the reaction network in the catalyzed poly-esterification of unsaturated carboxylic acids

78. Dufaure C.L., Mouloungui Z., Appl. Cat. A: General, vol.204, pp. 223-227, 2000
catalysed or uncatalysed esterification reaction of oleic acid with 2-ethyl hexanol

79. Timofeeva M.N., Maksimovskaya R.I., Paukshtis E.A., Kozhevnikov I.V.

J. Mol. Catal. A: Chemical, vol.102, pp. 73-77, 1995

Esterification of 2,6-pyridinedicarboxylic acid with n-butanol catalyzed by heteropoly acid $H_3PW_{12}O_{40}$ or its Ce(III) salt

80. Pozniczek J., Kulszewicz-Bajer I., Zagorska M., Kruczaka K., Dyrek K., Bielanski A., Pron A., J. Catal., vol 132, p.311, 1991

$H_3PMo_{12}O_{40}$ – doped polyacetylene as a catalyst for ethyl alcohol conversion

APPENDIX-A

SAMPLE CALCULATIONS

A.1 To prepare 10wt% PMo loaded 78μm-thick PSF membrane

23.86 ml DMF, 1.67 gr PSF (7wt% of DMF in ml), 0.167 gr PMo (10wt% of PSF in gr) was blended with respect to the procedure given above, then casted on a petri having 14cm diameter, then dried and annealed.

A.2 The procedure used for calculating the lactic acid conversions and the product distributions throughout the experiments

The procedure used for calculating the lactic acid conversions and the product distributions throughout the experiments were outlined by using the experimental data obtained with the 10wt% PMo loaded PSF catalyst.

Potassium hydroxide (KOH) solution, used in titrations, was standardized by using potassium hydrogen phthalate ($KHC_8H_4O_4$). Then, hydrochloric acid (HCl) solution was standardized by using the standard base solution.

$N_{KOH} = 1000.W_{KHC8H4O4} \ (gr) \ / \ MW_{KHC8H4O4} \ (g/gmol). \ V_{KOH} \ (ml)$

Examination of the unconverted lactic acid and the amount of lactoyllactic acid present, which is a normal component of aqueous

lactic acid solutions, in the product sample are done by means of two sequential acid-base titrations:

1. free acidity in the sample is determined by titrating a weighted amount of sample product against 0.1 N standardized KOH solution to the phenolphthalein end point.

$$F \ (wt\%) = [N_{KOH} \ (mol/lt).V_{KOH} \ (ml). \ MW_{lactic \ acid}(g/gmol)] \ / \ [\ 1000 \ (ml/lt). \ W_{sample} \ (g)].100$$

Where

F : free acidity as lactic acid, wt%

N_{KOH} : normality of KOH solution, mol/lt

V_{KOH} : volume of KOH solution used for the titration, ml

$MW_{lactic \ acid}$: molecular weight of lactic acid, 90.08 g/mol

W_{sample} : sample weight, g

2. An excess of alkali, KOH solution, is added to the titrated solution. After boiling for 5 min gently, solution is allowed to cool. Total acidity and the amount of polymeric lactic acid is determined by the back titration of the excess alkali with 0.1N standardized HCl solution.

$$T(wt\%) = [(N_{KOH} + N_{KOH, \ excess})(mol/lt).V_{KOH} \ (ml) - N_{HCl} \ (mol/lt).V_{HCl} \ (ml)].[MW_{lactic \ acid}(g/gmol) \ / \ (1000(ml/lt). \ W_{sample}(g))].100$$

where

T: total acidity as lactic acid, wt%

$N_{KOH, \ total}$: total volume of KOH solution including added excess, ml

N_{HCl}: normality of HCL solution, mol/lt

V_{HCl}: volume of HCl solution used for back titration, ml

Polymeric lactic acid ester, lactoyllactic acid, is the difference between acidities:

P (wt%) = T(wt%) – F(wt%)

Conditions for the 10wt% PMo loaded PSF membrane experimental run are as follows;

Table A.2.1 Experimental conditions

Temperature (T)=	50C	NKOH=	0,076 mol/lt
etOH/LA mole ratio =	1,0753	NHCL=	0,09 mol/lt
used membrane weight=			
loading (for used part)=		LA soln=	12 ml = 14,52 gr = 0.1612 mol
18cm2 used area		EtOH soln=	10 ml = 7,98 gr = 0.1735 mol
total membrane weight=	1,838 gr	rxn mixture=	22 ml = 22,5 gr
polymer amount=	1,68gr		
loading=	0,168gr		
thickness=	78 mcrmtr		

Lactic acid solution having 92 wt% total acidity, contains 73 wt% free acidity as lactic acid and 19 wt% as lactoyllactic acid. Ethanol solution was 99.5 wt%.

Table A.2.2. Initial ratio of species in the reaction medium

	wt% species	Gr species	Mol species
LA	0.471093	10.599593	0.117773
etOH	0.352893	7.9400925	0.1726107
H2O	0.0534	1.2015	0.06675
Ethyllact.	0	0	0
LLA	0.122613	2.7587925	0.01703

Initial mole fractions;	
$\theta1=N_{EtOH}/N_{LA}$	1.465622
$\theta2= N_{H2O}/N_{LA}$	0.566768
$\theta3= N_{LLA}/N_{LA}$	0.1446

Unconverted lactic acid was found from

P (wt%) = T(wt%) – F(wt%) equation as described.

Table A.2.3. Change of polymerized LA amount with respect to time

time(min)	smpl wgt	VKOH	VHCL	F(wt%)	T(wt%)	P(wt%)
0	1.0432	70	3	47.105061	51.504985	4.3999233
90	1.1388	66	3.5	40.684932	44.359852	3.674921
150	1.1664	64	3	38.518519	42.453704	3.9351852
210	1.2144	62.5	2.5	36.128953	40.242095	4.1131423
330	1.2575	59.5	3.2	33.215905	36.737177	3.5212724
450	1.237	59	3.5	33.482619	36.865804	3.3831851
570	1.3345	52	3	27.354065	30.793556	3.4394904
690	1.3088	50	3	26.81846	30.325489	3.5070293
810	1.2095	47	2.5	27.279041	31.408847	4.1298057

In the most general cases, when working at low water concentrations, gas chromatograph equipped with TCD detector produces larger signals than the actual amount of water present in the system.

FFAP column used for general esterification applications, detects alcohol, water and lactate ester. However, injected solution contains lactic and lactoyllactic acid at high concentrations. Therefore, a calibration methodology relating the wt% titration data with the resulting chromatograph signals is needed.

For this purpose, extensive calibration trials at varying concentrations were performed. Resulting differences between the total areas with respct to prepared solutions were analytically combined together with the estimation of relative response factors of the species at lactic and lactoyllactic acid free basis. Ethyl alcohol, which gave precise and definite peaks at the lowest retention time, was used as the reference component in calculations. From the calibration trials, best response factors were estimated representing the actual reaction concentrations.

Resulting areas were therefore corrected by multiplying with the corresponding relative response factor. Procedure is as follows:

$$(R.F.)species = [(area\ of\ EtOH\ /\ wt\%\ EtOH)\ /\ (\ area\ of\ species\ /\ wt\%\ species)]$$

relative response factors:

etOH= 1
H2O= 0.584885122
lactate= 1.255943377

Table A.2.4. Raw etOH, LA and H_2O fractions

time(min)	GCetOH	GCH2O	Gclact.	etOH crtd	H2O crtd	Lact crtd
0	15743	2596	0	15743	1518.3618	0
90	13142	3984	1855	13142	2330.1823	2329.775
150	12592	3158	2032	12592	1847.0672	2552.0769
210	13147	3513	2619	13147	2054.7014	3289.3157
330	12620	2822	3648	12620	1650.5458	4581.6814
450	4573	4080	3148	4573	2386.3313	3953.7098
570	11153	3047	4541	11153	1782.145	5703.2389
690	8910	2449	4428	8910	1432.3837	5561.3173
810	9233	2641	5354	9233	1544.6816	6724.3208

Actual lactic and lactoyllactic acid free basis weight and mole fractions are calculated;

Table A.2.5. Actual lactic and lactoyllactic acid free basis weight and mole fractions

	LA+LLA free wt%			LA+LLA free mole fractions		
time(min)	etOH	H2O	lact	etOH	H2O	lact
0	91.20369646	8.7963035	0	0.8022623	0.1977377	0
90	73.82334305	13.089473	13.087184	0.6569316	0.2976692	0.0453992
150	74.10919408	10.870764	15.020042	0.6878183	0.2578381	0.0543436
210	71.09938789	11.11189	17.788722	0.6680325	0.2668118	0.0651557
330	66.94169251	8.7551767	24.303131	0.6776152	0.2264836	0.0959013
450	41.90399339	21.866786	36.229221	0.3744469	0.4993501	0.126203
570	59.83887924	9.5616926	30.599428	0.622007	0.2539989	0.1239941
690	56.02469535	9.0066059	34.968699	0.6045388	0.2483655	0.1470957
810	52.7539636	8.8257422	38.420294	0.5842981	0.2498135	0.1658884

Since information about the mol fractions is available, conversion with respect to lactic acid esterification was calculated from the stoichiometric relations of material balances;

LA + EtOH $\leftrightarrow$ Ester + H_2O x_1

LLA + H_2O $\leftrightarrow$ 2LA x_2
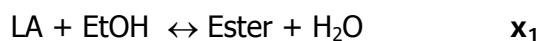
Table A.2.6. Stoichiometric relations

species	initial (mole)	change (mole)	final (mole)
LA	N_{LA0}	$- N_{LA0}.x_1 + 2. N_{LLA0}.x_2$	$N_{LA} = N_{LA0} - N_{LA0}.x_1 + 2. N_{LLA0}.x_2$
EtOH	N_{EtOH0}	$- N_{LA0}.x_1$	$N_{EtOH} = N_{EtOH0} - N_{LA0}.x_1$
Ester	N_{Ester0}	$+ N_{LA0}.x_1$	$N_{Ester} = N_{Ester0} + N_{LA0}.x_1$
H2O	N_{H2O0}	$+ N_{LA0}.x_1 - N_{LLA0}.x_2$	$N_{H2O} = N_{H2O0} + N_{LA0}.x_1 - N_{LLA0}.x_2$
LLA	N_{LLA0}	$- N_{LLA0}.x_2$	$N_{LLA} = N_{LLA0} - N_{LLA0}.x_2$

$$R_1 = (y_{ester} / y_{EtOH}) = [(N_{LA0}.x_1) / N_T] / [(N_{EtOH0} - N_{LA0}.x_1) / N_T]$$

$$R_2 = (y_{ester} / y_{H2O}) = [(N_{LA0}.x_1) / N_T] / [(N_{H2O0} + N_{LA0}.x_1 - N_{LLA0}.x_2) / N_T]$$

Table A.2.7. Mole fractions

time(min)	R1(Yest/YetOH)	R2(Yest/Yh2o)	X1
0	0	0	0
90	0.069108002	0.152515705	0.094739
150	0.079008692	0.210766489	0.1073178
210	0.097533705	0.244200941	0.1302443
330	0.141527671	0.423436025	0.1817092
450	0.337038417	0.252734508	0.3694516
570	0.199345155	0.48816769	0.2436035
690	0.243318871	0.592255102	0.2868238
810	0.283910475	0.664048728	0.3240923

Since x1 is known, x2, conversion relating to the lactoyllactic acid hydrolysis was calculated by expressing the titration data of the free acidity as mol free lactic acid.

Table A.2.8. Conversion relating to LLA hydrolysis calculation

time(min)	F(wt%)	gr free LA	mol free LA	X2
0	47.105061	10.598639	0.1177627	0
90	40.684932	9.1541096	0.1017123	-0.143689
150	38.518519	8.6666667	0.0962963	-0.2592223
210	36.128953	8.1290143	0.0903224	-0.3553563
330	33.215905	7.4735785	0.0830398	-0.3912368
450	33.482619	7.5335893	0.0837065	0.2775201
570	27.354065	6.1546647	0.0683852	-0.6075146
690	26.81846	6.0341534	0.0670461	-0.4973835
810	27.279041	6.1377842	0.0681976	-0.3347066

Using the material balance for the batch reactor, concentration (mol/lt) data were calculated.

Table A.2.9. Weight percent of species with respect to time

Time (min)	WLA	WetOH	Wlactate	WH2O	WLLA	Wtotal
0	10.598643	7.9393978	0	1.2013943	2.7586137	22.498049
90	9.1541132	7.4261887	1.3164928	1.4462578	2.7249896	22.068042
150	8.6666701	7.358048	1.4912885	1.508334	2.8405033	21.864844
210	8.1290175	7.2338533	1.809875	1.5863982	2.8676897	21.626834
330	7.4735815	6.9550638	2.5250306	1.7064876	2.7062658	21.366429
450	7.5335923	5.9380476	5.1338983	1.8994679	1.4166694	21.921676
570	6.1546671	6.6197773	3.3851135	1.9039786	2.5751357	20.638672
690	6.0341558	6.3856489	3.9857037	1.9618374	2.3517447	20.71909
810	6.1377866	6.1837628	4.5035855	1.9909738	2.1322504	20.948359

Table A.2.10. Concentrations of species with respect to time

time (min)	CLA	CetOH	Clactate	CH2O	CLLA
0	5.35285	7.8452547	0	3.0338241	0.7740218
90	4.6232895	7.3381311	0.5071236	3.6521661	0.7645874
150	4.3771061	7.2707984	0.5744563	3.8089242	0.7969987
210	4.1055644	7.1480764	0.6971784	4.0060561	0.8046267
330	3.7745361	6.8725927	0.972662	4.3093121	0.7593338
450	3.8048446	5.867636	1.9776187	4.7966362	0.3974942
570	3.1084177	6.5412819	1.3039728	4.8080266	0.7225409
690	3.0475534	6.3099297	1.535325	4.9541349	0.659861
810	3.0998922	6.1104375	1.7348172	5.0277116	0.5982745

APPENDIX B

REACTION RATE CALCULATION

Esterification reaction of lactic acid with ethyl alcohol was carried out in a batch reactor, then the general form of the mole balance is

$$dN_J / dt = \int_V rj \, dV$$

With the perfect mixing assumption, the variations in the rate of reaction through out the reactor volume was neglected. Then, the balance equation becomes

$$dN_J / dt = rj.V$$

with the constant-volume reactor assumption, reactor mole balance is expressed as

$$(1 / V).(dN_J / dt) = [d(Nj / V) / dt] = dCj / dt = rj$$

So, for the proposed esterification reactions, which are both reversible, to see the catalytic activity on the reaction rate, simple procedure was followed (for detailed rate calculation, see Engin Aytürk Ms Thesis, 2001)

$$r_{LA} = - (dc_{LA} / dt).(\text{liquid volume/amount of catalyst})$$

$$r_{LA} = - (\Delta Ci / \Delta ti). (\text{liquid volume/amount of catalyst})$$

$$r_{LA} = - \left[(C_2-C_1) / (t_2-t_1) \right] \Big|_{t_1+ (t_2-t_1)/2}$$

then, $- r_{LA}$ [=] moles / min-gr.catalyst

B.1. Loading is the variable

Table B.1.1. Concentration of LA versus time table wrt loaded catalyst amount used in reaction medium

time(min)	no cat.	5wt% (0.0835 gr pmo)	10wt%(0.168 gr pmo)	15wt% (0.2663 gr pmo)
0	5.3533182	5.3533182	5.35285	5.3533182
90	4.9358089	4.8893113	4.6232895	4.6249761
150	4.6164194	4.4674147	4.3771061	4.4260377
210	4.5426944	4.2804043	4.1055644	4.1700543
330	4.2374641	4.1022085	3.7745361	3.9540324
450	4.1485426	3.9092434	3.8048446	3.8343966
570	4.0340638	3.8246777	3.1084177	3.3549552
690	3.9868894	3.6871022	3.0475534	3.2516614
810	3.8969472	3.6355109	3.0998922	3.2743519

Liquid volume = 22 mlt

-ra = (moles/lt.min)*(liq rxn vol/cat.weight) calculations with respect to concentration versus time table;

Table B.1.2. Time versus reaction rate for used catalyst loadings in reaction

time(min)	5wt%	10wt%	15wt%
45	-0.2581988	-0.1249929	-0.07886
120	-0.08845	-0.0422879	-0.0268243
180	-0.0551293	-0.0265702	-0.0169841
270	-0.0352185	-0.0164552	-0.010701
390	-0.0233025	-0.0109573	-0.0071023
510	-0.0172022	-0.0076427	-0.0050134
630	-0.0135256	-0.0055092	-0.0037295
750	-0.0110754	-0.0046213	-0.0030946

B.2. Thickness is the variable

constant loading (0.168gr PMo)

concentration versus time table

Table B.2.1. Concentration of LA versus time table wrt catalytic film thickness

time(min)	no cat.	47 μm	78 μm	150 μm	300 μm
0	5.3533182	5.3532227	5.35285	5.3532227	5.3532227
90	4.9358089	4.7429218	4.6232895	4.7299983	5.1892857
150	4.6164194	4.5763348	4.3771061	4.5499582	4.8269
210	4.5426944	4.4375971	4.1055644	4.4375971	4.6759647
330	4.2374641	3.5920571	3.7745361	3.5920571	4.0006193
450	4.1485426	3.1888117	3.8048446	3.3547256	3.8146361
570	4.0340638	3.028714	3.1084177	3.0983663	3.7213313
690	3.9868894	3.0746553	3.0475534	3.2278773	3.6082939
810	3.8969472	3.0204071	3.0998922	3.0204071	3.4959309

Liquid volume = 22 mlt

-ra = (moles/lt.min)*(liq rxn vol/cat.weight) calculations with respect to concentration versus time table;

Table B.2.2. Reaction rate versus time wrt film thickness

time(min)	47mcrmtr	78mcrmtr	150mcrmtr	300mcrmtr
45	-0.1264317	-0.125057	-0.1260761	-0.1314825
120	-0.0437636	-0.0423096	-0.0435122	-0.0468444
180	-0.0282198	-0.0265839	-0.0280941	-0.0296291
270	-0.0167589	-0.0164636	-0.0167332	-0.0180352
390	-0.0097979	-0.0109629	-0.0100222	-0.0112464
510	-0.0068701	-0.0076466	-0.0071194	-0.0082929
630	-0.0054594	-0.0055121	-0.00565	-0.0065295
750	-0.0045796	-0.0046237	-0.0046875	-0.0053161

B.3. area is the variable

B.3.1. catalyst amount in reaction kept constant

Table B.3.1.1. LA concentration versus time table wrt film surface area

time(min)	no cat.	12cm2	18cm2	36cm2
0	5.3533182	5.35315	5.35285	5.3530464
90	4.9358089	5.1591953	4.6232895	4.781161
210	4.5426944	5.0040315	4.3771061	4.5882355
330	4.2374641	4.654913	4.1055644	4.2624225
450	4.1485426	4.2670036	3.7745361	3.9361622
570	4.0340638	4.1118399	3.8048446	3.5682821
690	3.9868894	4.034258	3.1084177	3.4545193
810	3.8969472	3.9566761	3.0475534	3.3107144

Liquid volume = 22 mlt

-ra = (moles/lt.min)*(liq rxn vol/cat.weight) calculations with respect to concentration versus time table;

Table B.3.1.2. Reaction rate versus time table wrt film surface area

time(min)	12cm2	18cm2	36cm2
45	-0.1219925	-0.1249929	-0.1276933
150	-0.0337144	-0.0338303	-0.035417
270	-0.0173503	-0.0177135	-0.0185867
390	-0.0114725	-0.0113921	-0.0119197
510	-0.0085603	-0.0083791	-0.0083433
630	-0.0067929	-0.006187	-0.0063206
750	-0.0056085	-0.0046278	-0.0051146

B.3.2 catalyst/polymer weight percent kept constant

Table B.3.2.1 Concentration of LA versus time table wrt variable area

time(min)	no cat.	12cm2	18cm2	36cm2	72cm2
0	5.3533182	5.3525227	5.35285	5.3531827	5.35314
90	4.9358089	4.8610624	4.6232895	4.3050799	4.6188275
210	4.5426944	4.8145787	4.3771061	3.4708627	4.3883806
330	4.2374641	4.2558237	4.1055644	3.2160175	4.1111838
450	4.1485426	3.9341879	3.7745361	2.9025175	3.9175603
570	4.0340638	3.8094021	3.8048446	2.7960706	3.8244912
690	3.9868894	3.6594774	3.1084177	2.4845971	3.6361909
810	3.8969472	3.6217056	3.0475534	2.3349645	3.5515178

Table B.3.2.2 Reaction rate versus time table wrt variable area

time(min)	12cm2	18cm2	36cm2	72cm2
45	-0.1919543	-0.1249929	-0.0605051	-0.0312352
150	-0.0545533	-0.0338303	-0.0146139	-0.008464
270	-0.0284116	-0.0177135	-0.0069818	-0.0044372
390	-0.0177604	-0.0113921	-0.0044227	-0.0029017
510	-0.0128412	-0.0083791	-0.0031499	-0.0021397
630	-0.0100264	-0.006187	-0.0023629	-0.0016692
750	-0.0082106	-0.0046278	-0.0018116	-0.0013508

APPENDIX C

EXPERIMENTAL DATA

Series C.1 esterification reaction at 50°C and 1:1 etOH/LA mole ratio with different area, constant loading (10 wt%), constant thickness (78 μm) PMo loaded PSF film

C.1.1 12cm^2, 78μm, 10wt% PMo loaded PSF membrane

Table C.1 Experimental conditions

T=	50C	**NKOH=**	0,080 mol/lt
etOH/LA mole ratio =	1,0753	**NHCL=**	0,097 mol/lt
used membrane weight=	0.03507 gr		
loading (for used part)=	0.00344 gr	**LA soln=**	12 ml = 14,52 gr
12cm2 used area		**EtOH soln=**	10 ml = 7,98 gr
total membrane weight	1.8745 gr	**rxn mixture= 22 ml= 22,5 gr**	
polymer amount=	1,6719 gr		
loading=	0,169gr		
thickness=	78 μm		

Table C.2. Initial ratio of species in the reaction medium

	wt% spe.	gr spe.	mol.spe.		**Initial mole fractions;**	
LA	0.471093	10.599593	0.117773		Tetha1=	1.465622
etOH	0.352893	7.9400925	0.1726107		Tetha2=	0.566768
H2O	0.0534	1.2015	0.06675		Tetha3=	0.1446
Ethyllact.	0	0	0			
LLA	0.122613	2.7587925	0.01703			

Table C.3. Titiration data

time(min)	smpl wgt	VKOH	VHCL
0	1.0853	71	2.5
90	1.1277	67	3
150			
210	1.1046	65	2.7
330	1.2304	64	2.8
450	1.2686	61	2.5
570	1.2672	59	2
690	1.2744	57	2.5
810	1.2651	56	3

Table C.4. Gas Chromatograph (GC) Data

time(min)	GCetOH	GCH2O	Gclact.	etOH crtd	H2O crtd	lact crtd
0	20007	4539	0	20007	2654.7936	0
90	13445	5020	4010	13445	2936.1233	5036.3329
150						
210	14494	2637	4885	14494	1542.3421	6135.2834
330	10797	4342	6282	10797	2539.5712	7889.8363
450	10262	2580	6373	10262	1509.0036	8004.1271
570	9750	2699	8655	9750	1578.6049	10870.19
690	9513	2373	8525	9513	1387.9324	10706.917
810	9057	3618	8740	9057	2116.1144	10976.945

C.1.2 18cm^2, 78μm, 10wt% PMo loaded PSF membrane

Table C.5. Experimental conditions

T=	50C	**NKOH**=	0,076 mol/lt
etOH/LA mole ratio =	1,0753	**NHCL=**	0,09 mol/lt
used membrane weight=	0.05255 gr		
loading (for used part)=	0.00512 gr	**LA soln=**	12 ml = 14,52 gr
18cm2 used area		**etOH soln=**	10 ml = 7,98 gr
total membrane weight=	1,8745 gr	**rxn mixture=**	22 ml = 22,5 gr
polymer amount=	1,68 gr		
loading=	0,168 gr		
thickness=	78 μm		

Table C.6. Initial ratio of species in the reaction medium

	wt% spe.	gr spe.	mol.spe.
LA	0.471093	10.599593	0.117773
etOH	0.352893	7.9400925	0.1726107
H2O	0.0534	1.2015	0.06675
Ethyllact.	0	0	0
LLA	0.122613	2.7587925	0.01703

initial mole fractions;	
tetha1=	1.465622
tetha2=	0.566768
tetha3=	0.1446

Table C.7. Titration Data

time(min)	smpl wgt	VKOH	VHCL
0	1.0432	70	3
90	1.1388	66	3.5
150	1.1664	64	3
210	1.2144	62.5	2.5
330	1.2575	59.5	3.2
450	1.237	59	3.5
570	1.3345	52	3
690	1.3088	50	3
810	1.2095	47	2.5

Table C.8. Gas Chromatograph (GC) Data

time(min)	GCetOH	GCH2O	Gclact.	etOH crtd	H2O crtd	lact crtd
0	15743	2596	0	15743	1518.3618	0
90	13142	3984	1855	13142	2330.1823	2329.775
150	12592	3158	2032	12592	1847.0672	2552.0769
210	13147	3513	2619	13147	2054.7014	3289.3157
330	12620	2822	3648	12620	1650.5458	4581.6814
450	4573	4080	3148	4573	2386.3313	3953.7098
570	11153	3047	4541	11153	1782.145	5703.2389
690	8910	2449	4428	8910	1432.3837	5561.3173
810	9233	2641	5354	9233	1544.6816	6724.3208

C.1.3 36cm^2, 78μm, 10wt% PMo loaded PSF membrane

Table C.9. Experimental conditions

T=	50C
etOH/LA mole ratio =	1,0753
used membrane weight=	0.1051 gr
loading (for used part)=	0,01032 gr
36cm2 used area	
total membrane weight=	1.8745 gr
polymer amount=	1.67 gr
loading=	0.167gr
thickness=	78 μm

NKOH= 0,094 mol/lt

NHCL= 0,098 mol/lt

LA soln= 12 ml = 14,52 gr

etOH soln= 10 ml = 7,98 gr

rxn mixture= 22 ml = 22,5 gr

Table C.10. Initial ratio of species in the reaction medium

	wt% spe.	gr spe.	mol.spe.
LA	0.471093	10.599593	0.117773
etOH	0.352893	7.9400925	0.1726107
H2O	0.0534	1.2015	0.06675
Ethyllact.	0	0	0
LLA	0.122613	2.7587925	0.01703

initial mole fractions;	
tetha1	1.465622
tetha2	0.566768
tetha3	0.1446

Table C.11. Titration data

time(min)	smpl wgt	VKOH	VHCL
0	1.1314	63	2.8
90	1.2331	57	3
210	1.2729	52	2.5
330	1.281	49	2.7
450	1.2877	47	3
570	1.2938	44	3.2
690	1.2993	42	3
810	1.3205	41.5	2.8

Table C.12. Gas Chromatograph Data

time(min)	GCetOH	GCH2O	Gclact.	etOH crtd	H2O crtd	lact crtd
0	14509	3795	0	14509	2219.639	0
90	13920	5351	4398	13920	3129.7203	5523.639
210	12821	5227	8322	12821	3057.1945	10451.961
330	12304	4961	9468	12304	2901.6151	11891.272
450	10694	6071	9998	10694	3550.8376	12556.922
570	9784	5634	9719	9784	3295.2428	12206.514
690	9101	6403	10792	9101	3745.0194	13554.141
810	9217	5444	11863	9217	3184.1146	14899.256

C.1.4 72cm^2, 78μm, 10wt% PMo loaded PSF membrane

Table C.13. Experimental conditions

T=	50C	**NKOH=**	0,089 mol/lt
etOH/LA mole ratio =	1,0753	**NHCL=**	0,095 mol/lt
used membrane weight=	0.2120 gr		
loading (for used part)=	0.02063gr	**LA soln=**	12 ml = 14,52 gr
72cm2 used area		**etOH soln=**	10 ml = 7,98 gr
total membrane weight=	1.8745 gr	**rxn mixture= 22 m l= 22,5 gr**	
polymer amount=	1.67 gr		
loading=	0.167 gr		
thickness=	78 μm		

Table C.14. Initial ratio of species in the reaction medium

	wt% spe.	gr spe.	mol.spe.		initial mole fractions;	
LA	0.471093	10.599593	0.117773		tetha1	1.465622
etOH	0.352893	7.9400925	0.1726107		tetha2	0.566768
H2O	0.0534	1.2015	0.06675		tetha3	0.1446
Ethyllact.	0	0	0			
LLA	0.122613	2.7587925	0.01703			

Table C.15. Titration data

time(min)	smpl wgt	VKOH	VHCL
0	1.14	67	3
90	1.2818	65	2.5
150			
210	1.3076	63	2.5
330	1.3293	60	2.8
450	1.3485	58	3
570	1.3575	57	3
690	1.3777	55	3.5
810	1.3849	54	3

Table C.16. Gas Chromatograph (GC) Data

time(min)	GCetOH	GCH2O	Gclact.	etOH crtd	H2O crtd	lact crtd
0	13077	5745	0	13077	3360.165	0
90	12438	4136	5246	12438	2419.0849	6588.679
150						
210	11413	4873	7009	11413	2850.1452	8802.9071
330	10251	7507	8875	10251	4390.7326	11146.497
450	9561	6835	9746	9561	3997.6898	12240.424
570	9039	9155	10749	9039	5354.6233	13500.135
690	9477	9269	12290	9477	5421.3002	15435.544
810	9312	8303	12156	9312	4856.3012	15267.248

Series C.2 esterification reaction at 50°C and 1:1 etOH/LA mole ratio with variable loading, constant area (18cm^2), constant thickness (78 μm) PMo loaded PSF film

C.2.1 18cm^2, 78μm, unloaded PSF membrane

Table C.17. Experimental conditions

T=	50C		**NKOH=**	0,08713 mol/lt
etOH/LA mole ratio =	1,0753		**NHCL=**	0,105 mol/lt
used membrane weight =	0.051 gr			
catalyst loading =	0 gr		**LA soln=**	12 ml = 14,52 gr
total membrane weight=	1.7136 gr		**etOH soln=**	10 ml = 7,98 gr
polymer amount =	1.67 gr		**rxn mixture=**	**22 ml = 22,5 gr**

Table C.18. Initial ratio of species in the reaction medium

	wt% spe.	gr spe.	mole spe.		initial mole ratios;	
LA	0.471093	10.599593	0.117773		**tetha1**	1.465622
etOH	0.352893	7.9400925	0.1726107		**Tetha2**	0.566768
water	0.0534	1.2015	0.06675		**tetha3**	0.1446
ethyllact.	0	0	0			
LLA	0.122613	2.7587925	0.01703			

Table C.19. Titration Data

time(min)	sample weight(gr)	VKOH (ml)	VHCL (ml)
0	1.1053	66.4	2.7
90	1.1338	62.8	2.7
150	1.1968	62	2.2
210	1.2123	61.8	2.5
330	1.2828	61	2.2
450	1.306	60.8	2.6
570	1.3033	59	3
690	1.2498	58	2.5
810	1.2566	57	2.7

Table C.20. Gas Chromatograph (GC) Data

time(min)	GCetOH	GCH2O	GClactate	etOH crrctd	H2O crrctd	lact.crrctd
0	15461	3832	0	15461	2241.2798	0
90	8874	1288	1761	8874	753.33204	2211.7163
150	12246	3371	3017	12246	1971.6477	3789.1812
210	12650	2936	4143	12650	1717.2227	5203.3734
330	13357	2556	4784	13357	1494.9664	6008.4331
450	10916	3328	4364	10916	1946.4977	5480.9369
570	9002	2671	4246	9002	1562.2282	5332.7356
690	11023	3645	5872	11023	2131.9063	7374.8995
810	10661	8324	6311	10661	4868.5838	7926.2587

C.2.2 esterification reaction without catalyst

Table C.21. Experimental conditions

T=   50C   **NKOH=**   0,0909 mol/lt
etOH/LA mole ratio =   1,0753   **NHCL=**   0,106 mol/lt

                                                   LA soln=   12 ml = 14,52 gr
                                                   etOH soln= 10 ml = 7,98 gr
                                                   rxn mixture= 22 ml = 22,5 gr

Table C.22. Initial ratio of species in the reaction medium

	wt% spe.	gr spe.	mole spe.
LA	0.471093	10.599593	0.117773
etOH	0.352893	7.9400925	0.1726107
water	0.0534	1.2015	0.06675
ethyllact.	0	0	0
LLA	0.122613	2.7587925	0.01703

initial mole ratios;	
tetha1	1.465622
tetha2	0.566768
tetha3	0.1446

Table C.23. Titration data

time(min)	samp w(gr)	VKOH (ml)	VHCl (ml)
0	1.09753	63.2	2.8
90	1.1305	60.3	2.5
150	1.17214	60	2
210	1.18341	59	2.8
330	1.2476	58.5	2.3
450	1.27653	58	2.8
570	1.18754	53	3.5
690	1.18435	50.8	2.8
810	1.19022	51	3.1

Table C.24. Gas Chromatograph data

time(min)	GCEtOH	GCH2O	Gcetlact	GCetOH cortd	GCH2O cortd	GC etlact cortd
0	16154	1626	0	16154	951.0232084	0
90	13270	4097	2874	13270	2396.274345	3609.581265
150	12074	4424	3495	12074	2587.53178	4389.522103
210	12560	4616	4038	12560	2699.829723	5071.499356
330	12130	3434	4765	12130	2008.495509	5984.570191
450	14049	4343	6044	14049	2540.156085	7590.921771
570	13127	7728	6590	13127	4519.992223	8276.666854
690	12196	6312	6477	12196	3691.79489	8134.745253
810	10109	3394	6242	10109	1985.100104	7839.598559

C.2.3 18cm^2, 78μm, 5wt% PMo loaded PSF membrane

Table C.25. Experimental conditions

T=	50C
etOH/LA mole ratio =	1,0753
used membrane weight=	0.0514 gr
loading (for used part)=	0.00242 gr
total membrane weight=	1.7988 gr
polymer amount=	1.6793 gr
loading=	0.0835 gr

NKOH=	0,075 mol/lt
NHCL=	0,093 mol/lt
LA soln=	12 ml = 14,52 gr
etOH soln=	10 ml = 7,98 gr
Rxn mixture=	22 ml = 22,5 gr

Table C.26. Initial ratio of species in the reaction medium

	wt% spe.	gr spe.	mol.spe.	initial mole fractions;	
LA	0.471093	10.599593	0.117773	tetha1=	1.465622
etOH	0.352893	7.9400925	0.1726107	tetha2=	0.566768
H2O	0.0534	1.2015	0.06675	tetha3=	0.1446
Ethyllact.	0	0	0		
LLA	0.122613	2.7587925	0.01703		

Table C.27. Titration data

time(min)	smpl wgt	VKOH	VHCL
0	1.039	72.5	3.2
90	1.1523	71.3	3.5
150	1.1577	70	3
210	1.2063	67	2.8
330	1.25	64.5	3.2
450	1.2579	62	3
570	1.3347	57	3.5
690	1.3466	58	3
810	1.3218	55	2.8

Table C.28. Gas Chromatograph data

time(min)	GCetOH	GCH2O	Gclact.	etOH crtd	H2O crtd	lact crtd
0	12724	2978	0	12724	1741.7878	0
90	13402	3575	1632	13402	2090.9642	2049.6996
150	12910	4907	3598	12910	2870.0312	4518.8844
210	12667	3690	3614	12667	2158.226	4538.9794
330	12659	3440	5004	12659	2012.0047	6284.7408
450	12222	3120	5374	12222	1824.8415	6749.4398
570	12081	3350	5811	12081	1959.3651	7298.2871
690	12140	3323	6485	12140	1943.5732	8144.7929
810	11840	3978	6456	11840	2326.6729	8108.3706

C.2.4 18cm^2, 78μm, 10wt% PMo loaded PSF membrane

Table C.29. Experimental conditions

T=	50C		NKOH=	0,076 mol/lt
etOH/LA mole ratio =	1,0753		NHCL=	0,09 mol/lt
used membrane weight=	0.05257 gr			
loading (for used part)=	0.00514 gr		LA soln=	12 ml = 14,52 gr
total membrane weight=	1,8748 gr		etOH soln=	10 ml = 7,98 gr
polymer amount=	1,68 gr		**rxn mixture=**	22 ml = 22,5 gr
loading=	0,168 gr			

Table C.30. Initial ratio of species in the reaction medium

	wt% spe.	gr spe.	mol.spe.
LA	0.471093	10.599593	0.117773
etOH	0.352893	7.9400925	0.1726107
H2O	0.0534	1.2015	0.06675
Ethyllact.	0	0	0
LLA	0.122613	2.7587925	0.01703

initial mole fractions;	
tetha1=	1.465622
tetha2=	0.566768
tetha3=	0.1446

Table C.31. Titration data

time(min)	smpl wgt	VKOH	VHCL
0	1.0432	70	3
90	1.1388	66	3.5
150	1.1664	64	3
210	1.2144	62.5	2.5
330	1.2575	59.5	3.2
450	1.237	59	3.5
570	1.3345	52	3
690	1.3088	50	3
810	1.2095	47	2.5

Table C.32. Gas Chromatograph (GC) data

time(min)	GCetOH	GCH2O	Gclact.	etOH crtd	H2O crtd	lact crtd
0	15743	2596	0	15743	1518.3618	0
90	13142	3984	1855	13142	2330.1823	2329.775
150	12592	3158	2032	12592	1847.0672	2552.0769
210	13147	3513	2619	13147	2054.7014	3289.3157
330	12620	2822	3648	12620	1650.5458	4581.6814
450	4573	4080	3148	4573	2386.3313	3953.7098
570	11153	3047	4541	11153	1782.145	5703.2389
690	8910	2449	4428	8910	1432.3837	5561.3173
810	9233	2641	5354	9233	1544.6816	6724.3208

C.2.5 18cm^2, 78μm, 15wt% PMo loaded PSF membrane

Table C.33. Experimental conditions

T=	50C		NKOH=	0,076 mol/lt
etOH/LA mole ratio =	1,0753		NHCL=	0,09 mol/lt
used membrane weight=	0.0556 gr			
loading in used part=	0.00751 gr		LA soln=	12 ml = 14,52 gr
total membrane weight=	1,9782 gr		etOH soln=	10 ml = 7,98 gr
polymer amount=	1,6719 gr		rxn mixture=	22 ml = 22,5 gr
loading=	0,2663 gr			

Table C.34. Initial ratio of species in the reaction medium

	wt% spe.	gr spe.	mol.spe.		initial mole fractions;	
LA	0.471093	10.599593	0.117773		tetha1	1.465622
etOH	0.352893	7.9400925	0.1726107		tetha2	0.566768
H2O	0.0534	1.2015	0.06675		tetha3	0.1446
Ethyllact.	0	0	0			
LLA	0.122613	2.7587925	0.01703			

Table C.35. Titration data

time(min)	smpl wgt	VKOH	VHCL
0	1.06	73	4
90	1.1597	69	3.5
150	1.1767	67	3
210	1.2247	65.7	3.5
330	1.2287	62.5	2.8
450	1.2569	62	3
570	1.2975	56	3.2
690	1.267	53	3.5
810	1.187	50	3

Table C.36. Gas Chromatograph data

time(min)	GCetOH	GCH2O	Gclact.	etOH crtd	H2O crtd	lact crtd
0	12632	3293	0	12632	1926.0267	0
90	11701	9896	2749	11701	5788.0232	3452.5883
150	13258	6544	4376	13258	3827.4882	5496.0082
210	13027	5539	6131	13027	3239.6787	7700.1888
330	12646	4906	7994	12646	2869.4464	10040.011
450	12489	4827	9761	12489	2823.2405	12259.263
570	12388	4214	9775	12388	2464.7059	12276.847
690	11919	4611	10014	11919	2696.9053	12577.017
810	11455	4242	10531	11455	2481.0827	13226.34

C.3 esterification reaction at 50°C and 1:1 etOH/LA mole ratio with variable area, constant loading (0.167 gr) , constant thickness (78 μm) PMo loaded PSF film

C.3.1 18cm^2, 78μm, 10wt% PMo loaded PSF membrane

Table C.37. Experimental conditions

T=	50C	**NKOH**=	0,076 mol/lt
etOH/LA mole ratio =	1,0753	**NHCL**=	0,09 mol/lt
used membrane weight=	0.05257 gr		
loading (for used part)=	0.00514 gr	**LA soln**=	12 ml = 14,52 gr
total membrane weight=	1,8748 gr	**etOH soln**=	10 ml = 7,98 gr
polymer amount=	1,68 gr	**rxn mixture**=	22 ml = 22,5 gr
loading=	0,168 gr		

Table C.38. Initial ratio of species in the reaction medium

	wt% spe.	gr spe.	mol.spe.
LA	0.471093	10.599593	0.117773
etOH	0.352893	7.9400925	0.1726107
H2O	0.0534	1.2015	0.06675
Ethyllact	0	0	0
LLA	0.122613	2.7587925	0.01703

initial mole fractions;	
tetha1	1.465622
tetha2	0.566768
tetha3	0.1446

Table C.39. Titration data

time(min)	smpl wgt	VKOH	VHCL
0	1.0432	70	3
90	1.1388	66	3.5
150	1.1664	64	3
210	1.2144	62.5	2.5
330	1.2575	59.5	3.2
450	1.237	59	3.5
570	1.3345	52	3
690	1.3088	50	3
810	1.2095	47	2.5

Table C.40. Gas Chromatograph (GC) data

time(min)	GCetOH	GCH2O	Gclact.	etOH crtd	H2O crtd	lact crtd
0	15743	2596	0	15743	1518.3618	0
90	13142	3984	1855	13142	2330.1823	2329.775
150	12592	3158	2032	12592	1847.0672	2552.0769
210	13147	3513	2619	13147	2054.7014	3289.3157
330	12620	2822	3648	12620	1650.5458	4581.6814
450	4573	4080	3148	4573	2386.3313	3953.7098
570	11153	3047	4541	11153	1782.145	5703.2389
690	8910	2449	4428	8910	1432.3837	5561.3173
810	9233	2641	5354	9233	1544.6816	6724.3208

C.3.2. 36cm^2, 78μm, 5wt% PMo loaded PSF Film

Table C.41. Experimental conditions

T=	50C	NKOH=	0,088 mol/lt
etOH/LA mole ratio =	1,0753	NHCL=	0,090 mol/lt
used membrane weight=	0.10318 gr		
loading (for used part)=	0.09832 gr	LA soln=	12 ml = 14,52 gr
total membrane weight=	1.7893 gr	etOH soln=	10 ml = 7,98 gr
polymer amount=	1.67 gr	rxn mixture=	22 ml = 22,5 gr
loading=	0,168gr		

Table C.42. Initial ratio of species in the reaction medium

	Wt% spe.	gr spe.	mol.spe.		initial mole fractions;	
LA	0.471093	10.5995925	0.117773		tetha1=	1.465622
etOH	0.352893	7.9400925	0.1726107		tetha2=	0.566768
H2O	0.0534	1.2015	0.06675		tetha3=	0.1446
Ethyllact	0	0	0			
LLA	0.122613	2.7587925	0.01703			

Table C.43. Titration data

time(min)	Smpl wgt	VKOH	VHCL
0	1.1769	70	3.5
90	1.2612	67	3
150	1.275	65	2.5
210	1.288	61	2.5
330	1.3033	57	2.8
450	1.362	54	3.2
570	1.3808	53	2.8
690	1.4	51.5	3
810	1.395	50.5	3.5

Table C.44. Gas Chromatograph Data

time(min)	GCetOH	GCH2O	Gclact.	etOH crtd	H2O crtd	lact crtd
0	14075	2722	0	14075	1592.0573	0
90	12642	3203	3050	12642	1873.387	3830.6273
150	13182	4328	4780	13182	2531.3828	6003.4093
210	12739	5071	5648	12739	2965.9525	7093.5682
330	12583	4453	5612	12583	2604.4934	7048.3542
450	12179	4339	7479	12179	2537.8165	9393.2005
570	11430	3335	7741	11430	1950.5919	9722.2577
690	11193	5020	8700	11193	2936.1233	10926.707
810	11246	3653	9077	11246	2136.5854	11400.198

C.4. esterification reaction at 50°C and 1:1 etOH/LA mole ratio with variable thickness, constant loading (wt%) , constant area (18 cm^2) PMo loaded PSF film

C.4.1 47μm, 18cm^2 , 10wt% PMo loaded PSF film

Table C.45. Experimental conditions

T =	50C	NKOH	0,076 mol/lt
etOH/LA mole ratio =	1,0753	NHCL	0,09 mol/lt
used membrane weight=	0.02836 gr		
loading (for used part)=	0.004679 gr	LA soln	12 ml = 14,52 gr
total membrane weight=	1,012 gr	etOH soln	10 ml = 7,98 gr
polymer amount=	0.835 gr	rxn mixture 22 ml = 22,5 gr	
loading=	0,168 gr		

Table C.46. Initial ratio of species in the reaction medium

	wt% spe.	gr spe.	mol.spe.		initial mole fractions;	
LA	0.471093	10.599593	0.117773		tetha1	1.465622
etOH	0.352893	7.9400925	0.1726107		tetha2	0.566768
H2O	0.0534	1.2015	0.06675		tetha3	0.1446
Ethyllact	0	0	0			
LLA	0.122613	2.7587925	0.01703			

Table C.47. Titration data

time(min)	smpl wgt	VKOH	VHCL
0	1.0309	71	3
90	1.098	67	3.5
150	1.104	65	3
210	1.121	64	2.5
330	1.2875	59.5	3.2
450	1.365	56	3.5
570	1.3345	52	3
690	1.264	50	3
810	1.2095	47	2.5

Table C.48. Gas Chromatograph data

time(min)	GCetOH	GCH2O	Gclact.	etOH crtd	H2O crtd	lact crtd
0	13368	4027	0	13368	2355.3324	0
90	14251	4560	3398	14251	2667.0762	4267.6956
150	12505	5225	3795	12505	3056.0248	4766.3051
210	13410	5006	4995	13410	2927.9349	6273.4372
330	13459	6647	6105	13459	3887.7314	7667.5343
450	12489	7581	7167	12489	4434.0141	9001.3462
570	12611	4192	7213	12611	2451.8384	9059.1196
690	10046	3647	6676	10046	2133.076	8384.678
810	12184	3954	8092	12184	2312.6358	10163.094

C.4.2 78μm, 18cm^2, 10wt% PMo loaded PSF membrane

Table C.49. Experimental conditions

T=	50C	NKOH=	0,076 mol/lt
etOH/LA mole ratio =	1,0753	**NHCL=**	0,09 mol/lt
used membrane weight=	0.05255 gr		
loading (for used part)=	0.00512 gr	**LA soln=**	12 ml = 14,52 gr
total membrane weight=	1,8745 gr	**etOH soln=**	10 ml = 7,98 gr
polymer amount=	1,68 gr	**rxn mixture=**	22 ml = 22,5 gr
loading=	0,168 gr		

Table C.50. Initial ratio of species in the reaction medium

	wt% spe.	gr spe.	mol.spe.
LA	0.471093	10.599593	0.117773
etOH	0.352893	7.9400925	0.1726107
H2O	0.0534	1.2015	0.06675
Ethyllact.	0	0	0
LLA	0.122613	2.7587925	0.01703

initial mole fractions;	
tetha1	1.465622
tetha2	0.566768
tetha3	0.1446

Table C.51. Titration data

time(min)	smpl wgt	VKOH	VHCL
0	1.0432	70	3
90	1.1388	66	3.5
150	1.1664	64	3
210	1.2144	62.5	2.5
330	1.2575	59.5	3.2
450	1.237	59	3.5
570	1.3345	52	3
690	1.3088	50	3
810	1.2095	47	2.5

Table C.52. Gas Chromatograph (GC) data

time(min)	GCetOH	GCH2O	Gclact.	etOH crtd	H2O crtd	lact crtd
0	15743	2596	0	15743	1518.3618	0
90	13142	3984	1855	13142	2330.1823	2329.775
150	12592	3158	2032	12592	1847.0672	2552.0769
210	13147	3513	2619	13147	2054.7014	3289.3157
330	12620	2822	3648	12620	1650.5458	4581.6814
450	4573	4080	3148	4573	2386.3313	3953.7098
570	11153	3047	4541	11153	1782.145	5703.2389
690	8910	2449	4428	8910	1432.3837	5561.3173
810	9233	2641	5354	9233	1544.6816	6724.3208

C.4.3. 150μm, 18cm^2, 10wt% PMo loaded PSF film

Table C.53. Experimental conditions

T=	50C	NKOH=	0,076 mol/lt
etOH/LA mole ratio =	1,0753	NHCL=	0,09 mol/lt
used membrane weight=	0.10087 gr		
loading (for used part)=	0.00468 gr	LA soln=	12 ml = 14,52 gr
18cm2 used area		etOH soln=	10 ml = 7,98 gr
		rxn mixture=	22 ml = 22,5 gr
total membrane weight=	3.600 gr		
polymer amount=	3.34 gr		
loading=	0,168 gr		

Table C.54. Initial rate of species in the reaction medium

	wt% spe.	gr spe.	mol.spe.
LA	0.471093	10.599593	0.117773
etOH	0.352893	7.9400925	0.1726107
H2O	0.0534	1.2015	0.06675
Ethyllac	0	0	0
LLA	0.122613	2.7587925	0.01703

initial mole fractions;	
tetha1	1.465622
tetha2	0.566768
tetha3	0.1446

Table C.55. Titration Data

time(min)	smpl wgt	VKOH	VHCL
0	1.0309	71	3
90	1.101	67	3.5
150	1.1104	65	3
210	1.121	64	2.5
330	1.2875	59.5	3.2
450	1.367	59	3.5
570	1.3045	52	3
690	1.204	50	3
810	1.2095	47	2.5

Table C.56. Gas Chromatograph Data

time(min)	GCetOH	GCH2O	Gclact.	etOH crtd	H2O crtd	lact crtd
0	13368	4027	0	13368	2355.3324	0
90	14251	4560	4398	14251	2667.0762	5523.639
150	12505	5225	4795	12505	3056.0248	6022.2485
210	13410	5006	4995	13410	2927.9349	6273.4372
330	13459	6647	6105	13459	3887.7314	7667.5343
450	12489	7581	7167	12489	4434.0141	9001.3462
570	12611	4192	7213	12611	2451.8384	9059.1196
690	10046	3647	6676	10046	2133.076	8384.678
810	12184	3954	8092	12184	2312.6358	10163.094

C.4.4. 300μm, 18cm^2, 10wt% PMo loaded PSF film

Table C.57. Experimental conditions

T=	50C	**NKOH=**	0,076 mol/lt
etOH/LA mole ratio =	1,0753	**NHCL=**	0,09 mol/lt
used membrane weight=	0.19213 gr		
loading (for used part)=	0.004681gr	**LA soln=**	12 ml = 14,52 gr
total membrane weight=	6.957 gr	**etOH soln=**	10 ml = 7,98 gr
polymer amount=	6.68 gr	**rxn mixture= 22 ml = 22,5 gr**	
loading=	0,168 gr		

Table C.58. Initial rate of species in reaction medium

	wt% spe.	gr spe.	mol.spe.
LA	0.471093	10.599593	0.117773
etOH	0.352893	7.9400925	0.1726107
H2O	0.0534	1.2015	0.06675
Ethyllact.	0	0	0
LLA	0.122613	2.7587925	0.01703

initial mole fractions;	
tetha1	1.465622
tetha2	0.566768
tetha3	0.1446

Table C.59. Titration Data

time(min)	smpl wgt	VKOH	VHCL
0	1.0309	71	3
90	1.041	69.5	3.5
150	1.095	68	3
210	1.0971	66	2.5
330	1.1463	59	3.2
450	1.192	58.5	3.5
570	1.201	57.5	3
690	1.174	54.5	3
810	1.1895	53.5	2.5

Table C.60. Gas Chromatograph Data

time(min)	GCetOH	GCH2O	Gclact.	etOH crtd	H2O crtd	lact crtd
0	12289	5461	0	12289	3194.0577	0
90	12965	4830	2498	12965	2824.9951	3137.3466
150	12989	4131	3446	12989	2416.1604	4327.9809
210	12715	4296	4082	12715	2512.6665	5126.7609
330	11563	4230	4593	11563	2474.0641	5768.5479
450	15318	4432	6333	15318	2592.2109	7953.8894
570	11327	4357	6991	11327	2548.3445	8780.3001
690	11486	4004	7596	11486	2341.88	9540.1459
810	11178	3954	7907	11178	2312.6358	9930.7443

C.5 Deactivation test for 18 cm^2 , 78 μm, 10 wt% PMo loaded PSF film

C.5.1   1st series of deactivation test for 18 cm^2 , 78 μm, 10 wt% PMo loaded PSF film

Table C.61. Experimental conditions

T=	50C	**NKOH=**	0,082 mol/lt
etOH/LA mole ratio =	1,0753	**NHCL=**	0,096 mol/lt
used membrane weight=	0.05257 gr		
loading (for used part)=	0.00514 gr	**LA soln=**	12 ml = 14,52 gr
total membrane weight=	1,8748 gr	**etOH soln=**	10 ml = 7,98 gr
polymer amount=	1,68 gr	**rxn mixture=**	**22 ml = 22,5 gr**
loading=	0,168 gr		

Table C.62. Initial rate of species in reaction medium

	wt% spe.	gr spe.	mol.spe.		initial mole fractions;	
LA	0.471093	10.599593	0.117773		tetha1	1.465622
etOH	0.352893	7.9400925	0.1726107		tetha2	0.566768
H2O	0.0534	1.2015	0.06675		tetha3	0.1446
Ethyllact.	0	0	0			
LLA	0.122613	2.7587925	0.01703			

Table C.63. Titration Data

time(min)	smpl wgt	VKOH	VHCL
0	1.081	69	3.2
90	1.1577	68	3
150	1.1858	66	3.5
210	1.2269	64	3
330	1.2631	58	2.8
450	1.258	55	2.5
570	1.3546	54	3
690	1.319	51	3
810	1.2918	49	2.8

Table C.64. Gas Chromatograph Data

time(min)	GCetOH	GCH2O	Gclact.	etOH crtd	H2O crtd	lact crtd
0	14037	6763	0	14037	3955.5781	0
90	13601	4676	2697	13601	2734.9228	3387.2793
150	13263	5416	3113	13263	3167.7378	3909.7517
210	13176	5383	4010	13176	3148.4366	5036.3329
330	12661	4239	5602	12661	2479.328	7035.7948
450	12639	4806	6520	12639	2810.9579	8188.7508
570	13101	3515	7207	13101	2055.8712	9051.5839
690	11933	4293	7573	11933	2510.9118	9511.2592
810	11710	4732	7631	11710	2767.6764	9584.1039

C.5.2 2nd series of deactivation test for 18 cm^2 , 78 μm, 10 wt% PMo loaded PSF film

Table C.65. Experimental conditions

NKOH=	0,082 mol/lt
NHCL=	0,096 mol/lt
LA soln=	12 ml = 14,52 gr
etOH soln=	10 ml = 7,98 gr
rxn mixture=	**22 ml = 22,5 gr**

Table C.66. Initial rate of species in reaction medium

	wt% spe.	gr spe.	mol.spe.		initial mole fractions;	
LA	0.471093	10.599593	0.117773		tetha1	1.465622
etOH	0.352893	7.9400925	0.1726107		tetha2	0.566768
H2O	0.0534	1.2015	0.06675		tetha3	0.1446
Ethyllact.	0	0	0			
LLA	0.122613	2.7587925	0.01703			

Table C.67. Titration Data

time(min)	smpl wgt	VKOH	VHCL
0	1.0152	64.8	3.8
90	1.1028	64.3	2.5
150			
210	1.1128	63	2.8
330	1.2073	57.5	3
450	1.223	56	2.7
570	1.2643	54.7	3
690	1.2974	51.5	2.5
810	1.3017	51	2.8

Table C.68. Gas Chromatograph Data

time(min)	GCetOH	GCH2O	Gclact.	etOH crtd	H2O crtd	lact crtd
0	13850	6561	0	13850	3837.4313	0
90	13149	5209	4016	13149	3046.6666	5043.8686
150						
210	12726	4436	5186	12726	2594.5504	6513.3224
330	12887	4749	6142	12887	2777.6194	7714.0042
450	12578	4773	7086	12578	2791.6567	8899.6148
570	11318	5231	7250	11318	3059.5341	9105.5895
690	12071	4577	8360	12071	2677.0192	10499.687
810	11027	5557	8593	11027	3250.2066	10792.321

C.5.3 4th series of deactivation test for 18 cm^2, 78 μm, 10 wt% PMo loaded PSF film

Table C.69. Experimental conditions

NKOH=   0,09 mol/lt
NHCL=   0,093 mol/lt

LA soln=   12 ml = 14,52 gr
etOH soln=   10 ml = 7,98 gr
rxn mixture= 22 ml = 22,5 gr

Table C.70. Initial rate of species in reaction medium

	wt% spe.	gr spe.	mol.spe.		initial mole fractions;	
LA	0.471093	10.599593	0.117773		tetha1	1.465622
etOH	0.352893	7.9400925	0.1726107		tetha2	0.566768
H2O	0.0534	1.2015	0.06675		tetha3	0.1446
Ethyllact.	0	0	0			
LLA	0.122613	2.7587925	0.01703			

Table C.71. Titration Data

time(min)	smpl wgt	VKOH	VHCL
0	1.1435	66.5	3
90	1.1834	64	2.5
210	1.2074	62	2.7
330	1.2368	60	3
450	1.269	58.5	2.8
570	1.2887	56	3.2
690	1.3035	53	2.5
810	1.3327	51	2.8

Table C.72. Gas Chromatograph Data

time(min)	GCetOH	GCH2O	Gclact.	etOH crtd	H2O crtd	lact crtd
0	15028	2876	0	15028	1682.12961	0
90	14880	3765	3898	14880	2202.09248	4895.6673
210	13739	4065	5177	13739	2377.55802	6502.0189
330	13073	3688	6711	13073	2157.05633	8428.636
450	12208	3678	7688	12208	2151.20748	9655.6927
570	11908	3817	8428	11908	2232.50651	10585.091
690	11658	3756	9124	11658	2196.82852	11459.227
810	11549	3871	9591	11549	2264.09031	12045.753

C.5.4   5th series of deactivation test for 18 cm^2 , 78 μm, 10 wt% PMo loaded PSF film

Table C.73. Experimental conditions

NKOH=   0,087 mol/lt
NHCL=   0,095 mol/lt

LA soln=   12 ml = 14,52 gr
etOH soln=   10 ml = 7,98 gr
rxn mixture= 22 ml = 22,5 gr

Table C.74. Initial rate of species in reaction medium

	wt% spe.	gr spe.	mol.spe.		initial mole fractions;	
LA	0.471093	10.599593	0.117773		tetha1	1.465622
etOH	0.352893	7.9400925	0.1726107		tetha2	0.566768
H2O	0.0534	1.2015	0.06675		tetha3	0.1446
Ethyllact.	0	0	0			
LLA	0.122613	2.7587925	0.01703			

Table C.75. Titration Data

time(min)	smpl wgt	VKOH	VHCL
0	1.122	67.5	3
90	1.1567	65	2.6
210	1.1496	64	2.2
330	1.1578	61	2.5
450	1.1816	58	3
570	1.2044	56	2.8
690	1.2379	55	3
810	1.2538	52	2.5

Table C.76. Gas Chromatograph Data

time(min)	GCetOH	GCH2O	Gclact.	etOH crtd	H2O crtd	lact crtd
0	15869	3422	0	15869	2001.4769	0
90	15418	3392	3959	15418	1983.9303	4972.2798
210	12866	3998	5242	12866	2338.3707	6583.6552
330	12193	3856	6848	12193	2255.317	8600.7002
450	11568	4342	8025	11568	2539.5712	10078.946
570	11265	3744	8084	11265	2189.8099	10153.046
690	10932	3970	9589	10932	2321.9939	12043.241
810	10473	3659	9483	10473	2140.0947	11910.111

C.5.5 6th series of deactivation test for 18 cm^2 , 78 μm, 10 wt% PMo loaded PSF film

Table C.77. Experimental conditions

NKOH=   0,088 mol/lt
NHCL=   0,090 mol/lt

LA soln=   12 ml = 14,52 gr
etOH soln=   10 ml = 7,98 gr
rxn mixture=22 ml = 22,5 gr

Table C.78. Initial rate of species in reaction medium

	wt% spe.	gr spe.	mol.spe.		initial mole fractions;	
LA	0.471093	10.599593	0.117773		tetha1	1.465622
etOH	0.352893	7.9400925	0.1726107		tetha2	0.566768
H2O	0.0534	1.2015	0.06675		tetha3	0.1446
Ethyllact.	0	0	0			
LLA	0.122613	2.7587925	0.01703			

Table C.79. Titration Data

time(min)	smpl wgt	VKOH	VHCL
0	1.1365	67.6	3
90	1.1584	61	2.8
210	1.1729	55.5	2.5
330	1.1846	54	3
450	1.1907	51	2.5
570	1.2045	49	2.7
690	1.2188	47.5	2.2
810	1.2208	47	2.5

Table C.80. Gas Chromatograph Data

time(min)	GCetOH	GCH2O	Gclact.	etOH crtd	H2O crtd	lact crtd
0	17163	2919	0	17163	1707.2797	0
90	17277	2667	2720	17277	1559.8886	3416.166
210	15922	2731	3614	15922	1597.3213	4538.9794
330	15885	2837	4942	15885	1659.3191	6206.8722
450	14517	1953	6731	14517	1142.2806	8453.7549
570	14010	3314	7042	14010	1938.3093	8844.3533
690	13457	3281	7585	13457	1919.0081	9526.3305
810	12875	3175	7998	12875	1857.0103	10045.035

C.6. Deactivation test for 18 cm^2 , 78 μm, 15 wt% PMo loaded PSF film

C.6.1 2nd series of deactivation test for 18 cm^2 , 78 μm, 15 wt% PMo loaded PSF film

Table C.81. Experimental conditions

NKOH=	0,093 mol/lt
NHCL=	0,095 mol/lt
LA soln=	12 ml = 14,52 gr
etOH soln=	10 ml = 7,98 gr
rxn mixture= 22 ml = 22,5 gr	

Table C.82. Initial rate of species in reaction medium

	wt% spe.	gr spe.	mol.spe.		initial mole fractions;	
LA	0.471093	10.599593	0.117773		**tetha1=**	1.465622
etOH	0.352893	7.9400925	0.1726107		**tetha2=**	0.566768
H2O	0.0534	1.2015	0.06675		**tetha3=**	0.1446
Ethyllact.	0	0	0			
LLA	0.122613	2.7587925	0.01703			

Table C.83. Titration Data

time(min)	smpl wgt	VKOH	VHCL
0	1.12	63	3.2
90	1.1583	58	3
210	1.1877	56	2.5
330	1.1903	52.5	2.8
450	1.2014	47.5	2.2
570	1.2198	46	2.8
690	1.237	45	3
810	1.2346	44	2.5

Table C.84. Gas Chromatograph Data

time(min)	GCetOH	GCH2O	Gclact.	etOH crtd	H2O crtd	lact crtd
0	15318	3027	0	15318	1770.4473	0
90	15156	2923	3893	15156	1709.6192	4889.3876
210	14240	2829	5513	14240	1654.64	6924.0158
330	13320	2916	6733	13320	1705.525	8456.2668
450	12833	3095	7271	12833	1810.2195	9131.9643
570	12061	3096	8741	12061	1810.8043	10978.201
690	12111	3200	9509	12111	1871.6324	11942.766
810	11648	3324	9956	11648	1944.1581	12504.172

C.6.2 3rd series of deactivation test for 18 cm^2, 78 μm, 15 wt% PMo loaded PSF film

Table C.85. Experimental conditions

NKOH =   0,087 mol/lt
NHCL =   0,092 mol/lt

LA soln =   12 ml = 14,52 gr
etOH soln =   10 ml = 7,98 gr
rxn mixture = 22 m l= 22,5 gr

Table C.86. Initial rate of species in reaction medium

	wt% spe.	gr spe.	mol.spe.
LA	0.471093	10.599593	0.117773
etOH	0.352893	7.9400925	0.1726107
H2O	0.0534	1.2015	0.06675
Ethyllact.	0	0	0
LLA	0.122613	2.7587925	0.01703

initial mole fractions;	
tetha1	1.465622
tetha2	0.566768
tetha3	0.1446

Table C.87. Titration Data

time(min)	smpl wgt	VKOH	VHCL
0	1.0638	64	3.3
90	1.1044	58	3
210	1.1137	55	2.5
330	1.1285	51	2.7
450	1.1369	47	3
570	1.1573	45	2.8
690	1.1728	42	2.5
810	1.1982	41	3

Table C.88. Gas Chromatograph Data

time(min)	GCetOH	GCH2O	Gclact.	etOH crtd	H2O crtd	lact crtd
0	15180	2720	0	15180	1590.8875	0
90	15071	2580	3165	15071	1509.0036	3975.0608
210	14253	2548	4802	14253	1490.2873	6031.0401
330	13405	2738	5326	13405	1601.4155	6689.1544
450	12817	2885	5523	12817	1687.3936	6936.5753
570	12434	3081	6490	12434	1802.0311	8151.0725
690	12106	3152	7105	12106	1843.5579	8923.4777
810	11799	3303	7828	11799	1931.8756	9831.5248

C.6.3   4th series of deactivation test for 18 cm^2 , 78 μm, 15 wt% PMo loaded PSF film

Table C.89. Experimental conditions

NKOH =   0,085 mol/lt
NHCL=   0,090 mol/lt

LA soln =   12 ml = 14,52 gr
etOH soln =   10 ml = 7,98 gr
rxn mixture = 22 ml = 22,5 gr

Table C.90. Initial rate of species in reaction medium

	wt% spe.	gr spe.	mol.spe.		initial mole fractions;	
LA	0.471093	10.599593	0.117773		**tetha1**	1.465622
etOH	0.352893	7.9400925	0.1726107		**tetha2**	0.566768
H2O	0.0534	1.2015	0.06675		**tetha3**	0.1446
Ethyllact.	0	0	0			
LLA	0.122613	2.7587925	0.01703			

Table C.91. Titration Data

time(min)	smpl wgt	VKOH	VHCL
0	1.0718	66	3
90	1.1033	62	
210	1.1159	60	
330	1.1364	58	
450	1.1487	54	
570	1.1522	52	
690	1.1845	50	
810	1.2006	49	

Table C.92. Gas Chromatograph Data

time(min)	GCetOH	GCH2O	Gclact.	etOH crtd	H2O crtd	lact crtd
0	15736	2885	0	15736	1687.3936	0
90	15210	2561	3740	15210	1497.8908	4697.2282
210	14350	2781	4574	14350	1626.5655	5744.685
330	13453	2235	5532	13453	1307.2182	6947.8788
450	12936	2167	6628	12936	1267.4461	8324.3927
570	12439	2804	7338	12439	1640.0179	9216.1125
690	12187	3032	8370	12187	1773.3717	10512.246
810	11851	3153	8934	11851	1844.1428	11220.598

APPENDIX-D

CHARACTERIZATION RESULTS

D.1. DSC RESULTS
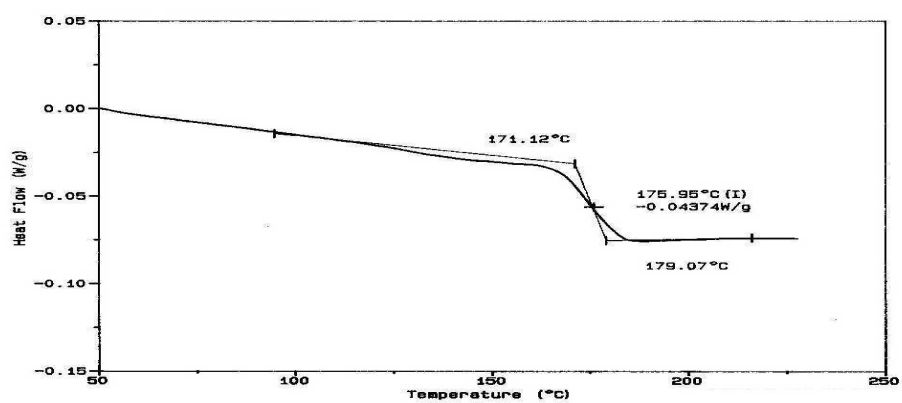
FigureD.1 DSC result for pure psf polymeric film
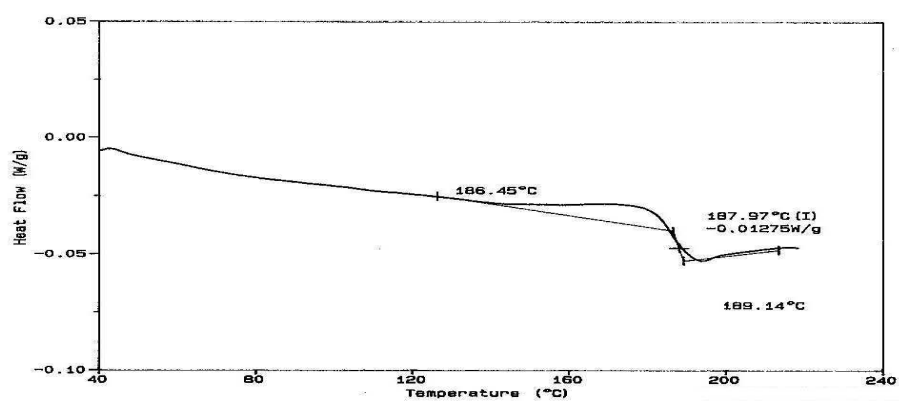
FigureD.2 DSC result for 5wt% pmo loaded 78 μm-psf catalytic film
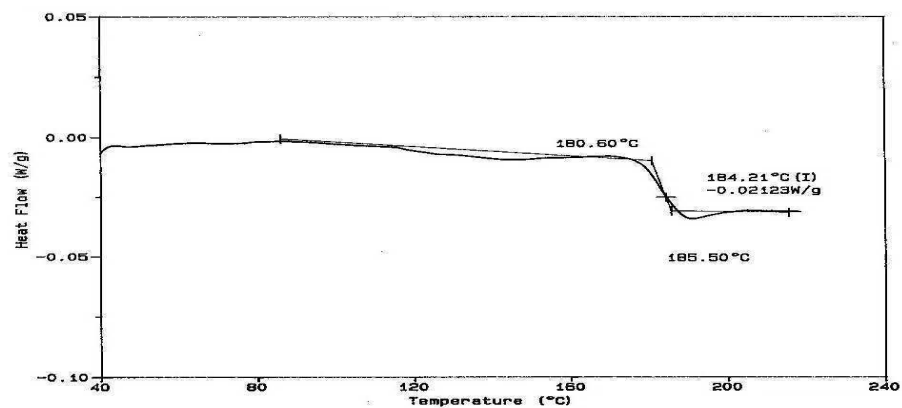
FigureD.3 DSC result for 10wt% pmo loaded 78 μm-psf catalytic film

D.2. TGA RESULTS
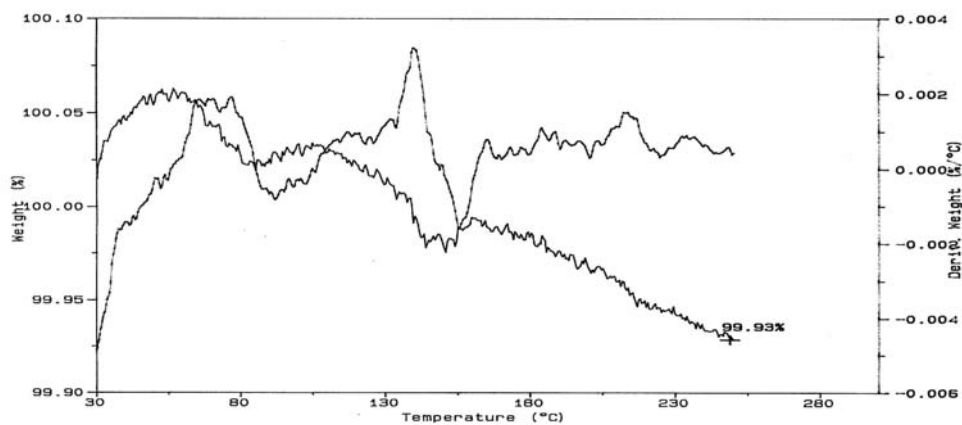
FigureD.4 TGA result for pellet psf
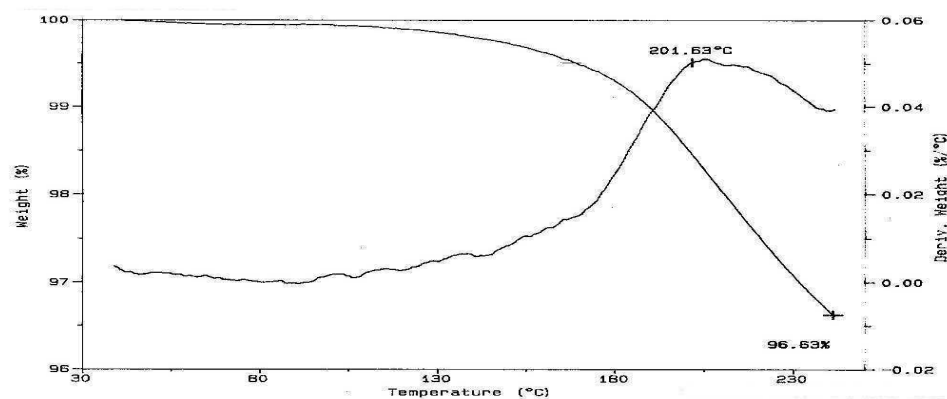
FigureD.5 TGA result for pure psf film
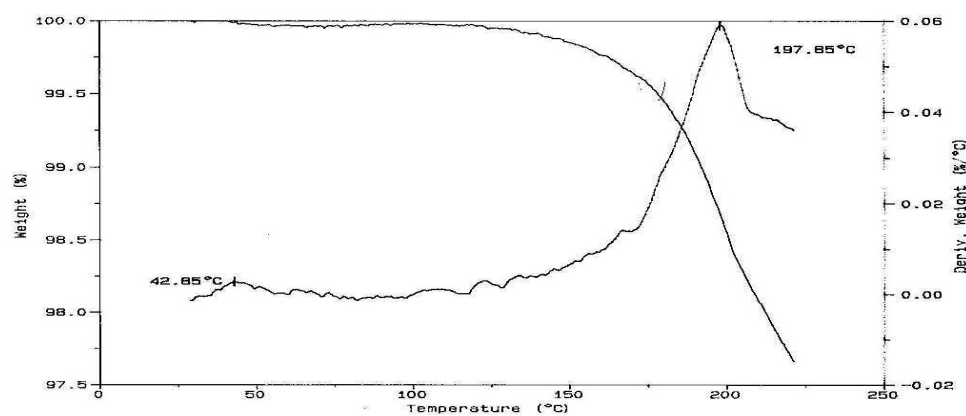
FigureD.6 TGA result for 5wt% pmo loaded 78 μm-psf catalytic film
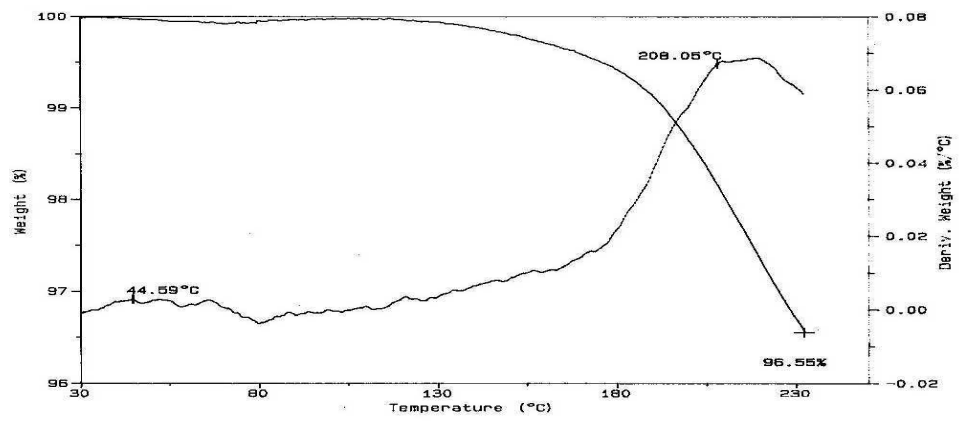
FigureD.7 TGA result for 10wt% pmo loaded 78 μm-psf film
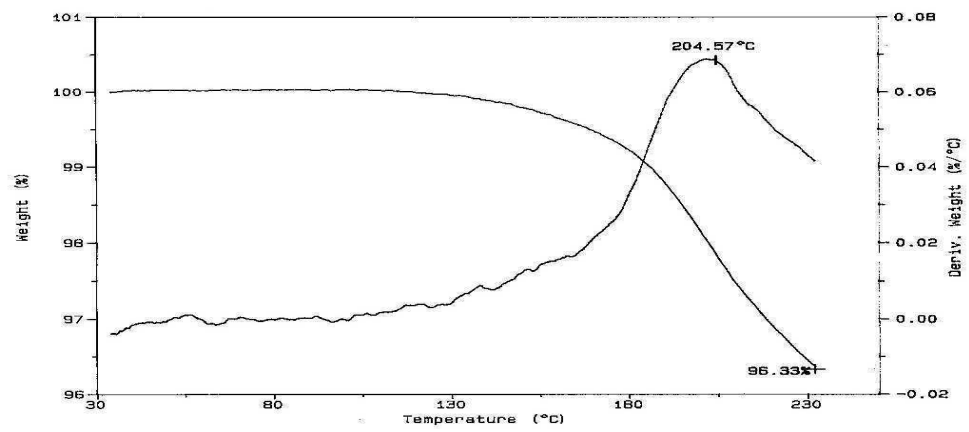
FigureD.8 TGA result for 15wt% pmo loaded 78 μm-psf film

D.3. SEM RESULTS
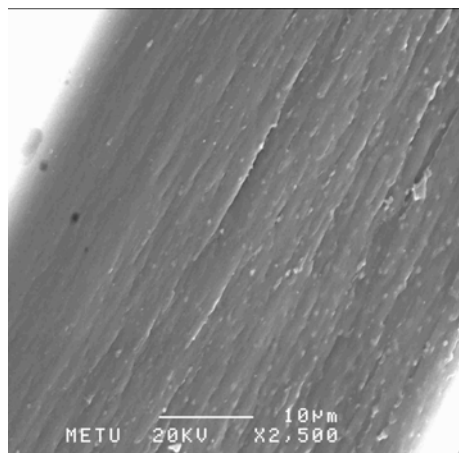
FigureD.9 crossectional SEM view of 5wt% pmo loaded 78μm-psf film
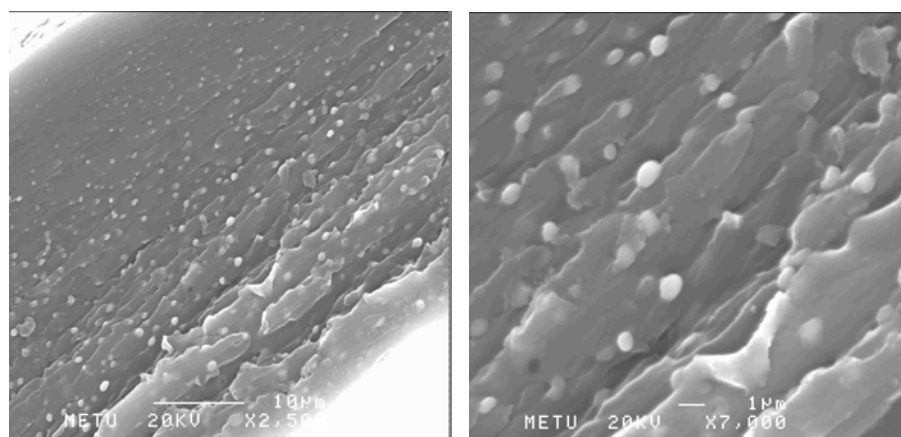
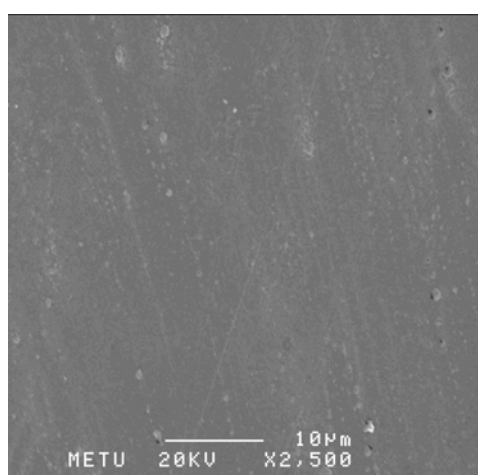**FigureD.10** crossectional SEM view of 10wt% pmo loaded 78μm-psf film
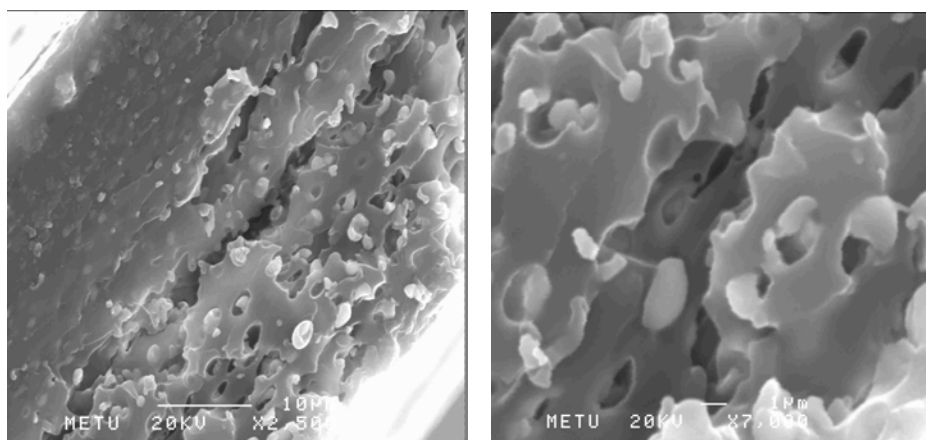
FigureD.11 crossectional SEM view of 15wt% pmo loaded 78μm-psf film
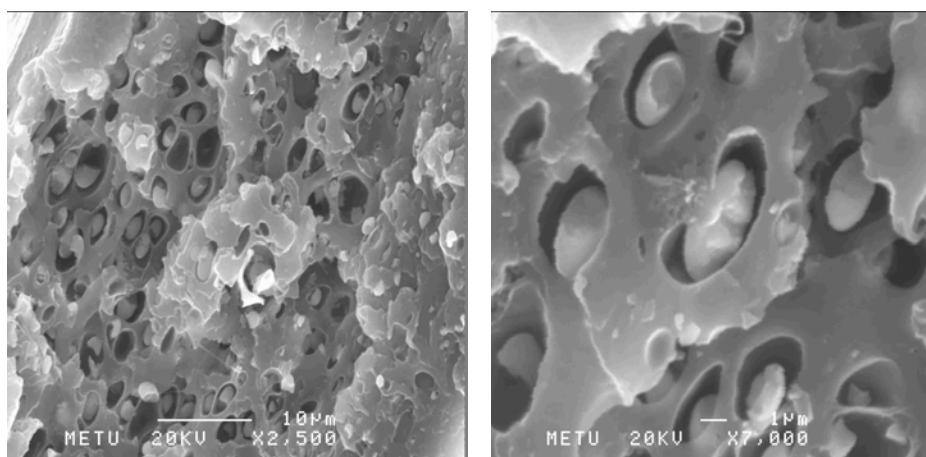
FigureD.12 crossectional SEM view of 10wt% pmo loaded 47μm-psf film
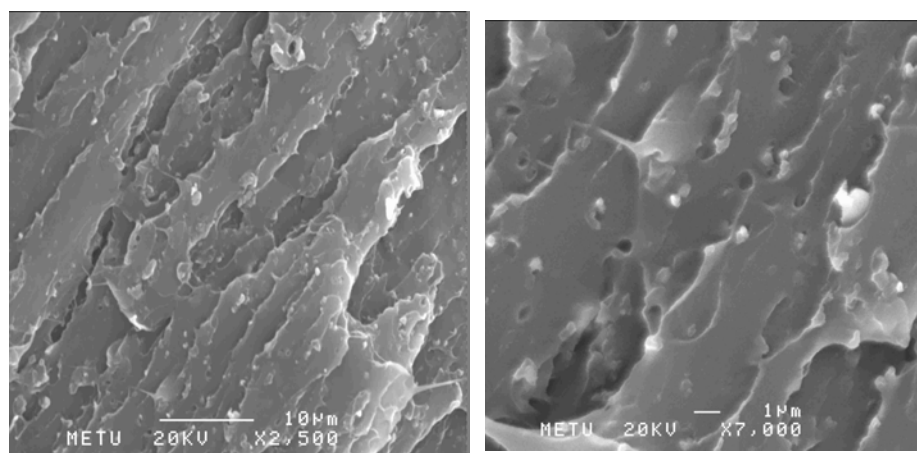
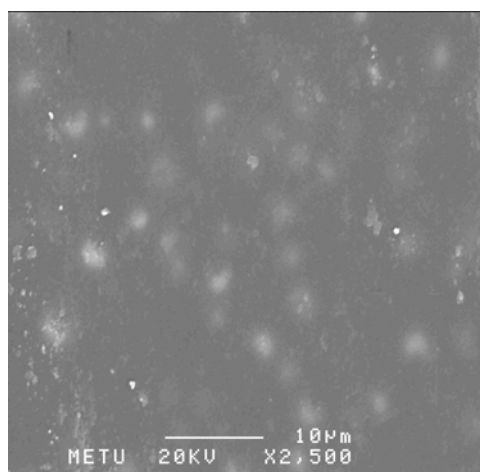**FigureD.13** cross-sectional SEM view of 10wt% pmo loaded 150μm-psf film
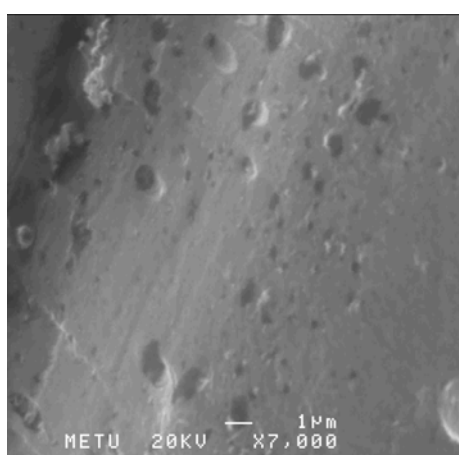
FigureD.14 top SEM view of 10wt% pmo loaded 300μm-psf film
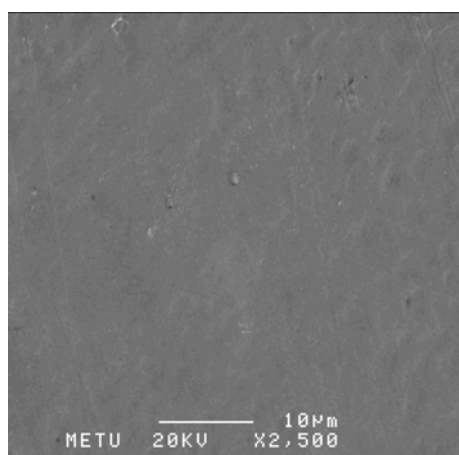
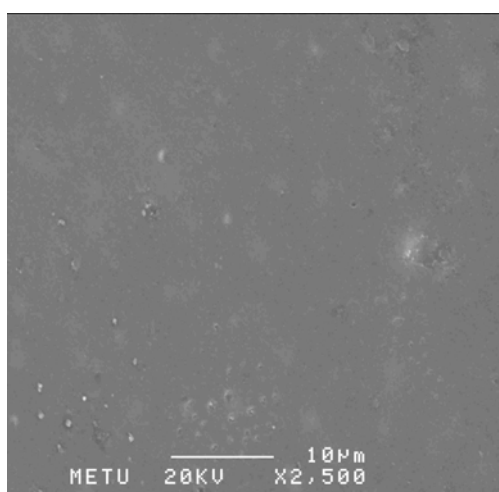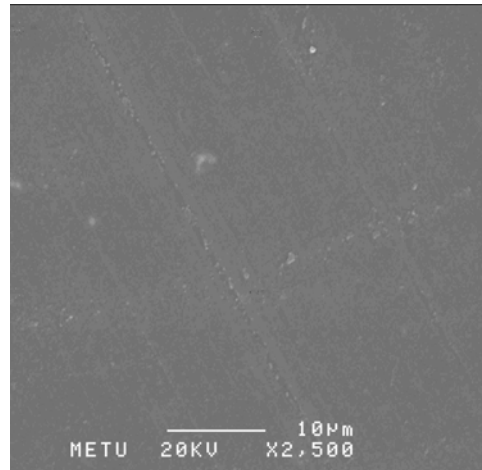**FigureD.15** top SEM view of 5wt% pmo loaded 78μm-psf film

FigureD.16 top SEM view of 10wt% pmo loaded 78μm-psf film

FigureD.17 top SEM view of 15wt% pmo loaded 78μm-psf film

FigureD.18 top SEM view of 10wt% pmo loaded 47μm-psf film

FigureD.19 top view of 10wt% pmo loaded 150μm-psf film